



Review

Metallophthalocyanine-based molecular materials as catalysts for electrochemical reactions

José H. Zagal^{a,**}, Sophie Griveau^b, J. Francisco Silva^a, Tebello Nyokong^c, Fethi Bedioui^{b,*}

^a Facultad de Química y Biología, Departamento de Química de los Materiales, Universidad de Santiago de Chile (USACH), Casilla 40, Correo 33, Santiago, Chile

^b Laboratoire de Pharmacologie Chimique et Génétique et d'Imagerie, UMR CNRS 8151/U INSERM 1022, Chimie-Paris Tech, Université Paris Descartes, ENSCP 11 rue Pierre et Marie Curie, 75231 Paris cedex 05, France

^c Department of Chemistry, Rhodes University, Grahamstown, South Africa

Contents

1. Introduction.....	2756
2. Metallophthalocyanine-based molecular electrodes.....	2756
3. Catalytic properties of MPcs in electrochemical reactions involving thiols.....	2759
3.1. Redox behavior of thiols at molecular phthalocyanine electrodes.....	2761
3.2. General trends in reactivity of macrocyclics for the oxidation of thiols.....	2763
4. Catalytic properties of MPc in electrochemical reduction of molecular oxygen.....	2768
4.1. Reaction pathways for the reduction of molecular oxygen.....	2768
4.2. Interaction of O ₂ with active sites and the redox mechanism.....	2769
4.3. One-electron reduction catalysts for the reduction of molecular oxygen.....	2774
4.4. Two to four-electron reduction catalysts for the reduction of molecular oxygen.....	2774
5. Catalytic properties of MPcs in electrochemical oxidation of nitric oxide NO.....	2777
6. Catalytic properties of MPcs in electrochemical oxidation of nitrite.....	2779
7. Catalytic properties of MPcs in electrochemical oxidation of hydrazine and hydroxylamine.....	2781
7.1. Electrooxidation of hydrazine.....	2781
7.2. Electrooxidation of hydroxylamine.....	2782
8. Catalytic properties of MPcs in electrochemical reactions involving other biologically and environmentally relevant compounds.....	2783
8.1. Phenols and organohalides.....	2783
8.2. Catecholamines.....	2784
9. Oxidation of glucose and other sugars at molecular phthalocyanine electrodes.....	2786
10. Conclusion and perspectives.....	2787
Acknowledgements.....	2787
References.....	2787

ARTICLE INFO

Article history:

Received 19 November 2009

Accepted 1 May 2010

Available online 11 May 2010

Keywords:

Metal phthalocyanine

Cobalt

Iron

Manganese

Nickel

Electrocatalysis

Modified electrodes

ABSTRACT

Metallophthalocyanines confined on the surface of electrodes are active catalysts for a large variety of electrochemical reactions and electrode surfaces modified by these complexes can be obtained by simple adsorption on graphite and carbon. However, more stable electrodes can be achieved by coating their surfaces with electropolymerized layers of the complexes, that show similar activity than their monomer counterparts. In all cases, fundamental studies carried out with adsorbed layers of these complexes have shown that the redox potential is a very good reactivity index for predicting the catalytic activity of the complexes. Volcano-shaped correlations have been found between the electrocatalytic activity (as $\log I$ at constant E) versus the Co(II)/(I) formal potential (E°) of Co-macrocyclics for the oxidation of several thiols, hydrazine and glucose. For the electroreduction of O₂ only linear correlations between the electrocatalytic activity versus the M(III)/M(II) formal potential have been found using Cr, Mn, Fe and Co phthalocyanines but it is likely that these correlations are “incomplete volcano” correlations. The volcano correlations strongly suggest that E° , the formal potential of the complex needs to be

* Corresponding author. Tel.: +33 1 53 10 12 98; fax: +33 1 53 10 12 92.

** Corresponding author.

E-mail addresses: jzagal@usach.cl (J.H. Zagal), fethi-bedioui@chimie-paristech.fr (F. Bedioui).

Thiol
Nitric oxide
Nitrite
Hydroxylamine
Hydrazine
Oxygen
Catecholamines
Phenol
Volcano plots

in a rather narrow potential window for achieving maximum activity, probably corresponding to surface coverages of an M-molecule adduct equal to 0.5 and to standard free energies of adsorption of the reacting molecule on the complex active site equal to zero. These results indicate that the catalytic activity of metallophthalocyanines for the oxidation of several molecules can be “tuned” by manipulating the E° formal potential, using proper groups on the macrocyclic ligand. This review emphasizes once more that metallophthalocyanines are extremely versatile materials with many applications in electrocatalysis, electroanalysis, just to mention a few, and they provide very good models for testing their catalytic activity for several reactions. Even though the earlier applications of these complexes were focused on providing active materials for electroreduction of O_2 , for making active cathodes for fuel cells, the main trend in the literature nowadays is to use these complexes for making active electrodes for electrochemical sensors.

© 2010 Elsevier B.V. All rights reserved.

1. Introduction

Metallophthalocyanines (MPcs) are extremely versatile materials. They belong to a class of transition metal complexes known as N4-macrocyclic complexes and they possess a N4 inner structure that is common in naturally occurring molecules such as chlorophyll, heme groups in hemoglobin, cytochrome c, vitamin B₁₂, etc. Due to their macrocyclic nature including extended π -systems, phthalocyanines are capable of undergoing fast redox processes, with minimal reorganizational energies and can act as mediators in electron transfer processes involving a great variety of molecules [1–5]. In this review we will concentrate our attention on the catalytic activity of phthalocyanines for electrochemical reactions. This was first reported four decades ago in a pioneering study by Jasinski [6,7] while searching for non-noble catalysts for the oxygen cathode in fuel cells. He showed that Co phthalocyanine is active for the reduction of O_2 . This triggered extensive research in many places in the world on N4 macrocyclic metal chelates as possible electrocatalysts for the reduction of O_2 for the development of low cost fuel cells, with the aim of replacing platinum, which is the best catalyst known for the reduction of O_2 . This topic has been the subject of several reviews [8–28] and the feasibility of using phthalocyanines in practical fuel cells has been shown recently [29].

MPcs constitute an interesting type of catalysts since they present several advantages over noble metals, not only because of the cost. In particular, they provide very interesting models for theoretical and experimental studies since their catalytic action can be described in terms of definite parameters such as chemical structure and chemical and physical properties. Their reactive centers are clearly identified and their reactivity can be modulated by changing the nature of the central metal or by modifying the structure of the macrocyclic ligand. Fig. 1 illustrates the structures of some metallophthalocyanines and related macrocyclic complexes that have been studied as catalysts for electrochemical reactions.

All the work published to date shows that MPcs have a very wide range of applications in electrochemistry varying from energy conversion devices to electrochemical sensors for the detection of molecules of biological and environmental relevance. In the earlier studies, most of the work was focused on the reduction of molecular O_2 but was later shown over the years that they catalyze a myriad of reactions. Some phthalocyanines and related macrocyclic complexes catalyze (i) the electrooxidation of formic acid [8,30], CO [8,29–33], SO_2 [34–36], oxalic acid [37–48], glucose [49–63], molecular hydrogen [64–68], H_2O_2 [67–69], hydrazine [8,30,47,70–88], nitrite [89,90], mercaptoethanol [91–93], L-cysteine [71,94–106], sulfide ion [107], thiocyanate [102,108,109], hydroxylamine [74,88,110–112], NO [113–119], dopamine [120–122], the evolution of oxygen [123,124] and the oxidation of phenols [125–128]; (ii) the electroreduction of H_2O_2 [129,130], protons [131], CO_2 [132–140], alkylchlorides [141,142], cystine [94,143], molecular nitrogen [144], N_2O [145,146], NO [147], nitrite [111], nitrate [148–150], thionyl chloride [151–167] and sulfonyl chloride [153]. They are also good

catalyst in hydrogenation reactions [165]. MPcs are also promising as electrode materials not only as catalysts but also as reactive species in lithium cells [166–168].

MPcs are also promising for promoting photocatalytic reactions. They can act as spectroscopic sensitizers deposited on semiconductor electrodes [169–188] and can have applications in solar energy conversion devices. The colour of phthalocyanines is modified when they undergo oxidation state changes involving the ligand and this can have applications in electrochromic devices [189–191]. Rare-earth diphthalocyanines are noticeable by their electrochromic reversibility which allows their use as electro-optic transducers in plate screens [192–194]. However we will not discuss these applications as they are beyond the scope of the present review.

2. Metallophthalocyanine-based molecular electrodes

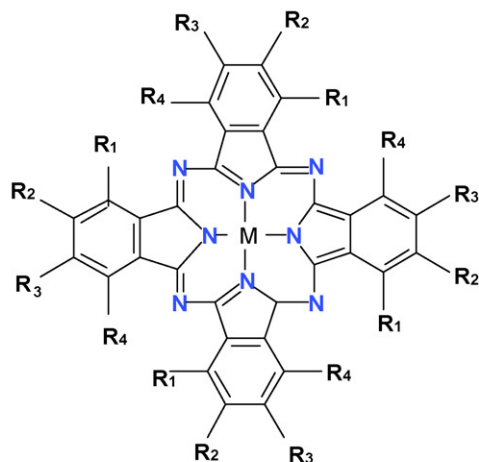
Most MPcs are insoluble in water and they can be confined on electrode surfaces, to yield “metallophthalocyanine-based molecular electrodes”. They can be attached to an electrode surface by vacuum sublimation, vapor deposition, precipitation, adsorption from a solution in an organic solvent or concentrated acid, polymerization by heat treatment in the presence of carbon powders (and the electrode is then made with the resulting mixture) and electrochemical polymerization, etc. Fig. 2 illustrates the different approaches for immobilizing MPcs on electrode surfaces. Adsorption of the complexes on graphite or carbon materials (see Fig. 2a) has been the preferred method of most authors due to its simplicity and because it provides reproducible results. The modified electrode can be characterized by simple techniques, like cyclic voltammetry which allows the estimation of the formal potentials of redox processes involving the immobilized complex and also the amount of electroactive molecules present on the electrode surface. In a typical experiment, the adsorption of monolayers of MPc is simply achieved by dipping the electrode into solutions of the complexes in an appropriate solvent for several minutes, or placing a drop of these solutions on the electrode surface and then rinsing with ethanol or other solvent to eliminate any excess of non-adsorbed complex.

The use of self-assembled monolayers (SAMs) of alkylthio-, arylthio- and thiol-derivatized phthalocyanines [57,82,102, 109,195–208] is a rather new and convenient method for immobilizing these macrocyclic complexes on gold surfaces. Indeed, thiol derivatized macrocyclic bound to a gold substrate via their thiol arms lead to the formation of reproducible and stable films of SAMs. A schematic representation of these SAMs is given in Fig. 2b–d. Such a monolayer of highly oriented molecules on a substrate is formed spontaneously by immersing a solid substrate into a solution containing the desired species with an appropriate functional group. Careful placement of thiol groups of the adsorbate can constrain the resulting molecule to a particular packing preference on the electrode surface (see Fig. 2b and c).

Another approach for modifying surfaces is to use polymeric phthalocyanines. Polymeric films containing MPCs can be formed on different conductive substrates by electropolymerizing a functionalized monomeric phthalocyanine directly onto a surface of

an electrode or by coating the electrode with a preformed polymer (Fig. 2e). Alternatively, these complexes can be incorporated into preformed polymers [131,139,209–224], plasma polymerized [224–227] onto substrates or formed by the Langmuir–Blodgett

(A) Phthalocyanine complexes



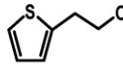
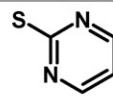
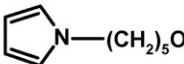
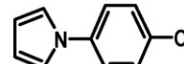
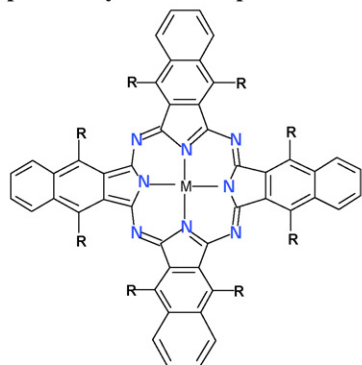
Octa (or more) substituted	Substituent	abbreviation
$R_1 = R_2 = R_3 = R_4$	= F	16(F)MPc
$R_1 = R_2 = R_3 = R_4$	= Cl	16(Cl)MPc
$R_1 = R_2 = R_3 = R_4$	= CN	16(CN)MPc
$R_1 = R_4 = H; R_2 = R_3$	= SBu	8 β (SBu)MPc
$R_1 = R_4 = H; R_2 = R_3$	= SC ₂ H ₄ OH	8 β (SC ₂ H ₄ OH)MPc
$R_1 = R_4 = H; R_2 = R_3$	= 2-Et-C ₆ H ₁₁ O	8 β (2-Et-C ₆ H ₁₁ O)
$R_2 = R_3 = H; R_1 = R_4$	= OBu	8 α (OBu)MPc
$R_1 = R_4 = H; R_2 = R_3$	= OC ₈ H ₁₆	8 β (OC ₈ H ₁₇)MPc
$R_1 = R_4 = H; R_2 = R_3$	= OCH ₃	8 β (OCH ₃)MPc
$R_1 = N(CH_3)_2; R_4 = R_2 = H; R_3$	= C(CH ₃) ₃	4 α (N(CH ₃) ₂)4 β ((CH ₃) ₃)MPc
Tetrasubstituted		
$R_1 = R_4 = R_2 = H; R_3$	= NH ₂	4 β (NH ₂)MPc
$R_1 = R_4 = R_2 = H; R_3$	= SCH ₂ Ph	4 β (SCH ₂ Ph)MPc
$R_1 = R_4 = R_2 = H; R_3$	= C(CH ₃) ₃	4 β (C(CH ₃) ₃)MPc
$R_1 = R_4 = R_2 = H; R_3$	= OBu	4 β (OBu)MPc
$R_1 = R_4 = R_2 = H; R_3$	= C(CH ₃) ₃ Ph	4 β (C(CH ₃) ₃ Ph)MPc
$R_1 = R_4 = R_2 = H; R_3$	= COCl	4 β (COCl)MPc
$R_1 = R_4 = R_2 = H; R_3$	= COOH	4 β (COOH)MPc
$R_1 = R_4 = R_2 = H; R_3$	= SC ₁₂ H ₂₅	4 β (SC ₁₂ H ₂₅)MPc
$R_1 = R_4 = R_2 = H; R_3$	=  (ethoxy thiophene: OETH)	4 β (OETH)MPc
$R_1 = R_4 = R_2 = H; R_3$	= OPhC(CH ₃) ₂ Ph	4 β (OPhC(CH ₃) ₂ Ph)MPc
$R_1 = R_4 = R_2 = H; R_3$	=  (mercapto pyrimidine: SMPy)	4 β (SMPy)MPc
$R_1 = R_4 = R_2 = H; R_3$	= NO ₂	4 β (NO ₂)MPc
$R_1 = R_4 = R_2 = H; R_3$	= OC ₅ H ₁₁	4 β (OC ₅ H ₁₁)MPc
$R_1 = R_4 = R_2 = H; R_3$	=  (pentoxypyrrole: OPePyr)	4 β (OPePyr)
$R_1 = R_4 = R_2 = H; R_3$	= OPh	4 β (OPh)MPc
$R_1 = R_4 = R_2 = H; R_3$	=  (phenoxypyrrole: PhPy)	4 β (PhPy)MPc
$R_1 = R_4 = R_2 = H; R_3 =$	= SO ₃ ⁻	4 β (SO ₃ ⁻)MPc
$R_1 = R_4 = R_2 = H; R_3$	= t-Bu	4 β (t-Bu)MPc

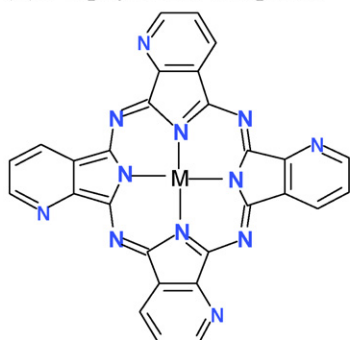
Fig. 1. Structures of some of the examined complexes.

(B) Naphthalocyanine complexes

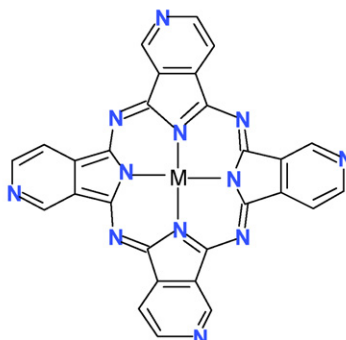


	Substituent	abbreviation
R	= H	MNc
R	= OBU	8α(OBU)Nc

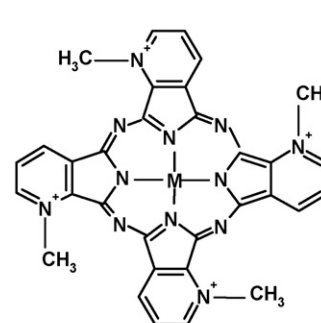
(C) Porphyrazine complexes



TPyr 2,3 MPz



TPyr 3,4 MPz



QTPy 2,3 MPz

(D) Porphyrins



	Substituent	abbreviation
R	= (C ₂ H ₅)	4(C ₂ H ₅)MP
R	= Ph(OCH ₃)	4(Ph(OCH ₃))MP
R	= Ph	4(Ph)MP
R	= PhNH ₂	4(PhNH ₂)MP
R	= SO ₃ ⁻	4(PhSO ₃ ⁻)MP
R	= F	20(F)PhMP

Fig. 1. (Continued).

method [198,228]. The electrochemical polymerization is an elegant, attractive and easy strategy for the immobilization of metal complexes [229–236] providing relatively stable films. The principle is based on the electrochemical oxidation (or reduction) of a polymerizable group present on the phthalocyanine ligand. The obtained polymeric films should be electronic conductors to ensure the continuous growth of the polymeric film and to allow electron transfer processes within the matrix. Pyrrole, thiophene and aniline-based monomers have been the most commonly used materials [234–237]. Such chemically substituted monomers have many interesting features including a high flexibility in their molecular design. Additionally, such materials offer the possibility of using either aqueous or organic solutions to carry out the electropolymerization. One of the first examples that involved the incorporation of MPcs into polypyrrole films was based on the ion-exchange properties of the oxidized polymer. Tetrasulfonated substituted complexes [238–245] have been introduced into polypyrrole films as counter-ions (or “doping” ions). Only few examples have described the electropolymerization of pyrrole-substituted MPcs [246–248]. Most studies of polymeric MPcs have involved the electrochemical polymerization of tetraaminoph-

thalocyanines (4β(NH₂)MPc) [77,119,137,230,249–255] which involves the oxidation of the amino group to form radicals that initiate condensation by attacking phenyl rings of neighboring molecules. An illustration of a hypothetical polymer coating is given in Fig. 2e. 4β(NH₂)MPc has been electropolymerized on glassy carbon electrode [77,119,121,252,253,256–262], ITO [77,241,258,260,262] and highly oriented pyrolytic graphite electrode [254]. Of the 4β(NH₂)MPc complexes, most studies have concentrated on 4β(NH₂)CoPc due the excellent electrocatalytic behavior of this complex towards a variety of electrochemical reactions.

Fig. 3 shows very schematically a hypothetical catalytic process promoted by “MPcs based molecular electrode”. The scheme is shown for a reduction process but a similar one can be shown for an oxidation process. In some reactions mediated by MPcs, the complex changes oxidation states upon interacting with the reacting molecule and it recovers its initial oxidation state by accepting or donating electrons to the electrode. So the electrode acts simply as a sink or a source of electrons that are exchanged with the surface-confined phthalocyanine molecule. As it will be discussed further, the formal potentials of the catalyst are correlated to the electro-

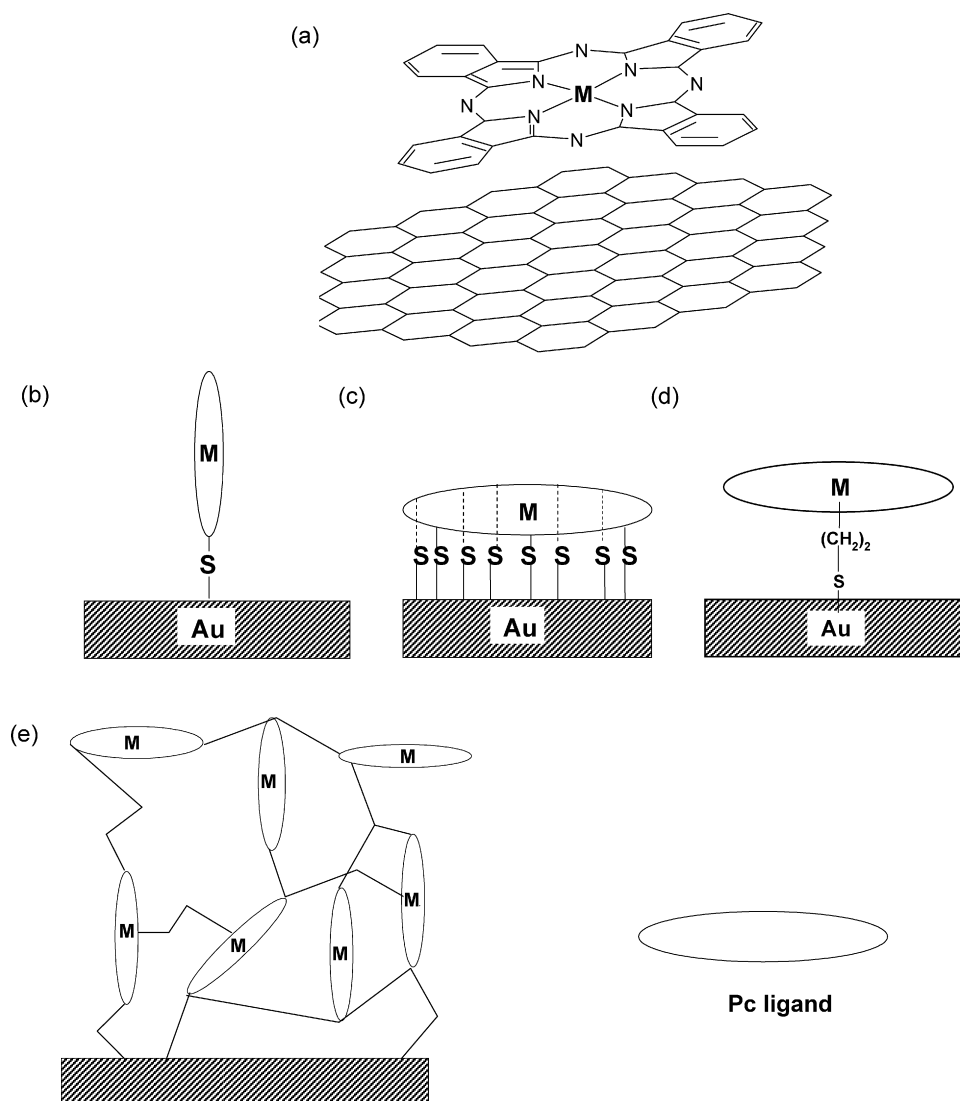


Fig. 2. Typical ways of immobilizing macrocyclic complexes on electrode surfaces: (a) with adsorption on graphite, (b) vertical and (c) octopus orientation of a thiol derivatized MPc complexes on gold to form SAMs; (d) axial ligation of MPc complex on 4-mercaptopyridine preformed SAM; (e) an illustration of a hypothetical polymer coating. Adapted from ref. [92].

catalytic activity. Table 1 recapitulates some significant examples of MPcs based molecular electrodes and their use for the activation of various analytes [263–320].

3. Catalytic properties of MPcs in electrochemical reactions involving thiols

Metallophthalocyanines and related complexes exhibit catalytic activity for the electrochemical oxidation of a great variety of thiols [14,21,100,274,284–287,290–292,321–338] and for the reduction of the corresponding disulfides [100]. These “*molecular phthalocyanine electrodes*” act by lowering the overpotential of oxidation or reduction of the target molecules [14]. Studies of the electrooxidation of thiols to give the corresponding disulfides have shown that the catalytic activity of the molecular electrodes strongly depends on the nature of the central metal, with cobalt derivatives exhibiting the highest activity [14]. The rates of the electrochemical oxidation of thiols are also strongly dependent of the nature of the N_4 -macrocyclic ligand.

The electrocatalytic oxidation of thiols and many other reactions discussed in this review can be considered as inner-sphere reactions since a bond between a sulfur atom and the active site

is expected to occur before or when the electron transfer takes place [14]. In some cases, this interaction can be so strong that the catalytic process is inhibited as the active sites are blocked by the reacting molecules bound to the active sites in the phthalocyanine. Indeed, in the case of polymeric tetraaminocobalt phthalocyanine poly-4 β (NH_2)CoPc deposited on transparent indium tin oxide (ITO) electrodes, there is *in situ* evidence that an adduct is formed between this molecule and 2-mercaptoethanol (2-ME) [292,329]. This adduct, if it is labile, could be a precursor in the electrocatalytic process of oxidation of thiols. Further, electroreflectance spectroscopy studies on Co and Fe tetrasulfonated phthalocyanines adsorbed on the basal plane of highly oriented pyrolytic graphite electrodes have demonstrated that under open-circuit conditions, in basic deaerated aqueous solutions, the thiol, L-cysteine, reduces the metal in the adsorbed phthalocyanine from M(II) to M(I) [330] suggesting that the M(II)/M(I) redox couple in the phthalocyanine plays a role in the catalytic process.

In earlier studies of the electrocatalytic activity of MPcs for the oxidation of thiols such as 2-ME and 2-aminoethanethiol [290,333,334,338–340] the catalytic activity (measured as current at constant potential) followed a linear correlation with the redox potential (driving force) of the complex, when immobilized on

Table 1
Summary of studied analytes using MPC complexes^a.

Oxidative detection	M in MPC	Selected ring substituents	Electrodes	Modification methods	References
Oxidation					
Dopamine	Fe, Ni, Fe, Co	NH ₂ , SO ₃ [−] , H	CF, GCE, ITO	CPE, polymer, adsorption	[121,268–273,312,316]
Serotonin	Ni	SO ₃ [−] , H, NH ₂	CF	Polymer, CPE	[268,312]
Noradrenaline, adrenaline	Ni	SO ₃ [−]	CF	Polymer	[312]
Vitamin B1	Mn	H		CPE	[315]
Glycine	Mn	NH ₂	ITO, GCE	Polymer	[260]
Glucose, H ₂ O ₂	Co	H, 4(Ph)P	GCE	Adsorption	[50–58,69]
Cysteine, homocysteine, N-acetylcysteine	Co, Mn, Fe, Rh, Os, Ru, Mo	NO ₂ , NH ₂ , SO ₃ [−] , H, C-(CH ₃) ₃ , COOH, alkylthio, phenoxy pyrrole, ethoxy thiophene, ethyloxy, neopentoxy, methoxy	GCE, Au, OPGE, VCE, CF, silica gel	CPE, polymer, adsorption, electrodeposition, SAM, preformed SAM	[52,92,99,100,101,103,108,248,284–289,299,314,317,320]
r-GSH	Co	H, ethoxy thiophene, NH ₂	VCE, CME, GCE, OPGE	CPE, adsorption, SPCE, polymer	[52,93,103,293,296,300,302,311,314]
2-ME	Co, Fe	NH ₂ , SO ₃ [−] , H, methoxy, ethoxy thiophene, Cl, ethoxy	OPGE, VCE, GCE, CF, Au, OPGE, graphite	Polymer, adsorption, SPCE, SAM	[92,93,99,275,100,101,106,290,292,294,295,297,314]
2-MESA	Co	NH ₂ , H	GCE, OPGE, VCE	Polymer, adsorbed	[106,298]
DEAET, ethanethiol, methanethiol, propanethiol	Co	H, alkylthio, NH ₂	BPPGE/SWCNT	Electrosorption	[291,301,314,319]
SCN [−] , penicillamine	Co, Fe	H, alkylthio	Au, GCE	Adsorption, SAM, preformed SAM	[108,101,109,317]
NO	H ₂ , Co, Cr, Fe, Mn, Zn, Cu	SO ₃ [−] , H	GCE, CF	Homogeneous, electrodeposition, adsorption, polymer	[113–119,230]
NO ₂ [−]	Co, Ni, Fe, Mn, Ti, Cr	Alkylthio, NH ₂ , phenoxy, benzyloxy, 4- <i>tert</i> -butylphenoxy	Au, GCE	Polymer, SAM, adsorption, electrodeposition	[89,119,277–282,314]
Hydrazine	Co, Fe, Ru, Fe	SO ₃ [−] , H, NH ₂	GCE, RDE, OPGE, zeolite, Au	Polymer, adsorption, CPE, preformed SAM	[76–79,81,82,111,283]
Hydroxylamine	Ru	H	BPG, RDE	Adsorption	[111,112]
Phenol, 4-CP, PCP, 4-NP	Co, Ni	H, phenoxy pyrrole	GCE, VCE	Adsorption, SPCE, polymer, CPE	[126,265–267]
Cresol	Co	H	GCE	Adsorption	[266]
Amitrole	Co, Fe	H		CPE	[313]
Asulum	Co	NH ₂	BPPGE/MWCNT	Polymer	[318]
Reduction					
Cystine	Co, Fe, Mn	Ethyloxy, SO ₃ [−] , H	Graphite, OPGE	Adsorption	[302]
Dithiobis(ethanol)	Co, Fe	SO ₃ [−] , H, NH ₂ , ethoxy thiophene,	Au, VCE, GCE, OPGE	SAM, adsorption, polymer	[100,101,292,274,297]
NO	Co, H ₂	SO ₃ [−] , H,	GCE	Electrodeposition, homogeneous, adsorption	[117,118,275]
NO ₂ [−]	Co, Ru	H, TPyr2, 3Pz, QTPyr2, 3Pz	GCE, RDE	Electrodeposition	[111,276]
TCA, DBB, t-DBCH	Ni, Cu, Co	H	GCE, OPGE	Adsorption, membrane	[263,264]
Oxygen	Co, Mn, Fe, Ru,	H, NH ₂ , SO ₃ [−] , Cl, CN pentoxy pyrrole, ethoxy thiophene, mercaptopyrimidine, phenoxy pyrrole	GCE, graphite, CF, OPGE, Pt, EPPGE, Au, zeolite, ITO	CPE, adsorption, polymer, homogeneous	[79,81,130,214,262,303–305,306–308,309,310]

CPE: carbon paste electrode, SAM: self-assembled monolayer, CF: carbon fiber, GCE: glassy carbon electrode, OPGE: ordinary pyrolytic graphite electrodes BPG: basal-plane pyrolytic graphite, VCE: vitreous carbon electrode, SPCE: screen printed carbon electrode, CME: carbon microelectrode, ITO: indium tin oxide, MWCNT: multi-walled carbon nanotube, EPPGE: edge plane pyrolytic graphite electrode, RDE: rotating disk electrode, BPG: basal-plane pyrolytic graphite, BPPGE: basal plane pyrolytic graphite electrode. r-GSH: reduced glutathione, 2-ME: mercaptoethanol, 2-MESA: mercaptoethanesulfonic acid, 4-CP: 4-chlorophenol, 4-NP: 4-nitrophenol, PCP: pentachlorophenol, TCA: trichloroacetic acid, DBB: 1,2-dibromobutane, DBCH: 1,2-dibromocyclohexane, DEAET: 2-(diethylamino) ethanethiol.

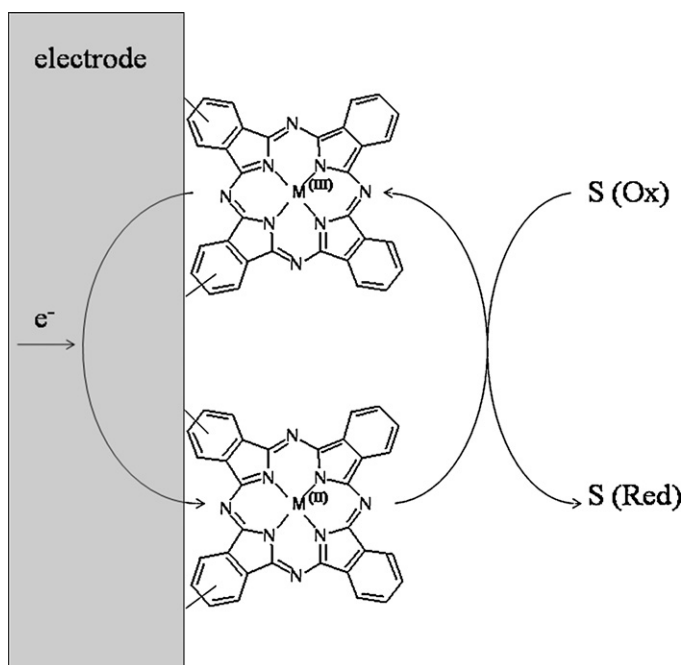


Fig. 3. Scheme of a catalytic process promoted with MPcs based molecular electrode.

graphite electrodes. The activity increases as the $M(II)/M(I)$ formal potential of the catalyst becomes more negative, that is to say, the activity increases when the driving force of the catalyst decreases. This is contrary to what is expected on thermodynamic grounds. In contrast, for the reduction of 2-mercaptodisulfide the activity increases as the $Co(II)/Co(I)$ becomes more negative [296], that is the activity increases when the driving force of the catalyst increases (as expected), since the latter is a reduction reaction. However, it was shown later that if complexes exhibiting formal potentials in a wide range are examined, the complete correlation follows a volcano-shape [92,295,340]. Indeed for the oxidation of 2-ME in a study using five cobalt complexes including porphyrins and phthalocyanines bearing $Co(II)/Co(I)$ redox potentials in the range -1.2 V to -0.6 V, a volcano plot was obtained [295] with Co-tetraaminophenylporphyrin having a $Co(II)/Co(I)$ formal potential at ca. -0.9 V versus SCE showing the highest activity. More correlations of this type were reported later using adsorbed substituted metallo tetraphenylporphyrins and metallo phthalocyanines with Co as the central metal with substituents on the N_4 ligand, using both electron-donor and electron-acceptor groups to modulate the $Co(II)/Co(I)$ redox potentials in a wide range [340]. The volcano correlations indicate that the redox potential of the catalyst needs to be “tuned” in a rather narrow potential range for achieving maximum activity. These observations have an impact on the search for catalysts for applications in electrocatalysis and the development of electrochemical sensors as will be discussed further [321].

In this section we focused on the description of some significant recent examples reported in the literature related to the electro-activation of thiols by “molecular phthalocyanine electrodes”. It is aimed at showing how the redox and electrocatalytic activities of the electrodes can be finely tuned in order to control the electron transfer rates. Also, a tentative elucidation of a possible empirical correlation between the experimentally established data and theoretical calculations will be reported and discussed. Table 2 shows a selection of thiols activated by several types of “molecular phthalocyanine electrodes”.

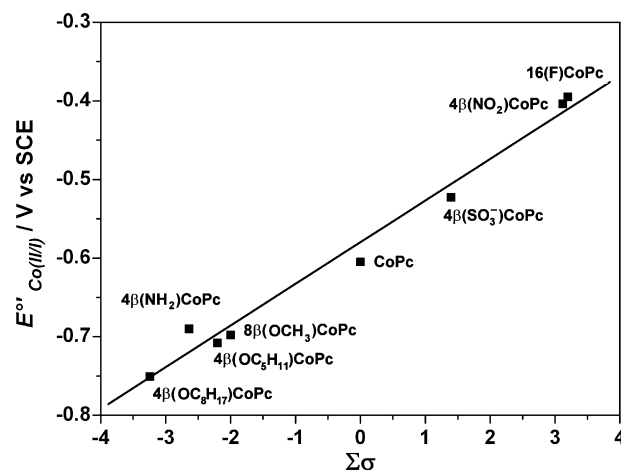


Fig. 4. Dependence of the $Co(II)/(I)$ formal potential of the adsorbed CoPcs with the sum of the Hammett parameters of the substituent on the ligand. Adapted from ref. [92].

3.1. Redox behavior of thiols at molecular phthalocyanine electrodes

As stated in the first part, the catalytic activity of the MN4 complexes strongly depends on the nature of the central metal but also on the nature of the ligand. We will also describe below the studies that support the influence of these parameters on the catalytic activity towards the oxidation of thiols.

All adsorbed CoPcs complexes exhibit a reversible pair of peaks between -0.8 and 0.0 V versus SCE that has been tentatively assigned to the $Co(II)/Co(I)$ reversible process [338]. As expected, the formal potential of the $Co(II)/Co(I)$ redox process shifts to more negative values by the effect of electron donating groups ($8\beta(OC_8H_{17})CoPc$, $8\beta(OCH_3)CoPc$, $4\beta(OC_5H_{11})CoPc$ and $4\beta(NH_2)CoPc$) since these groups increase the electron density on the metal center, facilitating the oxidation of the Co center compared to H-substituted CoPc. The opposite effect is observed for electron withdrawing groups, as the formal potential shifts to more positive values in comparison to CoPc. This is illustrated in Fig. 4 that shows a linear correlation between the $Co(II)/Co(I)$ formal potential and the sum of the Hammett parameters σ of some examples of substituents on the ligand. This shows that the redox potential of Co phthalocyanine can be modulated, by choosing the appropriate substituents on the ligand. This is true for phthalocyanines of other metals, as has been shown in a series of papers by Lever and co-workers [21,88,111,146].

Fig. 5 illustrates a typical cyclic voltammogram for $4\beta(OC_5H_{11})CoPc$ adsorbed on OPG, after adding 1 mmol L^{-1} of 2-mercaptoethanol (2-ME) to 0.5 mol L^{-1} NaOH solution [339]. A large oxidation current is observed starting at -0.5 V versus SCE, which corresponds to the electrocatalytic oxidation of 2-ME at the molecular phthalocyanine electrode. The appearance of the oxidation peak at $E_p = +0.38$ V versus SCE is concomitant with the reduction peak at -0.75 V versus SCE, during the reverse scan. This large cathodic peak is related to the reduction of the corresponding disulfide. Oxidation of 2-ME on the bare OPG electrode is only observed as a peak at $+0.07$ V versus SCE with no reduction peak in the potential range examined. This clearly shows that cobalt phthalocyanine layer not only acts as a catalyst towards the oxidation of 2-ME but also for the reduction of the corresponding disulfide. This has also been observed for the oxidation of 2-ME on Fe phthalocyanines and the more active the catalysts, the smaller the separation between the 2ME oxidation peak and the disulfide reduction peak [290].

Table 2
A selection of peak potentials for the detection of thiols on MPC modified electrodes versus Standard calomel electrode (SCE). Potentials reported versus Ag/AgCl have been corrected to versus SCE using -0.045 V conversion factor.

MPC ^a	Electrode ^b	Modification method ^b	Analyte ^c	E_p (V) versus SCE	Medium	References
Cysteine						
CoPc	Clay/Hg	Incorporated inside	Cysteine	-0.47	pH 7.4	[288]
4 β (COOH)CoPc, 4 β (SO ₃ ⁻)CoPc, CoPc, 4 β (C(CH ₃) ₃)CoPc, 4 β (NO ₂)CoPc	GCE	Electrodeposition	Cysteine	0.63 to $+0.78$	pH 3.5	[284]
8 β (SBu)FePc, 8 β (SBu)CoPc, 8 β (SC ₂ H ₄ OH)FePc, 8 β (SC ₂ H ₄ OH)CoPc	Au	SAM	Cysteine	-0.03 to $+0.16$ $+0.29$ to $+0.46$	pH 9 pH 4	[108,285]
4 β (OETH)CoPc	VCE	Adsorbed	Cysteine	-0.11	0.5 M NaOH	[100]
4 β (PhPy)CoPc	VCE	Adsorbed	Cysteine	-0.04	0.5 M NaOH	[100]
4 β (SMPy)CoPc	GCE	Adsorbed	Cysteine	$+0.12$	pH 4	[99]
4 β (PhPy)CoPc	GCE	Polymer	Cysteine	$+0.46$	pH 4	[248]
4 β (OETH)CoPc	Au	SAM	Cysteine	$+0.36$	pH 4	[101]
CoPc, FePc, MnPc	Au	Preformed SAM	Cysteine	$+0.14$, $+0.16$	pH 4	[102]
CoPc	CME	Micromolded C	Cysteine	0.50^d	pH 5.5	[103]
RhPc(Cl)(py), OsPc(py) ₂ , RuPc(py) ₂ , 4 β (SO ₃ ⁻)OMoPc	GCE	Adsorption	Cysteine	$+1.05$ to $+1.15$	pH 7.2	[286]
	Carbon	CPE	Cysteine	$+0.25$	0.05 M H ₂ SO ₄	[287]
2-ME						
FePc 8 β (OCH ₃)FePc	OPGE	Adsorption	2-ME	-0.28 , -0.33	pH 10.5	[290]
4 β (NH ₂)CoPc	VCE	Adsorption	2-ME	-0.29 , -0.32	0.5 M NaOH	[274]
4 β (OETH)CoPc	Au	SAM	2-ME	$+0.74$	pH 4	[101]
4 β (OETH)CoPc	VCE	Adsorbed	2-ME	-0.22	0.5 M NaOH	[100]
4 β (PhPy)CoPc	VCE	Adsorbed	2-ME	-0.12	0.5 M NaOH	[100]
4 β (SMPy)CoPc	GCE	Adsorbed	2-ME	-0.4	pH 11	[99]
CoPc	Carbon	SPCE	2-ME	$+0.12$	pH 7.4	[93]
			2-ME	-0.35	\sim pH 13	
CoPc	VCE	Polymer	2-ME	-0.45	0.5 M NaOH	[292]
4 β (NH ₂)CoPc	VCE	Polymer	2-ME	-0.05	0.5 M NaOH	[295]
CoPc/SWCNT	GCE	Adsorption	2-ME	-0.15	0.1 M NaOH	[297]
Other						
8 β (SBu)FePc, 8 β (SBu)CoPc	Au	SAM	Homocysteine	$+0.48$, 0.40	pH 4	[108]
8 β (SC ₂ H ₄ OH)FePc, 8 β (SC ₂ H ₄ OH)CoPc	Au	SAM	Homocysteine	$+0.50$, 0.41	pH 4	[108]
8 β (SBu)FePc, 8 β (SBu)CoPc	Au	SAM	Penicillamine	$+0.54$, 0.41	pH 4	[108]
8 β (SC ₂ H ₄ OH)FePc, 8 β (SC ₂ H ₄ OH)CoPc	Au	SAM	Penicillamine	$+0.51$, 0.40	pH 4	[108]
8 β (SBu)FePc, 8 β (SBu)CoPc	Au	SAM	Thiocyanate	$+0.74$, 0.69	pH 4	[108]
8 β (SC ₂ H ₄ OH)FePc, 8 β (SC ₂ H ₄ OH)CoPc	Au	SAM	Thiocyanate	$+0.69$	pH 4	[108]
CoPc, FePc, MnPc	Au	Preformed SAM	Thiocyanate	$+0.51$, $+0.54$	pH 4	[109,317]
4 β (NH ₂)CoPc/MWCNT	BPPGE	Electrosorption	DEAET	$+0.54$	pH 7	[319]
4 β (NH ₂)CoPc	VCE	Polymer	Dithiobis (ethanol)	-0.89	0.5 M NaOH	[274]
4 β (OETH)CoPc	Au	SAM	Dithiobis (ethanol)	-0.65	pH 4	[101]
4 β (OETH)CoPc	VCE	Adsorbed	Dithiobis (ethanol) r-GSH	-1.1 , -0.14	0.5 M NaOH	[100]
4 β (PhPy)CoPc	VCE	Adsorbed	r-GSH	-0.08	0.5 M NaOH	[100]
4 β (SMPy)CoPc	GCE	Adsorbed	r-GSH	-0.19	pH 11	[99]
CoPc	Carbon	SPCE	r-GSH	$+0.34$	pH 7.4	[93]
			r-GSH	-0.05	\sim pH 13	
CoPc	VCE	Polymer	Dithiobis (ethanol)	-0.9	0.5 M NaOH	[292]
CoPc	CME	Micromolded C	Glutathionine, homocysteine	0.50	pH 5.5	[103]
				0.35		
4 β (OC ₅ H ₁₁)MPC	OPGE	Adsorbed	2-HEDS	-0.9	0.2 M NaOH	[296]
CoPc/SWCNT	GCE	Adsorption	Dithiobis (ethanol)	-0.95	0.1 M NaOH	[297]
CoPc	OPGE	Adsorbed	2-MESA	-0.047	0.1 M NaOH	[298]
4 β (NH ₂)CoPc	VCE	Adsorbed	2-MESA	-0.14	0.1 M NaOH	[298]
		Polymer		-0.14		

^a py: pyridine; MWCNT: multi-walled carbon nanotube; SWCN: single-walled carbon nanotube.

^b OPGE: ordinary pyrolytic graphite electrode; GCE: glassy carbon electrode; CPE: carbon paste electrode; VCE: vitreous carbon electrode; SPCE: screen printed carbon electrode; OPGE: ordinary pyrolytic graphite electrodes; BPPGE: basal plane pyrolytic graphite electrode; SAM: self-assembled monolayer.

^c r-GSH: reduced glutathionine, 2-ME: mercaptoethanol, 2-MESA: mercaptoethanasulfonic acid, DEAET: 2-(diethylamino) ethanethiol.

^d versus Pt wire quasi-ref electrode.

The catalytic activity of MPCs for the oxidation of thiols is strongly dependent on the nature of the metal in the macrocycle [14,21,321]. When comparing the activity of phthalocyanines of different metals for the oxidation of 2-ME, the highest activity was shown by CoPc and FePc [91]. CoPc and 4 β (SO₃⁻)CoPc complexes were the most active (compared to MnPc, FePc, NiPc and CuPc) for the electrocatalytic oxidation of L-cysteine [74].

The catalytic activity of ring substituted 4 β (NO₂)CoPc, 4 β (NH₂)CoPc, 4 β (C(CH₃)₃)CoPc, 4 β (SO₃⁻)CoPc and 4 β (COOH)CoPc adsorbed onto glassy carbon electrode increased with the ring substituent as follows: 4 β (COOH)CoPc > 4 β (C(CH₃)₃)CoPc > 4 β (SO₃⁻)CoPc > 4 β (NH₂)CoPc > 4 β (NO₂)CoPc. The potential for the catalytic oxidation of L-cysteine was closely related to the

Co(III)/Co(II) couple of the CoPc species in acid media and to Co(II)/Co(I) couple in basic media [284]. The Fe(II)/Fe(I) couple has also been associated with the electrocatalytic oxidation of L-cysteine by 4 β (SO₃⁻)FePc [330].

The study on the effect of ring substituents on the electrocatalytic behavior of iron phthalocyanines (4 β (SO₃⁻)FePc, 4 β (COOH)FePc, 8 β (OCH₃)FePc, 16(F)FePc and FePc) adsorbed on ordinary pyrolytic graphite electrode, for the oxidation of 2-ME [53], showed that complexes containing electron-withdrawing groups ($-\text{CO}_2^-$, $-\text{SO}_3^-$, Cl^-) shifted the catalytic peak to more positive potentials, and the ones containing electron-donating methoxy groups to more negative potentials [290] as discussed above for Co complexes. The catalytic activity was measured by

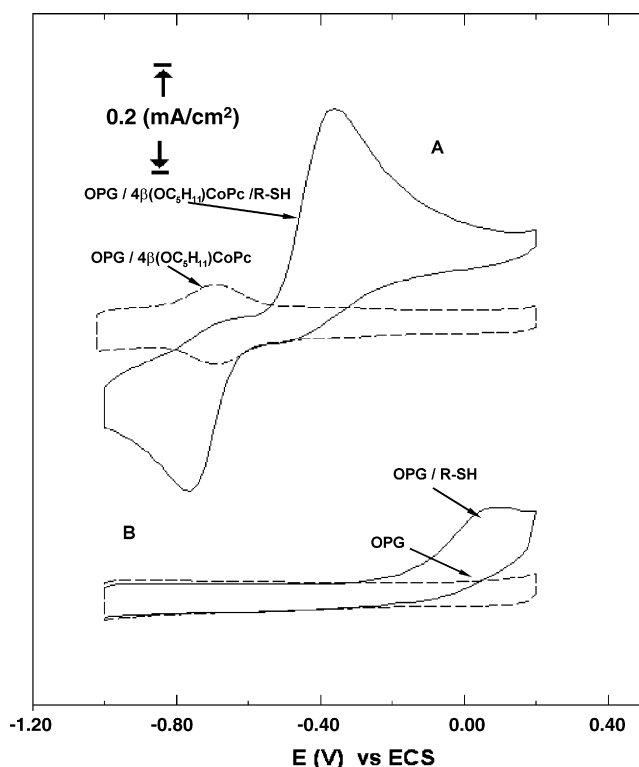


Fig. 5. Typical cyclic voltammogram of the response of an OPG/4 β (OC₈H₁₇)CoPc electrode recorded in a 0.1 M NaOH deaerated solution containing 0.001 M 2-mercaptoethanol. The response of the unmodified OPG is also shown. Scan rate: 0.1 V/s.

Taken from ref. [339].

the difference in peak potentials between the oxidation peak of the RSH and the reduction peak of the product (RSSR). That is, the lower the potential peak separation of the RSH/RSSR couple, the higher the catalytic activity. Based on this observation, the catalytic activities of the complexes increase as follows: 8 β (OCH₃)FePc > FePc > 4 β (COOH)FePc > 4 β (SO₃⁻)FePc > 16(F)FePc [290]. Similarly, 8 β (OC₈H₁₇)CoPc monomer adsorbed onto graphite electrodes shows a higher catalytic activity towards oxidation of 2-ME than adsorbed 4 β (SO₃⁻)CoPc or CoPc due to the electron-donating ability of the ethylhexyloxy substituents in the former [333]. These differences in activities can be attributed to the different redox properties of the complexes, as it will be discussed further on.

Platinum group metal monophthalocyanines adsorbed on glassy carbon electrode catalyze the oxidation of L-cysteine depending on the nature of axial ligands [286]. When DMSO or cyanide were employed as axial ligands, catalytic activity was observed and ring-based redox processes were implicated in the catalytic process.

Oxidation of L-cysteine on MPc-SAMs formed from thiol substituted MPc complexes, was observed at lower potentials compared to the potential observed for its oxidation on unmodified CoPc [96,293,341,342]. The overpotentials for oxidation of homocysteine, L-cysteine and penicillamine are slightly lower on alkylthio substituted FePc complexes compared to the corresponding CoPc ones [108], however the latter was less susceptible to fouling [108]. Of a series of MPc-4-MPy-SAM (M=Fe, Mn, Co and 4-MPy=4-mercaptopyridine) used for catalytic oxidation of L-cysteine, FePc-4-MPy-SAM showed better catalytic activity [102].

The sensitivity and stability of poly-4 β (NH₂)CoPc were much higher than for adsorbed monomer for 2-ME oxidation [274] or to be similar to that of adsorbed 4 β (NH₂)CoPc (on vitreous carbon electrode) in terms of current and peak potential [335] for L-

cysteine and reduced glutathione showing that only a few external layers of the polymer are electroactive. Poly-4 β (NH₂)CoPc shows catalytic activity for both the oxidation of thiols and the reduction of the corresponding disulfides [274].

In addition to studies on adsorbed monomers, polymers and SAMs, other methods of electrode modifications for the detection of thiols have been explored. CoPc supported on poly(2-chloroaniline) was active for the electrooxidation of 2-ME, reduced glutathione and hydrazine [293]. The use of CoPc composite electrode resulted in the lowering of overpotential for glutathione oxidation by 0.75 V [343] compared to the unmodified carbon electrode. Also, MPc modified carbon paste electrodes have been employed by several authors for the analysis of thiols. Carbon paste electrodes incorporating OMo^V(OH)Pc catalyze the oxidation L-cysteine with a considerable reduction in overpotential [287], and it was proposed that the oxidation of L-cysteine is mediated by Mo^{VI}Pc species [287].

Very few metalloporphyrins have been investigated for the oxidation of thiols [292]. For example studies using electropolymerized aminophenyl and hydroxyphenyl cobalt porphyrins have shown some activity [292,344] but they are less active than phthalocyanines. These differences in behavior have been attributed to a different electrocatalytic mechanism and/or to differences in the polymer film conductivities. However, as it will be discussed further on, Co porphyrins exhibit Co(II)/(I) formal potentials which are much more negative than those of phthalocyanines, so the interaction of the sulfide ion with the Co(II) center to form a Co(I) adduct is less favorable with porphyrins.

3.2. General trends in reactivity of macrocyclics for the oxidation of thiols

It is very important in electrocatalysis to be able to make predictions about the eventual catalytic activity of an electrode. This is especially important if the active electrode contains a metal complex having a reactivity that can be controlled by its molecular and electronic structure. However the theory of electrocatalysis is still underdeveloped. Predictions of reactivities, with a few notable exceptions, have been thus far mainly based on correlative approaches. Along these lines, most of the work published has been focused on the electrocatalytic activity of pure metals, alloys or metal oxides for well known reactions such as hydrogen evolution, hydrogen oxidation, O₂ evolution or O₂ reduction which are the reactions occurring in H₂/O₂ fuel cells and water electrolyzers. Crucial parameters that correlate with catalytic activity are heats and free energies of adsorption of intermediates that account for the degree of interaction of the reacting molecule with the active sites located on the metal or metal oxide surface [345–361]. The adsorption phenomenon lowers activation energies for the processes. In relation to the electrocatalytic activity of electrodes modified with metallophthalocyanines or complexes in general there are no models available. However correlations can be found if the reactivity is compared versus some parameter that accounts for the reactivity of the active site which is the central metal. One useful parameter is the redox potential of the complex and can be easily determined by cyclic voltammetry, under the same conditions (pH, electrolyte composition, temperature) employed for the kinetic measurements. As shown recently, non-linear correlations are found between the redox potential of the metal complex and the catalytic activity, expressed as log *i* at constant potential or potential at constant current density. This is not only valid for the oxidation of thiols but also for many other reactions promoted by these MN4 complexes [14,27,321] as it will be discussed further down.

Tafel plots are very common in kinetic studies of electrode processes. They correlate currents or current densities (*i* or *I*) with electrode potentials (*E* versus a reference electrode potential) or

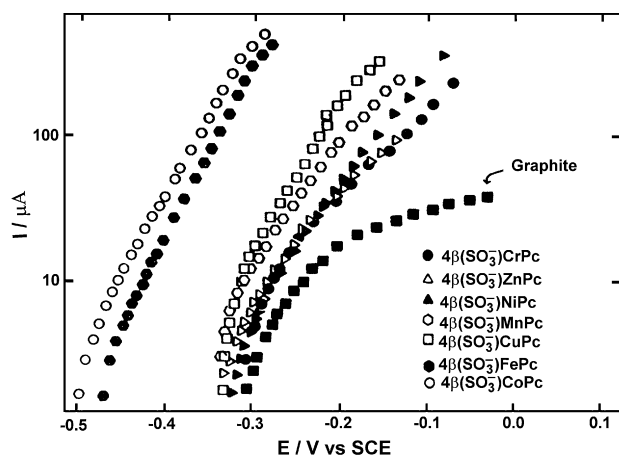


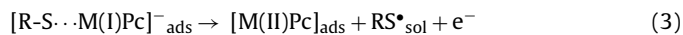
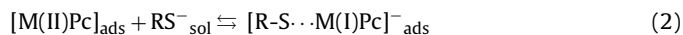
Fig. 6. Tafel plots for the oxidation of 2-ME on graphite modified with M-tetrasulfonated phthalocyanines. Response of graphite also shown. pH 10.1 Adapted from Fig. 11 in ref. [91].

overpotentials η . The overpotential $\eta = E - E_{\text{eq}}$ is a measure of the departure from the equilibrium E_{eq} . The current density is the current divided by the area of the electrode. The electrical current flowing through the electrode is proportional to the reaction rate, and the electrode potential is proportional to the driving force. The rate of an electrochemical reaction increases exponentially with the electrode potential. For a chemical reaction the driving force is ΔG° , the standard free energy of the reaction. For an electrochemical reaction, the driving force of the reaction can be modified by the electrode potential, since $\Delta G = -nFE$ where E is the potential of the cell. For a reduction reaction the driving force can be increased by applying a negative potential. The opposite is true for an oxidation. The Tafel equation is: $\log i = \log i_0 + \eta/b$ where i is the current density, i_0 is the exchange current density, b is the Tafel slope and η is the overpotential. $\eta = E - E_{\text{eq}}$ where E is the potential and E_{eq} is the equilibrium potential of the reaction versus a reference electrode (given by the Nernst equation).

A Tafel plot is a graph of $\log i$ versus E , and according to the equation it should be linear, with a slope of $1/b$. So essentially a Tafel plot is a plot of $\log(\text{reaction rate})$ versus driving force. A bit far from equilibrium these plots are linear and the Tafel slope $\delta E / \delta \log i$ provides information about the rate determining step. A common slope is 0.118 V/decade indicating that the reaction rate is increased 10 times if the potential applied to the electrode is increased by 0.118 V, for an oxidation process. A Tafel slope close to 0.118 V/decade is indicative that the first one-electron transfer is rate determining. A Tafel slope close to 0.059 V/decade indicates that the first fast electron transfer is followed by a slow chemical step. A Tafel slope close to 0.040 V indicates that the first fast electron transfer is followed by a slow electron transfer step. For catalytic processes the smaller the Tafel slope the better since it indicates the magnitude of applied potential required to increase the rate 10 times, the lower the energy required to push the reaction. The Tafel equation is an empiric equation and a more rigorous correlation between the current and the potential is given by the Butler–Volmer equation and the interested reader can consult several text books available in electrochemistry.

Fig. 6 illustrates a series of Tafel plots obtained with pyrolytic graphite modified with tetrasulfonated phthalocyanines of Cr, Mn, Co, Fe, Ni, Cu and Zn for the oxidation of 2-mercaptoethanol. The response of the bare graphite is also shown. The slopes of the lines range from 0.10 to 0.120 V/decade suggesting that the first one-electron transfer step is rate determining, for the oxidation of 2-ME with all catalysts. The most active one is $4\beta(\text{SO}_3^-)\text{CoPc}$ as the Tafel lines appear at lower potentials. The least active is bare graphite,

since the Tafel lines (which are linear only at low potentials) appear at the more positive potentials. Plots similar to those in **Fig. 6** are obtained with other phthalocyanines and also for the oxidation of other thiols, so it can be proposed that the rate determining step for the oxidation of thiol is step (3) in the mechanism depicted below. The oxidation of thiols in alkaline media most likely involves the formation of a bond between the metal center in the complex and the sulfur atom in the thiolate. The complete reaction scheme is:



where “sol” and “ads” stand for species in solution or adsorbed on the electrode, respectively. Step 4 is fast and irreversible. A crucial step is step 2, which involves the formation of a Co–S bond, with a partial reduction of the metal center in the catalyst and partial oxidation of the bound thiol molecule.

As pointed out above, the redox potential can be used as a parameter of reactivity as reduction of the metal center is involved in step 2. Two approaches can be used to modify and modulate the redox potential of the complexes: (a) by changing the metal but keeping the same phthalocyanine ligand or (b) keeping the metal but changing the ligand by using different substituted phthalocyanines.

By using approach (a) **Fig. 7** compares the reactivity of two families of MPC for the oxidation of 2-ME, namely unsubstituted and tetrasulfonated phthalocyanines [331,333,334]. The activity as $\log i$ (current density) at constant potential has been plotted versus the redox potential of the first reduction process of the catalyst (called “formal redox potential of the catalyst”). This redox potential might involve the M(II)/(I) couple for Cr, Mn, Co and Fe but might involve the ligand for Ni and Cu. Since these redox potentials are obtained from the potential of voltammetric peaks at which the surface concentration of oxidized species is equal to the surface concentrations of reduced species, these potentials are then formal potentials “ E° ”. In **Fig. 7** a linear correlation is observed for both families of phthalocyanines and the activity increases as the redox potential becomes more positive. One would expect this on thermodynamic grounds if the formal potential of the catalyst represents part of the driving force of the reaction (apart from the electrode potential, which in this case has been kept constant). However, activity should also increase if the affinity of the central metal for the thiol increases, i.e. as the M–Co energy bond increases. In the data shown in **Fig. 7** the effect of the ligand depends on the nature of the central metal. When comparing CrPc with $4\beta(\text{SO}_3^-)\text{CrPc}$, CrPc is more active than $4\beta(\text{SO}_3^-)\text{CrPc}$. In contrast $4\beta(\text{SO}_3^-)\text{CuPc}$ is more active than CuPc but in both cases no deviations are observed from the linear correlation, so the redox potential is a good reactivity index for these complexes no matter what central metal or what ligand is considered.

An interesting feature in the correlations of **Fig. 7** is that the slopes for both families of phthalocyanines are different. For unsubstituted MPCs, the slope is 0.070 V/decade whereas for $4\beta(\text{SO}_3^-)\text{MPCs}$ the slope is 0.14 V/decade. These slopes are not Tafel slopes since the data were obtained at constant potential (constant driving force of the electrode) and the driving force was varied by changing the redox potential of the catalyst but essentially, they have a similar meaning to Tafel slopes, since these slopes are $(\delta E^\circ / \delta \log i)_E$, where E° is the formal potential of the catalyst instead of $(\delta E / \delta \log i)_{E^\circ}$, the Tafel slopes obtained for a given catalyst (constant E°). On the other hand, Tafel slopes obtained from plots of $\log i$ versus potential for all catalysts included in **Fig. 6** are less than 0.118 V/decade [91,333], and depend on the particular

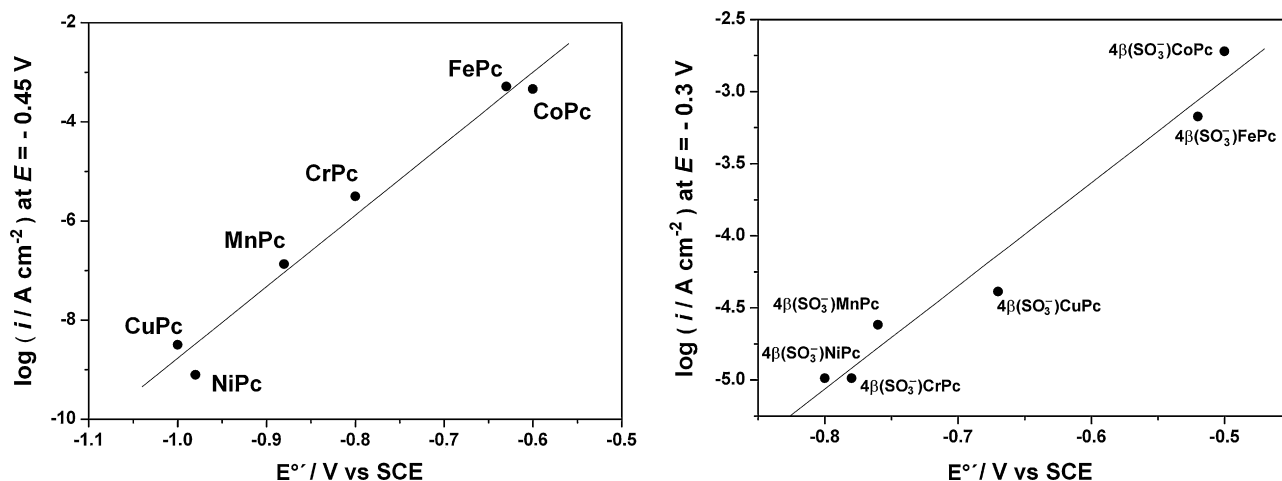


Fig. 7. (Left) Plots of $\log i$ (current density in A cm^{-2}) at constant potential versus the redox potential of MPcs and $4\beta(\text{SO}_3^-)\text{MPc}$ s for the oxidation of 2-ME in 0.2 M NaOH. Data obtained from mass transport corrected Tafel plots at -0.45 V. Data for $4\beta(\text{SO}_3^-)\text{MPc}$ taken from Fig. 6. (Right) Plot of $\log i$ (current density in A cm^{-2}) at constant potential versus the Co(II)/(I) formal potential of different CoPcs confined on an OPG electrode for the oxidation of 2-aminoethanethiol in 0.2 M NaOH. Data obtained for mass transport corrected Tafel plots at -0.20 and at -0.35 V versus SCE. Adapted from ref. [92].

Table 3

Tafel slopes for the oxidation of 2-mercaptoethanol on different MPcs at 25°C , pH 12.8.

Catalyst	Slope in V/decade	$RT/(1-\beta)F$	β
NiPc	0.150	$2.54RT/F$	0.61
CuPc	0.136	$2.30RT/F$	0.57
MnPc	0.127	$2.15RT/F$	0.53
CrPc	0.099	$1.68RT/F$	0.40
CoPc	0.127	$2.15RT/F$	0.53
FePc	0.113	$1.91RT/F$	0.48

catalyst. As seen from the data in Tables 3 and 4, the slopes tend to be lower for the most active catalysts, so the symmetry factor β varies between 0.28 and 0.65. The Tafel slope is $2.3RT/\beta F$ and for a symmetrical energy barrier $\beta = 0.5$ and the slope is 0.118 V/decade, that indicates that the first electron transfer is rate determining.

Slopes close to 0.118 V are also observed for the oxidation of other thiols like L-cysteine catalyzed by several metallophthalocyanines [95], the oxidation of mercaptoacetate [340] and aminoethanethiol [338]. The values of the Tafel slopes have been used to justify that the transfer of one electron in step 3 is rate controlling in alkaline media. The linear dependence of $\log i$ on the redox potential in Fig. 7 indicates that the free energy of adsorption of the thiol on the active sites is proportional to the redox potential of the catalyst. If this is true, the slope would be $\beta' \Delta G_{\text{ads}}$ where ΔG_{ads} would account for the thermodynamics of step 2. Note that β' is a Brönsted coefficient not necessarily equal to the transfer coefficient β , linked to the r.d.s. 3. This is generally observed for correlations of this type when comparing the electrocatalytic activity of metals [344–353]. Similar correlations to those in Fig. 7 are found for the oxidation of L-cysteine

Table 4

Tafel slopes for the oxidation of 2-mercaptoethanol on different $4\beta(\text{SO}_3^-)\text{MPc}$ s at 25°C , pH 10.1.

Catalyst	Slope (V/decade)	$RT/(1-\beta)F$	β
$4\beta(\text{SO}_3^-)\text{CrPc}$	0.167	$2.83RT/F$	0.65
$4\beta(\text{SO}_3^-)\text{NiPc}$	0.120	$2.03RT/F$	0.51
$4\beta(\text{SO}_3^-)\text{MnPc}$	0.114	$1.93RT/F$	0.48
$4\beta(\text{SO}_3^-)\text{CuPc}$	0.0958	$1.62RT/F$	0.38
$4\beta(\text{SO}_3^-)\text{MePc}$	0.082	$1.39RT/F$	0.28
$4\beta(\text{SO}_3^-)\text{CoPc}$	0.093	$1.58RT/F$	0.37

Taken from ref. [91].

on MPcs and $4\beta(\text{SO}_3^-)\text{MPcs}$ with similar slopes [331,333,334], so these correlations seem to be independent of the nature of the thiol. However, only Mn, Fe and Co and probably Cr exhibit redox processes located on the metal, namely the M(II)/M(I) process while for Ni and Cu the redox potential plotted in Fig. 7 involves the ligand. Thus, when different central metals are compared, different frontier orbitals in the metal could be involved for each particular case, when adsorption of RS^- takes place. For example for complexes having central metals like Fe and Co, which have a frontier orbital with more d character, one would expect a stronger interaction of the metal with the thiol than, for example, Cu.

Since the redox potential (formal potential) of the catalyst is a good reactivity index for predicting the catalytic activity of these complexes, it is interesting to compare the activity of complexes using approach (b), i.e. by keeping the same metal center but modulating the redox potential by placing different substituents (electron-withdrawing or electron-donating groups) on the phthalocyanine ligand. Fig. 8 compares the catalytic activity of different iron phthalocyanines versus the Fe(II)/Fe(I) formal potential for the oxidation of 2-ME [290]. In contrast to what is observed for phthalocyanines of different metals, the activity decreases as the formal potential of the catalyst becomes more positive and the

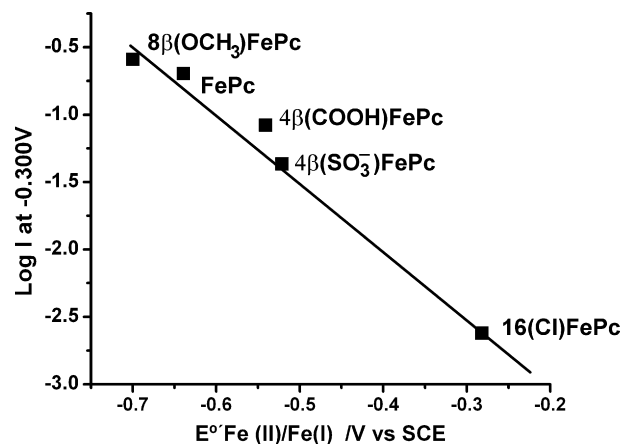


Fig. 8. Plot of $\log I$ at constant E , versus $E^\circ \text{Fe(II)/Fe(I)}$ for the oxidation of 2-ME at pH 10 on OPG modified with different FePcs. Adapted from ref. [290].

Table 5
Variation of the slope (in V/decade) of plots of $\log i$ versus E° for the oxidations of several thiols in basic media (pH 13) catalyzed by Co phthalocyanines confined on graphite.

Electrode potential (V versus SCE)	2-Aminoethanethiol	2-Mercaptosulfonic acid	L-Cysteine	2-Mercaptoethanol
–0.450				–0.234
–0.400				–0.267
–0.350	–0.180			–0.283
–0.300	–0.220			–0.273
–0.250	–0.261			
–0.200	–0.286	–0.225	–0.220	–0.300
–0.150		–0.250	–0.218	
–0.100		–0.257	–0.224	
–0.050		–0.240	–0.220	

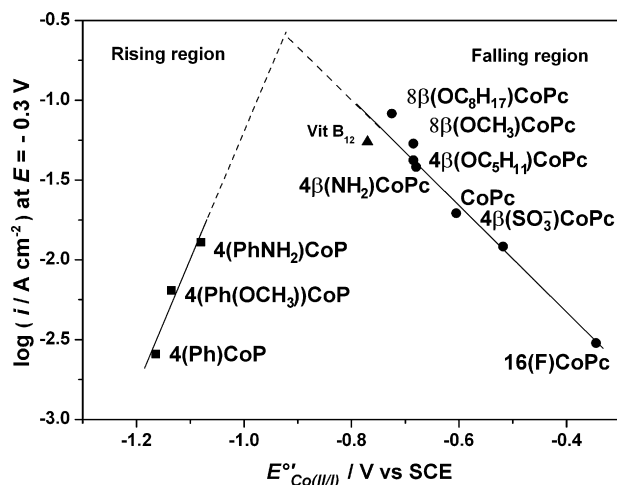


Fig. 9. Volcano plot for the oxidation of 2-ME in 0.1 M NaOH, on OPG modified with different cobalt N4 macrocycles. Data obtained from Tafel plots at $E = -0.30$ V versus SCE (currents in A cm^{-2} corrected for mass transport). Adapted from ref. [92].

slope ($\delta E^\circ / \delta \log i$)_E is -0.205 V/decade (-3.47RT/F) for $E = -0.30$ V versus SCE and -0.370 V/decade (-6.27RT/F) for $E = -0.25$ V versus SCE. Similar results were reported for the oxidation 2-ME [333] and for the oxidation of aminoethanethiol [338] on different Co phthalocyanines. For cobalt substituted phthalocyanines, the slopes of the plots of $\log i$ versus redox potential are also negative and potential-dependent for the oxidation of several thiols, as illustrated in Table 5.

In order to explore a wider range of Co(II)/Co(I) redox potentials, cobalt porphyrins together with cobalt phthalocyanines and vitamin B₁₂ (aquocobalamine) were investigated and the results are included in Fig. 9 for the oxidation of 2-ME. In this case a volcano-shaped curve is obtained, with a region where the activity increases with the formal potential of the catalyst and another region where the activity decreases. The slope, ($\delta E^\circ / \delta \log i$)_E of the rising portion of the volcano is 0.110 V/decade or 1.86RT/F and the falling portion has a reciprocal slope of -0.245 V/decade or -4.15RT/F . The slope of the rising portion of the volcano is similar to the Tafel slopes obtained from Tafel plots for single catalysts (see Fig. 6). Similar results are obtained for the oxidation of 2-ME when glassy carbon is used instead of pyrolytic graphite [295] (see Tables 6 and 7), which shows that the cor-

Table 6
Tafel slopes for the oxidation of mercaptoacetate for catalysts on the rising side of the volcano plot of Fig. 10.

Catalyst	Tafel slope	Tafel slope
20(F)PhCoP	0.092	1.56RT/F
4(PhSO ₃ [−])CoP	0.103	1.74RT/F
4(PhNH ₂)CoP	0.093	1.58RT/F

Table 7
Tafel slopes for the oxidation of mercaptoacetate for catalysts on the falling side of the volcano plot of Fig. 10.

Catalyst	Tafel slope (V/decade)	Tafel slope
Vitamin B ₁₂	0.091	1.54RT/F
8β(OC ₈ H ₁₇)CoPc	0.079	1.34RT/F
4β(OC ₅ H ₁₁)CoPc	0.077	1.31RT/F
8β(OC ₃ H ₇)MPc	0.078	1.32RT/F
CoPc	0.094	1.59RT/F
4β(SO ₃ [−])CoPc	0.075	1.27RT/F
16(F)CoPc	0.085	1.44RT/F
4β(NH ₂)CoPc	0.095	1.61RT/F

relations do not depend on the substrate used for confining the complexes.

A volcano-shaped correlation is also obtained for the oxidation of 2-mercaptoacetate and the data are illustrated in Fig. 10. The volcano correlation includes again several types of macrocyclic complexes, i.e. Co porphyrins, Co phthalocyanines and cyanocobalamin (vitamin B₁₂). As observed for the oxidation of 2-ME a linear region of positive slope (0.112 V/decade) is observed and then a region where activity decreases with the formal potential of the catalysts with a slope equal to -0.171 V/decade.

It is well-known in heterogeneous catalysis and electrocatalysis [345–361] that a volcano-shape curve is obtained when the activity of the catalyst (logarithm of current density) for a given reaction is plotted versus a parameter related to the ability of the catalyst to form chemical bonds with reactants, reaction intermediates or products [298,350–360]. So in some cases that we have discussed before, where linear correlations are obtained, these are probable

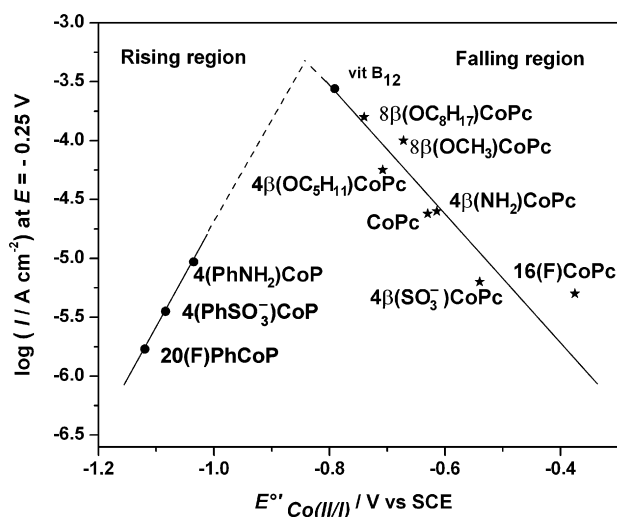


Fig. 10. Volcano plot for the oxidation of 2-mercaptoacetate in 0.1 M NaOH, on OPG modified with different cobalt N4 macrocycles. Data obtained from Tafel plots at $E = -0.250$ V versus SCE (currents in A cm^{-2} corrected for mass transport). Adapted from ref. [92].

“incomplete” volcano correlations. These relations are very important as they serve as guidelines in the search of new catalysts for any given reaction. It is important for these correlations to be valid that the rate determining step of the reaction is the same for all catalysts, and this is the case for the data reported in Figs. 9 and 10. Heats of adsorptions of the molecules on different catalysts or bond energies between active site and the adsorbed molecule are generally used in volcano plots [345]. In the case of the data in Figs. 9 and 10, the redox potential is used since heats and free energies of adsorption of thiols on the different metal N_4 -macrocycles, to best of our knowledge, are not available in the literature. However the formal potential is related to the reactivity of the metal center towards the thiol through adduct formation and to the thermodynamics of this process (step 2). Thus, the data in the volcano plots can be explained according the above written mechanism (the thiolate is used since all data were obtained in alkaline media (pH in the range 10–13). Since the active sites (the metal center in the phthalocyanine) are well separated from the neighboring phthalocyanine molecule, it is expected that the free energy of adsorption of thiolate molecules on the metal centers is independent of coverage. Then it seems suitable to use a Langmuir isotherm [345,362,363] for the adsorption of thiolate molecules on the metal centers as follows:

$$\frac{\theta}{1-\theta} = aRS_{sol}^{-} \exp \frac{-\Delta G_{RS^{-}}}{RT} \quad (5)$$

where θ is the coverage of thiolate RS^{-} and $\Delta G_{RS^{-}}$ is the free energy of adsorption of RS^{-} (as $[R-S \cdots M(1)Pc]$ in Eq. (2) relative to aRS_{sol}^{-} , the solution activity of the thiolate. $\Delta G_{RS^{-}}$ is essentially the free energy of step 2. Solving for θ , one obtains:

$$\theta = \frac{aRS_{sol}^{-} \exp(-\Delta G_{RS^{-}}/RT)}{[1 + aRS_{sol}^{-} \exp(-\Delta G_{RS^{-}}/RT)]} \quad (6)$$

$-\Delta G_{RS^{-}}$ could depend on electrode potential since the process involves a charged species and could also depend on coverage. If one assumes that the electrochemical r.d.s. has a rate constant of $k = C \exp + (1-\beta)EF/RT$ at $\theta = (1-\theta) = 0.5$ (where E is the potential on some nominal scale and C is a constant). Assuming that the barrier height is changed by $+\beta' \Delta G_{RS^{-}}$ in the presence of adsorption keeping in mind that adsorption acts on the initial state (step 2) whereas E affects step 3 which involves the transfer of one electron. Note that β' is a Brönsted coefficient (not necessarily identical with β) which is the symmetry factor related to the symmetry of the energy barrier for electron transfer step 3. As seen from the bottom of the energy well for $RS_{(ads)}^{-}$, the barrier height changes by $-(1-\beta')\Delta G_{RS^{-}}$ in the presence of adsorption, compared with its standard state value at $\theta = 0.5$. The rate of the r.d.s. is therefore:

$$v = \theta C \exp + \left[\frac{(1-\beta') \Delta G_{RS^{-}}}{RT} \right] \exp + \left[\frac{(1-\beta)EF}{RT} \right] \quad (7)$$

$$v = aRS_{sol}^{-} C \exp - \left[\frac{\beta' \Delta G_{RS^{-}}}{RT} \right] \exp + \frac{[(1-\beta)EF/RT]}{[1 + aRS_{sol}^{-} \exp(-\Delta G_{RS^{-}}/RT)]} \quad (8)$$

At low θ coverages, $aRS_{sol}^{-} \exp(-\Delta G_{RS^{-}}/RT) \ll 1$, this corresponds to the rising side of the volcano and the rate is:

$$v = aRS_{sol}^{-} C \exp - \left[\frac{\beta' \Delta G_{RS^{-}}}{RT} \right] \exp + \left[\frac{(1-\beta)EF}{RT} \right] \quad (9)$$

The first exponential term of the equation depends on the thermodynamics of step 2 and the second term depends on the potential and it is constant in a volcano plot since the rates are compared at fixed potential E . So the rate can be rewritten as:

$$v = aRS_{sol}^{-} C' \exp - \left[\frac{\beta' \Delta G_{RS^{-}}}{RT} \right] \quad (10)$$

The hypothetical slope $(\delta E^{\circ}/\delta \log i)_E$ of the rising side of the volcano is then $RT/F\beta'$, and if the energy barrier is symmetrical $\beta' = 0.5$ the slope is $2RT/F$ or 0.118 V/decade. Experimental values are close to this figure.

For the falling side of the volcano, θ is high and $aRS_{sol}^{-} \exp(-\beta' \Delta G_{RS^{-}}/RT) \gg 1$. The rate is then:

$$v = C \exp + \left[\frac{(1-\beta') \Delta G_{RS^{-}}}{RT} \right] \exp + \left[\frac{(1-\beta)EF}{RT} \right] \quad (11)$$

Again, the second exponential term is constant since E is constant. Under high coverage conditions the rate becomes zero order in RS^{-} so the rate in the falling side of the volcano is:

$$v = C' \exp + \left[\frac{1 - \beta' \Delta G_{RS^{-}}}{RT} \right] \quad (12)$$

and the slope of the declining portion of the volcano would be $-2RT/F$. Experimental values are larger (absolute value) than -0.118 V/decade.

From this simplified analysis, catalysts on the rising and falling side of the volcano should have the same Tafel slope, provided that $\Delta G_{RS^{-}}$ does not depend on the electrode potential (a mathematical treatment for the case where $\Delta G_{RS^{-}}$ depends on the potential as been given elsewhere [92] and it is too long to describe here).

The numerical deduction given above predicts that β' should have the same value for both branches, but Figs. 9 and 10 show that this is not the case. However, the rising branch (weak adsorption, positive ΔG , low θ) may have very differently shaped energy wells than those for the falling branch (strong adsorption, negative ΔG , high θ), so the change in β' with coverage may not be surprising. In all cases, the rising branch of the volcanoes shows slopes almost one-half of those corresponding to the falling branch [295].

It can be concluded that (i) β (the symmetry factor for the electrochemical step) seems to depend on the nature of the catalyst which indicates that the shape of the energy wells might vary to some degree for each catalyst (as seen for the variation of Tafel slopes), (ii) variations in the slopes on both sides of the volcanos or incomplete volcanos might also reflect changes in the shape of energy wells with adsorption and (iii) the rising portion of the volcano corresponds to low coverages and a maximum activity should be achieved at $\theta = 0.5$.

In general, the slopes observed experimentally are close to, but less than $2RT/F$ (0.118 V/decade) and indicate that the formal potential of the catalyst is directly proportional to $\Delta G_{RS^{-}}$ as:

$$\Delta G_{RS^{-}} \approx -nEF^{\circ'} + C'' \quad (13)$$

So replacing $\Delta G_{RS^{-}}$ in Eq. (10) gives for the rising portion of the volcano:

$$v \approx aRS_{sol}^{-} C''' \exp + \left[\frac{\beta' n EF^{\circ'}}{RT} \right] \text{ assuming } n = 1 \quad (14)$$

and C''' contains all terms in the exponential that are constant. So a plot of $\log i$, which is proportional to $\log v$, versus $E^{\circ'}$ would have a reciprocal slope of $+2.303RT/F\beta'$ (assuming $n=1$) or $+0.118$ V/decade, for β' values ca. 0.5. This slope is similar to a Tafel slope of $+2.303RT/F\beta'$ that is obtained for kinetic measurements with a single catalyst ($E^{\circ'}$ constant) from plots of $\log i$ versus E . So the rising side of a volcano essentially represents a plot of $\log v$ (or $\log i$) versus driving force of the catalyst ($E^{\circ'}$) at constant E whereas a Tafel plot represents a plot of $\log v$ (or $\log i$) for a given catalyst versus driving force of the electrode (E) at constant $E^{\circ'}$.

Replacing $\Delta G_{RS^{-}}$ in Eq. (12), for the falling side of the volcano we have:

$$v = C''' \exp - \left[\frac{(1-\beta')nEF^{\circ'}}{RT} \right] \quad (15)$$

so the slope $(\delta E^\circ / \delta \log i)_E$ in the falling side of a volcano of $\log i$ versus E° would be $2.303RT/F(1 - \beta')$ or ca. -0.118 V/decade for $\beta' = 0.5$. Thus, increasing the formal potential increases the reactivity of the metal center in the macrocycle towards the thiol. However, increasing the formal potential beyond a certain value becomes detrimental since this stabilizes the adduct (shifting the equilibrium of step 2 to the right), blocking the active sites. This can explain the declining portion of the volcano plots, that includes most of the catalysts studied. $\Delta G^\circ_{\text{ads}}$ is >0 for the ascending portion of the volcano (low coverages $\theta \ll 1$). The maximum activity should be achieved when $\Delta G_{\text{ads}} = 0$ [345] and $\theta = 0.5$ (equilibrium constant equal to 1 for step 1 under standard conditions). Then currents decrease for values of $\Delta G_{\text{ads}} < 0$ which correspond to the high coverage region ($\theta \sim 1$). However an explanation is still needed for the slopes near $-4RT/F$ in the declining portion of the volcano, i.e. for the unsymmetry of the experimental volcano correlations. They might reflect a different shape of the energy well for high coverages which will affect the values of β' .

The data in Figs. 9 and 10 clearly show that MN_4 -macrocylic complexes with formal potentials corresponding to an optimum situation for the interaction of the thiol with the active sites will have the highest activity. This corresponds to the Sabatier principle in heterogeneous catalysis that an interaction of the reacting molecule with the active sites needs to be not too weak, not too strong for optimum catalytic activity [345–360]. For the oxidation of 2-mercaptoethanol the highest activity is observed for $E^\circ = -0.93$ V versus SCE for catalysts adsorbed on graphite and at $E^\circ = -0.95$ V versus SCE for catalysts adsorbed on glassy carbon [295] whereas for 2-mercaptoacetate oxidation maximum activity is achieved for $E^\circ = -0.85$ V versus SCE. For the oxidation of aminoethanethiol, maximum activity is observed for $E^\circ = -1.02$ V and for cysteine $E^\circ = -1.01$ V [344]. A plot of the pK_a of the thiol versus E° max gives a linear correlation, indicating once again that the maximum in the volcano is related to the reactivity of the sulfur in the thiol [344]. So the optimum formal potential depends on the nature of the thiol.

4. Catalytic properties of MPc in electrochemical reduction of molecular oxygen

Amongst the non-noble metals candidates, phthalocyanines have appeared as promising catalysts to replace platinum in fuel cells. Unfortunately, the stability of metallo phthalocyanines in a fuel cell environment is tempered by the formation of oxygen-based radical intermediates that can attack the ligand during the O_2 reduction process, with the generation of species that present much lower catalytic activity than the original phthalocyanine. In this section we will discuss the catalytic properties of metallophthalocyanines for the electrochemical reduction of molecular oxygen in aqueous media. The different factors that affect their catalytic activity will be discussed such as the nature of the central metal, the

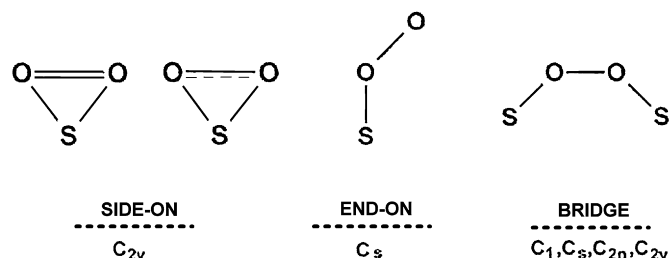
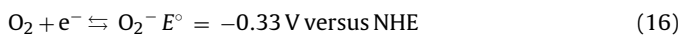


Fig. 11. Possible configurations for molecular oxygen for its interaction with active sites on the electrode surface.

nature of the ligand and the effect of substituents on the phthalocyanine ring. Catalytic activity of different metallomacrocyclics will be discussed in terms of the different reduction pathways of O_2 that they promote, i.e. two versus four electron reduction pathways.

4.1. Reaction pathways for the reduction of molecular oxygen

The electrochemical reduction of oxygen in aqueous media is a complex multielectron process that occurs via two main pathways: one involving the transfer of two electrons, to give hydrogen peroxide and the direct four-electron pathway to give water. The latter involves the rupture of the O–O bond and releases the most energy. The nature of the electrode strongly influences the preferred pathway. Most electrode materials catalyze the reaction only via two electrons to give hydrogen peroxide. The several possible pathways are given in Table 8. In strongly alkaline solutions or in organic solvents, O_2 is reduced via the transfer of a single electron to give superoxide ion



As mentioned above, in order to obtain the maximum free energy or the highest oxidant capacity of O_2 when this molecule reacts on the cathode of a fuel-cell, O_2 needs to be reduced via four electrons. Most common electrode materials only promote the two-electron pathway, which releases almost one half the free energy compared to that of the four-electron pathway. This can be attributed in part to the high dissociation energy of the O–O bond (118 kcal/mol). Fig. 11 illustrates the possible orientations that O_2 can adopt when it interacts with an active site. The four-electron reduction of dioxygen to give water involves the rupture of the O–O bond and requires the interaction of dioxygen with one site (single site, side-on, see Fig. 11) or with two active sites simultaneously (dual site, bridge, see Fig. 11) on the electrode surface. When dioxygen interacts or binds to a site, as depicted in Fig. 11, the energy of the O–O bond decreases, favoring the rupture of the bond since electrons accepted by the oxygen molecule will occupy antibonding π^* orbitals. On platinum, O_2 reduction occurs almost entirely via four electrons [361]. A “bridge cis” type of interaction is favor-

Table 8
Possible pathways for the oxygen reduction in aqueous media.

Mode of interaction	Oxygen reduction pathways	
	Acidic medium	Basic medium
Bridge (or) Trans	$\text{O}_2 + 2\text{H}^+ + 2e^- \rightarrow 2\text{OH}_{\text{ads}}$ $2\text{OH}_{\text{ads}} + 2\text{H}^+ + 2e^- \rightarrow 2\text{H}_2\text{O}$ Overall direct reaction: $\text{O}_2 + 4\text{H}^+ + 4e^- \rightarrow 2\text{H}_2\text{O}; E^\circ = 1.23 \text{ V versus NHE}$	$\text{O}_2 + 2\text{H}_2\text{O} + 2e^- \rightarrow 2\text{OH}_{\text{ads}} + 2\text{OH}^-$ $2\text{OH}_{\text{ads}} + 2e^- \rightarrow 2\text{OH}^-$ Overall direct reaction: $\text{O}_2 + 2\text{H}_2\text{O} + 4e^- \rightarrow 4\text{OH}^-; E^\circ = 0.401 \text{ V versus NHE}$
End-on	$\text{O}_2 + \text{H}^+ + e^- \rightarrow \text{HO}_{2,\text{ads}}$ $\text{HO}_{2,\text{ads}} + \text{H}^+ + e^- \rightarrow \text{H}_2\text{O}$ Overall indirect reaction: $\text{O}_2 + 2\text{H}^+ + 2e^- \rightarrow \text{H}_2\text{O}_2; E^\circ = 0.682 \text{ V versus NHE}$ with $\text{H}_2\text{O}_2 + 2\text{H}^+ + 2e^- \rightarrow 2\text{H}_2\text{O}; E^\circ = 1.77 \text{ V versus NHE}$	$\text{O}_2 + \text{H}_2\text{O} + e^- \rightarrow \text{HO}_{2,\text{ads}} + \text{OH}^-$ $\text{HO}_{2,\text{ads}} + e^- \rightarrow \text{HO}_2^-$ Overall indirect reaction: $\text{O}_2 + \text{H}_2\text{O} + 2e^- \rightarrow \text{HO}_2^- + \text{OH}^-; E^\circ = -0.076 \text{ V versus NHE}$ with $\text{HO}_2^- + \text{H}_2\text{O} + 2e^- \rightarrow 3\text{OH}^-; E^\circ = 0.88 \text{ V versus NHE}$

able on Pt, as illustrated in Fig. 11, which involves two metal sites since the Pt–Pt separation in certain crystallographic orientations is optimal for this type of interaction. It is very important then to develop low cost catalysts that decrease the overpotential of the reduction of oxygen and that can also promote the four-electron reduction.

Several reviews have appeared in the literature dealing with the electrocatalytic activity of MN4 complexes for the reduction of dioxygen [12–14,16–19,23–25,364,365]. MN4 complexes are also interesting because they provide models where active centers can be identified and their catalytic activity can also be modulated by changing the structure of the macrocyclic ligand or by changing the central metal as discussed above for the oxidation of thiols. Fe and Mn phthalocyanines, at low overpotentials promote the four-electron reduction with rupture of the O–O bond [14,16,18,361,366], without the formation of hydrogen peroxide. In contrast Co, Ni and Cu phthalocyanines promote the reduction of O₂ only via two-electron to give hydrogen peroxide [16,366] as the main product. Polymerized Co tetraamino phthalocyanines promote the four-electron [367,368] reduction whereas polymerized Fe tetraaminophthalocyanines only promote the two-electron reduction [310] in contrast to their monomeric counterparts. The catalytic activity of metal macrocyclics is correlated to the M(III)/M(II) redox potential of the complexes, the more positive the redox potential, the higher the activity. This trend is the opposite to what is expected from a simple redox catalysis mechanism, which is generally observed for the reduction of O₂ catalyzed by immobilized enzymes.

Most studies have been performed with the metal chelates confined on an electrode surface, generally graphite or carbon supports. Heat treatment in an inert atmosphere increases both the stability and catalytic activity [369–374]. Since the support can act as an axial ligand, the properties of the complexes in solution or on the adsorbed state could be different. So most studies discussed here have been carried out with the complexes immobilized on graphite or carbon supports. Smooth electrodes have been used to study mechanistic aspects of the reaction.

4.2. Interaction of O₂ with active sites and the redox mechanism

O₂ reduction involving more than one electron is an inner sphere reaction and involves an interaction of dioxygen with an active site as depicted in Fig. 11. The outer-sphere reduction of dioxygen involves the transfer of one single electron to give superoxide and probably occurs at the outer Helmholtz plane. The kinetics of this outer-sphere reaction are independent of the nature of the catalyst and do not involve an interaction of dioxygen with the electrode surface. Since we are interested in studying the electrocatalysis of the reaction we will focus our discussion on the inner sphere reduction mechanisms.

The interaction of molecular oxygen with the MN4 catalyst involves binding to the d-orbitals of the central metal in the macrocyclic structure and will be influenced by the electronic density located on those orbitals. Two different possible interactions, end-on and side-on, of the orbitals of the dioxygen molecule with the orbitals of the metal in the MN4 molecule occur, as illustrated in Fig. 11. For end-on M–O₂ complexes, the major interaction for both σ and π bonding occurs with the π^* antibonding orbitals of the O₂. The σ interaction is essentially between the metal 3d_{z²} and the in plane antibonding π_g^s orbital of dioxygen, where the superscript refers to whether or not the orbital is symmetric “s” (or antisymmetric “a”) with respect to the MO₂ plane. This can be viewed as an electron transfer from the metal ion to O₂. The π interaction involves essentially the metal 3d_{yz} and the 1 π_g^a (π antibonding antisymmetric orbital) on the O₂ and can be visualized as a back-bonding interaction. In both interactions the π_u^s and π_u^a (bonding

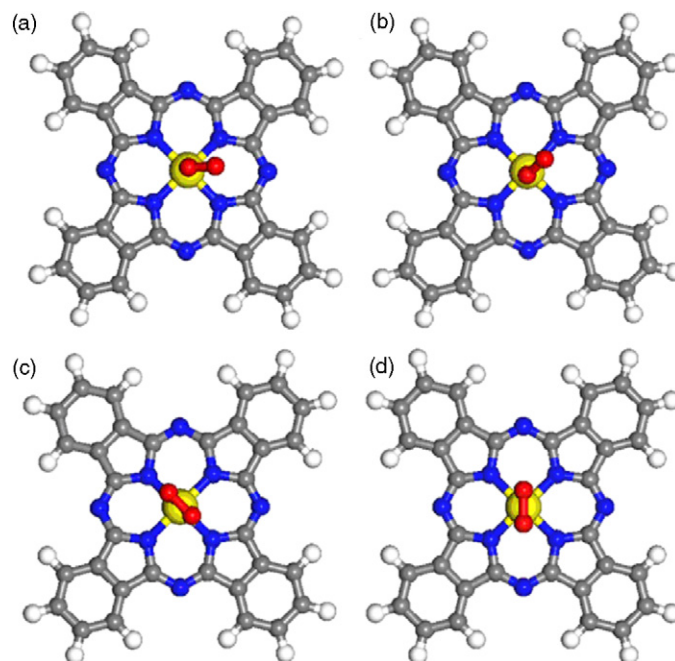


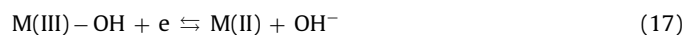
Fig. 12. Optimized structural configurations for the O₂ adsorbed on FePc and CoPc molecules. Parts (a) and (b) are two end-on configurations; parts (c) and (d) are two side-on configurations. The central yellow ball represents metal Fe or Co atom, the central two red balls represent the adsorbed O₂ molecule, blue balls represent N atoms, gray balls represent C atoms and light white balls represent H atoms. (For interpretation of the references to color in this figure legend, the reader is referred to the web version of the article.)

From reference [377], reproduced from permission from Taylor and Francis.

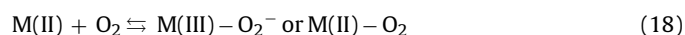
π orbitals symmetric and antisymmetric respectively) play a lesser role in the composition of the bonding orbitals [375–378]. For the side-on interaction, a 3d_{z²} orbital of the metal will interact with the 1 π_s^u bonding orbital (back-bonding interaction) and a 3d_{xz} with a 1 π_g^s antibonding orbital of dioxygen. Fig. 12 shows the optimized structural configurations for the O₂ adsorbed on FePc and CoPc molecules [377].

Shi and Zhang conducted a density functional theory study of metal phthalocyanines and metal porphyrins [379] to investigate the dioxygen-binding abilities and their relation with the catalytic activity. They investigated both end-on and side-on binding modes. They also evaluated the electronic properties of the complexes such as the ionization potential and Mulliken charge. They also studied the effect of substituents on the ligand on the electronic properties of the complexes. The catalytic activity varied linearly with the ionization potential. The ionization potential correlates directly with the redox potential of the catalysts, based on previous studies by Zagal and co-workers [18,331,334,375]. Cobalt porphyrins have high ionization potentials, which make them better catalysts than the iron counterparts. In contrast with other phthalocyanines, iron derivatives have large ionization potentials and better oxygen-binding ability which makes them good catalysts for O₂ reduction [379]. As discussed further down, these theoretical studies correlate well with experimental studies that demonstrate that the redox potential (proportional to the ionization potential) is related to the catalytic activity of metal phthalocyanines.

The active site in the phthalocyanine usually involves the M(II) state, so in alkaline solution a step will require the reduction of M(III):



An adduct will be formed as follows:



The adduct will undergo reduction as follows:



The mechanism above is applicable to Mn and Fe complexes. In the case of Co complexes, Co(III) is probably not formed upon its interaction with the dioxygen molecule since the Co(III)/(II) redox process occurs at much more positive potentials than the Fe(III)/Fe(II) process but step 17 is still crucial since the catalytically active site is Co(II) [14,19]. Density functional theory calculations [377,378] have indicated that O₂ interacts with CoPc via an end-on interaction whereas for FePc both end-on and side-on interactions are plausible. As it will be discussed further, Fe phthalocyanines promote the four-electron reduction of O₂ and this can be attributed to a side-on interaction of O₂ with the Fe complexes, which facilitates the rupture of the O–O bond.

When making comparisons between different catalysts, it is important that the redox potentials or formal potentials are measured in the same conditions. This implies that the same electrolyte and the same pH are used since M(III)/M(II) redox couples are pH dependent [366,379–381]. Co and Fe phthalocyanines exhibit the highest activity for the reduction of O₂ but they behave differently: Co complexes exhibit Co(III)/Co(II) transition that is far more positive than the onset potential for O₂ reduction whereas for Fe complexes the onset potential for O₂ reduction is very close to the Fe(III)/Fe(II) process [14,18,19,366]. There is *in situ* spectroscopic evidence for the fact that reversible transitions for the adsorbed macrocycles involve the M(III)/M(II) couples [19,382,383] for both Co and Fe phthalocyanines. For example, for experiments conducted on Fe phthalocyanine adsorbed on ordinary pyrolytic graphite, Scherson et al. demonstrated that evidence for the redox transition assigned to Fe(III)/Fe(II) involving a metal-based orbital was supported by Fe K-edge XANES [382,383] (X-ray absorption near edge structure) recorded *in situ* in 0.5 M H₂SO₄ as illustrated in Fig. 13. The adsorption edge of Fe(II)Pc (recorded at the same potential indicated in the insert) shifted strongly to higher energies upon oxidation from Fe(II) to Fe(III).

The total driving force of the reaction is given by the applied potential and also by the M(III)/M(II) formal potential of the catalyst, so the catalytic activity could be correlated with the formal potential of the catalyst as discussed before for the oxidation of thiols. Many authors have discussed this issue and it is yet not clear what sort of correlation should be expected. Reduction should occur at the potential of reduction of the M(III)O₂[−] adduct and not at the potential of the M(III)/M(II) couple. The latter should only be observed if the reaction were outer-sphere. For the particular case of iron phthalocyanines and other macrocyclics, O₂ reduction starts at potentials very close to the Fe(III)/Fe(II) couple [14,18,23]. In contrast, for cobalt macrocyclics reduction of O₂ starts at potentials much more negative than those corresponding to the Co(III)/Co(II) couple [366]. Several authors have reported correlations between activity (measured as potential at constant current) and the M(III)/M(II) formal potential and volcano-shaped curves have been obtained [13,366,384,385]. This could indicate that the redox potential needs to be located in an appropriate rather narrow window to achieve maximum activity as discussed before for the oxidation of thiols. In other words a M(III)/M(II) formal potential that is too negative (easily oxidizable metal center) or a M(III)/M(II) formal potential that is too positive (metal center that is more difficult to oxidize) does not favor the catalysis. However more recent studies [304,331,334,375] have shown that when comparing families of metallophthalocyanines, linear correlations are obtained when plotting log *k* or log *I* (rate constant or current at fixed potential, respectively) versus the M(III)/M(II) formal potential, as illustrated in Fig. 14A (first order rate constants were calculated as $k = I/nAFc$ where *I* is the current at a given potential, *n* is the total number of electrons transferred, which is 2 for the

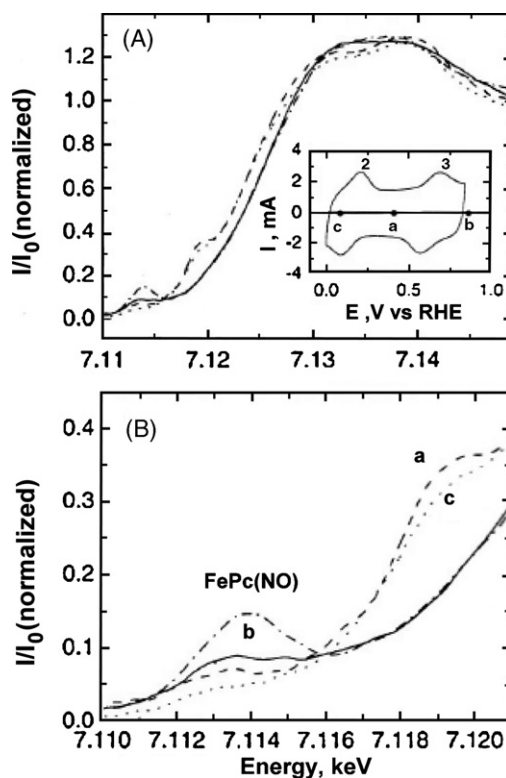


Fig. 13. (A) *In situ* FeK-edge XANES of FePc/KB in 0.5 M H₂SO₄ at 0.4 V (a, dashed line), 0.84 V (b, solid line) and 0.08 V (c, dotted line). (B) Same as A in an enlarged scale. Insert: cyclic voltammogram of FePc/KB recorded at 10 mV s^{−1} in H₂SO₄ where a, b, and c indicate the potential at which XANES spectra was recorded. From reference [383], reproduced from permission from the American Chemical Society.

hydrogen peroxide pathway and 4 for the reduction to H₂O, *A* is the area in cm², *F* is the Faraday constant and *c* is the oxygen concentration in moles per cm³). One linear correlation is obtained for Cr, Mn and Fe complexes and these metals have configurations d⁴ (Cr), d⁵ (Mn) and d⁶ (Fe) and another linear correlation is obtained for Co complexes, which have a d⁷ configuration. Shi and Zhang [379] have conducted theoretical studies that show that the ionization potential of the complexes *IP* is correlated the redox potential of Co and Fe phthalocyanines and porphyrins. So the catalytic activity should also be correlated with *IP* so plots of log *k* versus *IP* also give linear correlations (see Fig. 14B and C). The lines in Fig. 14A are parallel with a slope close to 0.15 V/decade. The line in Fig. 14B has a slope of 1.25 eV/decade and 1.1 eV/decade for Fig. 14C demonstrating that *IP* is a good reactivity index for these Co and Fe phthalocyanines and also for TPyr3,4FePz. It is possible that the declining straight lines are part of an incomplete volcano correlation. If so, the slope (δ*E*^o/δ log *i*)_{*E*} of 0.15 V/decade might have a physical meaning, as discussed for the oxidation of thiols [92]. So using similar arguments to those discussed for the oxidation of thiols, the slope of 0.15 V/decade would correspond to the falling region of an incomplete volcano. If the lines in Fig. 14 correspond to a declining portion of a volcano, then the log of currents should be used instead of log *k* since the calculation of log *k* assumes that the surface concentration of adsorbed reacting O₂ molecules and the surface concentration of free sites are constant and this is not necessarily true on the falling side of a volcano. However, the shape of the curves in Fig. 14 is not going to change when using log *I* since the kinetic currents are proportional to *k*. For the data in Fig. 14, the driving force of the catalyst increases as the formal potential of the catalysts becomes more negative. So if Δ*G*_{adsO₂} is the free energy of step 18, then the more negative the formal potential of the catalyst, the more nega-

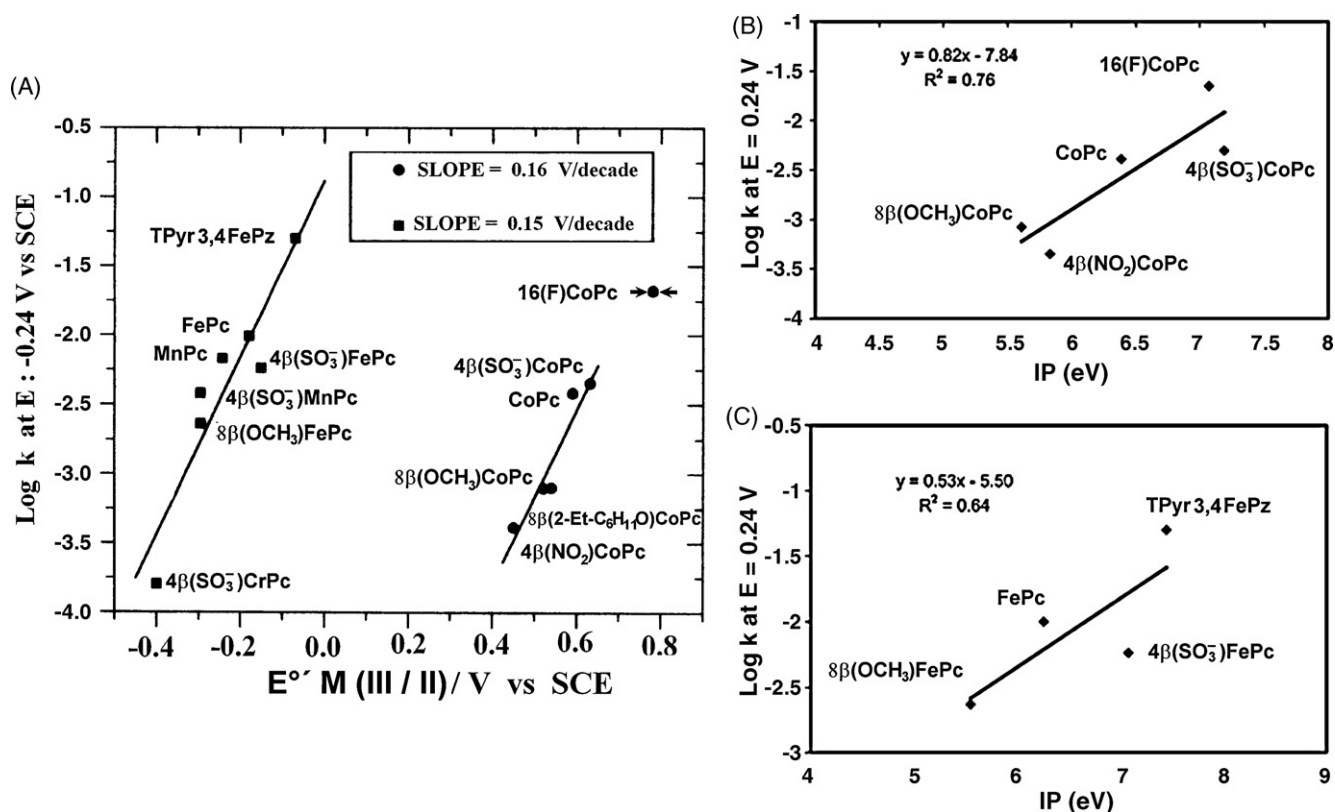


Fig. 14. (A) Plot of $\log k$ (at constant potential) versus the $M(III)/(II)$ formal potential and (B and C) ionization potential IP of MN4 macrocyclic for the reduction of molecular oxygen in 0.2 M NaOH. Adapted from ref. [331] and [379].

tive ΔG_{adsO_2} . So the rate of the falling region of the volcano would be (note that we do not use rate constants but rates):

$$\nu = C \exp + \left[\frac{\beta' \Delta G_{adsO_2}}{RT} \right] \exp - \left[\frac{\beta E F}{RT} \right] \quad (20)$$

and since kinetic data are compared at constant E , the second exponential term is constant so Eq. (20) can be rewritten as:

$$\nu = C' \exp + \left[\frac{\beta' \Delta G_{adsO_2}}{RT} \right] \quad (21)$$

so assuming that

$$\Delta G_{adsO_2} \approx nFE^{\circ'} + C'' \quad (22)$$

$$\nu = C''' \exp + \left[\frac{\beta' E^{\circ'}}{RT} \right] \quad (23)$$

where C''' contains the constant exponential terms.

So Eq. (23) predicts a reciprocal slope $(\delta E^{\circ'} / \delta \log i)_E$ of the plot of $\log \nu$ versus $E^{\circ'}$ of $2.303RT / \beta F$, which for values of $\beta' = 0.5$ gives a slope of 0.118 V/decade. This is not far from the experimental values.

The data in Fig. 14A indicate that more positive redox potentials will increase the catalytic activity up to a certain point if the correlation is an “incomplete volcano”. The $M(III)/M(II)$ redox potential of some macrocyclics can be shifted in the positive direction with heat-treatment. For example when iron tetraphenyl porphyrin [372], 4(Ph)FeP, is heat treated the $Fe(III)/(II)$ redox transition is shifted from 0.2 V versus RHE for fresh 4(Ph)FeP to 0.4 V for 4(Ph)FeP heat treated at 700 °C. Intermediate redox potentials are obtained for heat treatments at intermediate temperatures [372]

and the catalytic activity increases with heat treatment, showing that a more positive redox potential of the catalyst favors the O_2 reduction reaction rate.

An alternative explanation for the results in Fig. 14 (activity decreases as the driving force of the catalyst increases) is that the electronic coupling between the donor (MPc) and the acceptor (O_2) decreases as the electron-donating capacity of the substituents increases, due to a shift in the energy of the frontier orbitals of the metallophthalocyanine [332,386,387]. The shift in the energy of the frontier orbital with substituents on cobalt phthalocyanines has been calculated by Schlettwein and Yoshida [332] and Cárdenas-Jirón and co-workers [296] using PM3 and ZINDO/S semi-empirical theoretical calculations and using DFT by Shi and Zhang [379]. There are several approaches to estimate the electronic coupling matrix elements between the donor and the acceptor in electron transfer reactions. One of them considers the energy difference between the LUMO of the electron acceptor and the HOMO of the electron donor [388] but this requires knowledge of the distance that separates the donor from the acceptor. This is not simple for an inner sphere reaction where the $M-O_2$ distance could vary from complex to complex. Another reactivity index that can be used to rationalize the data in Fig. 14 is the concept of molecular hardness which is a commonly used criterion to predict reactivities in organic reactions and was proposed by Pearson [389,390]. The hardness η of a single molecule is approximately one-half the energy gap of the HOMO–LUMO, so the larger the gap the greater the hardness of the molecule and the higher its stability (the harder the molecule the lower its reactivity). On the contrary, a molecule with a narrow HOMO–LUMO gap (soft molecule) will be very reactive. Now for a donor–acceptor pair it is better to use the concept of donor–acceptor hardness η_{DA} which is one-half the difference between the energy of the LUMO of the

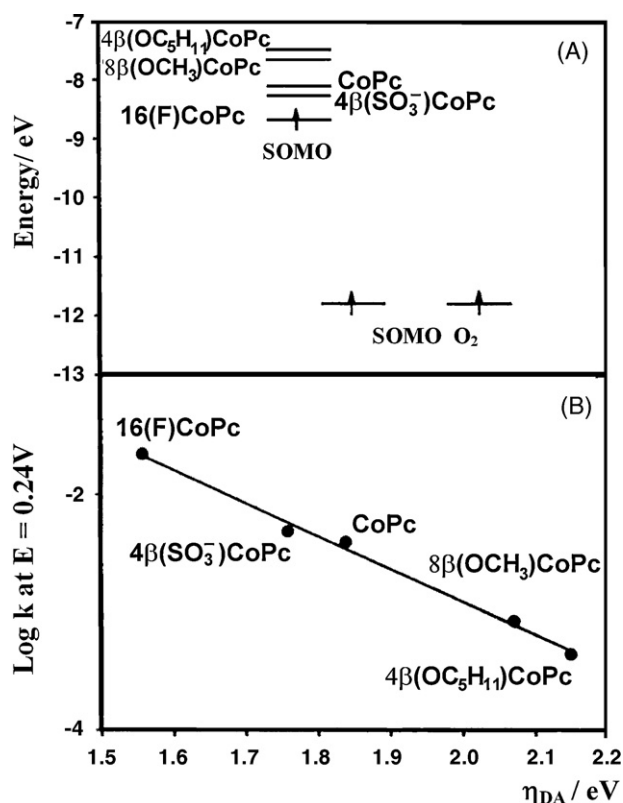


Fig. 15. (A) Relative energies of frontier orbitals of dioxygen and substituted CoPcs. For simplicity, only one electron is shown on the SOMO of the CoPcs. (B) Plot of $\log k$ (at constant potential) versus the donor-acceptor intermolecular hardness for the different O_2 -CoPc pairs. Adapted from ref. [386].

acceptor (O_2 molecule) and the energy of the HOMO of the donor (metal complex).

$$\eta_{DA} = -\frac{1}{2}(\epsilon_{LUMO\text{acceptor}} - \epsilon_{HOMO\text{donor}}) \quad (24)$$

Also, the donor-acceptor intermolecular hardness is one half the difference between the ionization potential of the donor and the electron affinity of the acceptor.

$$\eta_{DA} = -\frac{1}{2}(I_{\text{donor}} - A_{\text{acceptor}}) \quad (25)$$

The ionization potential is directly proportional to the redox potential of the catalyst as shown in theoretical studies by Shi and Zhang [379]. For a gas phase reaction involving the transfer of a single electron this will be equivalent to ΔG° . For the particular case of Co-phthalocyanine in its ground state, the highest occupied molecular orbital is occupied with a single electron (doublet state) so it corresponds to a single occupied molecular orbital (SOMO). The same is valid for molecular oxygen, which in its ground state has two unpaired electrons in two degenerate π^* anti-bonding orbitals. So the formation of an adduct $CoPc-O_2$ involves the interaction of two SOMOs and η_{DA} is given by:

$$\eta_{DA} = \frac{1}{2}(\epsilon_{SOMO\text{acceptor}} - \epsilon_{SOMO\text{donor}}) \quad (26)$$

Fig. 15 illustrates the calculated energy levels of the SOMOs of different cobalt phthalocyanines with respect to the SOMO of dioxygen using PM3. Electron-withdrawing substituents (sulfonate, fluoro) on the phthalocyanine ring stabilize the SOMO and the opposite is true for electron donating groups (methoxy and neopentoxy). So electron-withdrawing groups, even though they decrease the electron density on the cobalt (more positive

redox potential) they also decrease the gap between the energy of the SOMO of the phthalocyanine and the energy of the SOMO of dioxygen. The bottom of Fig. 15 shows that $\log k$ for O_2 reduction increases as the chemical hardness of the system decreases or as the softness of the system increases the reactivity increases. The trend in reactivity is exactly the same as that illustrated in Fig. 14. So molecular hardness can be used as a criterion for reactivity of these systems when comparing complexes that bear the same structure, and could explain why, for example perfluorinated phthalocyanine, which has the most positive redox potential (the most oxidant) is the best catalyst for O_2 reduction in the series of cobalt phthalocyanines examined since one would expect, on thermodynamic grounds that the best catalyst should be that one having the most negative redox potential. However, the concepts discussed before need to be taken with care since the metal-free phthalocyanine molecule (~ 1.8 eV HOMO-LUMO energy gap, which is quite small) is not very reactive and rather stable. It would be interesting to use the Klopman-Salem equation to describe the reactivity of the one system with respect to the other one. According to this equation a hard-hard reaction is fast because of a large Coulombic attraction and a soft-soft reaction is fast because of a large interaction between the HOMO of the nucleophile and the LUMO of the electrophile. To the best of our knowledge, there are no reports in the literature that use the Klopman-Salem equation to describe the reactivity of phthalocyanines.

In order to understand the dioxygen-binding difference between phthalocyanines and porphyrins, with cobalt and iron as central metals, Shi and Zhang [379] examined electronic structures using density functional theory. They calculated Mulliken charges on central atoms of metal macrocyclic complexes. They find that electron-withdrawing substituents (HSO_3 , F) of M-X-Pc increase as expected the positive charge on both central metal atoms (Co and Fe), and electron-donating substituents (methoxy, neopentoxy, phenyl) diminish the charge on central metal atoms (Co and Fe). For phthalocyanine systems, they find that the central metal has less charge compared to porphyrins. They attribute this to the better electron-donating ability of the phthalocyanine ligand compared to the porphyrin one, that has a frontier orbital (HOMO) of lower energy and higher ionization potential than that of Pc. The calculated charges on Co in phthalocyanine and porphyrin systems are in the range of 0.18–0.21 and 0.24–0.26, respectively. For Fe, they are in the range of 0.31–0.40 and 0.43–0.45, respectively. They find that the Co atom generally has a small Mulliken charge than the corresponding Fe atom due to lower d orbital energies of cobalt. The HOMO energies calculated for CoPcs were lower than that of molecular oxygen (except for $8\beta(OCH_3)CoPc$, which has a higher HOMO energy). The 3d orbitals of Co in CoPcs were even lower in energy. An electron-donating substituent has the effect of raising the Co 3d orbital energy, the energy gap between the interaction orbitals of Co and O_2 diminishes, so the binding energy increases. This disagrees with the explanation given by Zagal and Cardenas-Jirón [386] that stated that the electronic coupling between the donor (CoPcs) and the acceptor (O_2) decreases as the electron-donating capability of the substituents increases. Shi and Zhang obtained a theoretical correlation very similar to that illustrated in Fig. 14 B and C, where they plot experimental values of $\log k$ versus the ionization potential IP. They conclude [379] that the catalytic activity of the metal-macrocyclics is related to its ionization potential and dioxygen-binding ability.

For substituted cobalt phthalocyanines, the catalytic activity decreases linearly with dioxygen binding ability so for cobalt phthalocyanines the activity is associated with weak dioxygen binding ability. For Fe complexes they claim [379] that the reverse is true but the dispersion of the data does not allow to draw this conclusion. However the clear correlation obtained with Co phthalocyanines strongly suggest that the data in Fig. 14A corre-

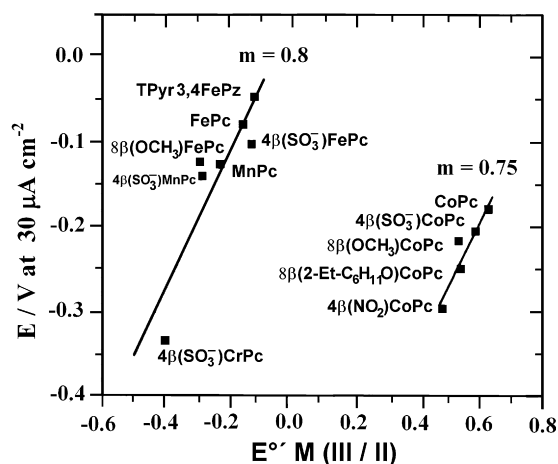


Fig. 16. Plot of $\log E$ (at constant current) versus the $M(III)/(II)$ formal potential of the MN4 macrocyclic for the reduction of oxygen in 0.2 M NaOH. Adapted from ref. [331].

sponds to the falling region of an incomplete volcano since the decrease in the activity with driving force is associated with strong adsorption of O_2 on the Co sites. These authors explain the differences in reactivity between phthalocyanines and porphyrins. Cobalt porphyrins have high ionization potentials, making them better catalysts than the corresponding iron derivatives. In contrast, for phthalocyanines, iron complexes have large ionization potentials and better dioxygen-binding ability, which make them better catalysts than Co derivatives. Therefore, their calculations [379] predict very well the catalytic activities found experimentally in spite of the fact that the influence of the solvent has not been considered.

Quantum theories of elementary heterogeneous electron transfer (ET) reactions in polar media have been extended to reactions which proceed through active intermediate electronic surface band states or bands. On the basis of this theoretical framework Ulstrup [391] has interpreted experimental data obtained for the reduction of molecular oxygen catalyzed by metal phthalocyanines. When comparing activities of complexes by plotting constant potential versus redox potential of the catalyst, linear correlations are also obtained (see Fig. 16) as predicted theoretically [391]. Essentially, Fig. 16 is a plot of driving force versus driving force. This carries the assumption that the $M(III)/M(II)$ redox potential provides a

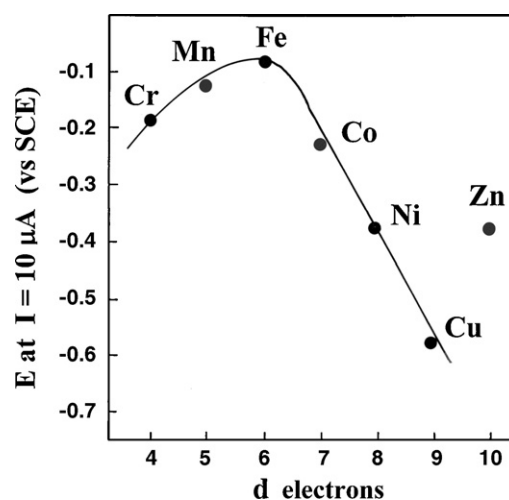


Fig. 17. Volcano plot for the electrocatalytic activity of different $4\beta(SO_3^-)MPcs$ adsorbed on graphite for O_2 reduction in 0.1 M NaOH, as a function of the number of d-electrons in the metal. From reference [14], reproduced with permission of Elsevier.

measure of the driving force of the catalysts and this might not necessarily be true for inner sphere reactions.

Not all metals of the first transition series exhibit $M(III)/M(II)$ processes so if one compares macrocyclics of different metals it is convenient to use another parameter, for example the number of d electrons in the metal (Fig. 17). Here it can be clearly seen that Fe derivatives exhibit the highest activity, followed by Mn and Co and the correlation also illustrates a common observation in catalysis that metals with nearly half filled d-energy levels exhibit the highest activity. So a redox type of mechanism does not operate for metals that do not exhibit the $M(III)/M(II)$ transition in the potential window examined for O_2 reduction. This is the case for Ni, Cu and Zn phthalocyanines. It is important to comment at this point that in order to obtain catalytic activity, the frontier orbital of the MN4 needs to have some d character. In fact, the most active catalysts included in the data (Cr, Mn, Fe, Co) have frontier orbitals with d character [392]. In the case of CuPc, Fig. 18 [334] compares the frontier orbitals of CoPc and CuPc and it is quite clear that CoPc shows a well defined d_{z^2} orbital sticking out of the plane of the phthalocyanine whereas CuPc does not and shows very low activity for O_2 reduction. There is experimental evidence to support this

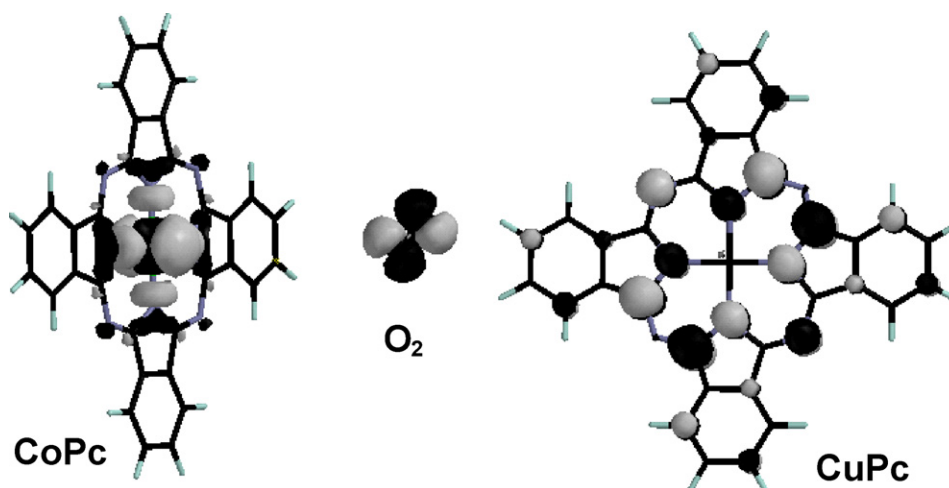


Fig. 18. Illustration of the frontier orbitals involved in the interaction of cobalt phthalocyanine with O_2 . From reference [334], reproduced with permission of Elsevier.

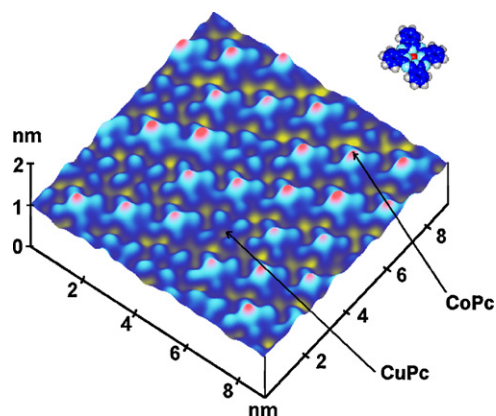


Fig. 19. STM surface plot image of CoPc and CuPc coadsorbed on the (1 1 1) plane of Au. From reference [393], reproduced with permission of the American Chemical Society.

using tunneling electron microscopy. By this technique Hipps et al. [393] have been shown a strong d-orbital dependence on the images of metal phthalocyanines (see Fig. 19). Unlike CuPc where the metal appears as a hole in the molecular image [393], the highest point in the molecular image [393]. The benzene regions of CoPc and CuPc show the same height. So, essentially images are in agreement with those predicted by theoretical calculations.

Even though most authors agree that the M(II) state is the active site for O_2 reduction [13,17–19,23,25,370,376,378,379,383], it has been proposed that Fe(I) could also play a role in the electrocatalytic process in the case of FePc and FeNc [394–396]. This was based on electroreflectance experiments that indicated that Fe(I) interacts with O_2 whereas Fe(II) does not. However, many authors have shown experimental evidence that O_2 reduction commences at potentials much more positive than those corresponding to the Fe(II)/Fe(I) [14,16–19,366]. On the contrary, the reduction currents are observed at potentials close to the potential of the Fe(III)/Fe(II) couple, so it seems unlikely that Fe(I) could be the active site. Worse, as shown from rotating ring-disk experiments, Fe(I) only favors the 2 electron reduction in contrast to Fe(II) [14,370,397] so catalytic activity when scanning the potential in the negative direction with electrodes containing FePcs decreases as Fe(I) is formed.

Another factor that affects the catalytic activity is the amount of metal complex present on the electrode surface. In general, this is evaluated from cyclic voltammograms, measuring the electrical charge under reversible peaks. This carries the assumption that all adsorbed catalyst gives an electrochemical signal. This might not necessarily be true and there could be a fraction of complexes present on the surface that are electrochemically silent. It is assumed that the “electroactive” adsorbed species are also active for the reduction of O_2 . O_2 reduction currents are directly proportional to the amount of catalyst [398,399], when the catalyst is adsorbed on the electrode surface indicating that the reaction is first order in the surface concentration of catalyst. This was not true for cases where the catalyst is incorporated to the surface by vapor deposition or when the catalyst is deposited from solutions and the solvent is completely evaporated [399]. This can be explained by the formation of multilayers where the metal active centers are not all completely accessible to O_2 . This is also the case for polymerized multilayers of $4\beta(NH_2)CoPc$, where it has been shown that only the outermost layer was active for the reduction of O_2 [367,368]. Scherson and co-workers have also reported that when $(4Ph(OCH_3)FeP)_2O$ is deposited on a porous support, 30% of the amount deposited is electrochemically active [400] and Anson and co-workers [401] have found that for $16(CN)CoPc$ and $16(F)CoPc$ complexes that were deposited from solutions where the solvent

was completely evaporated, only 30% of the amount deposited was electrochemically active. Finally, van der Putten et al. [402] have observed catalytic activity with vacuum deposited layers in spite of the fact that these layers are electrochemically silent. As pointed out before when multilayers of metal phthalocyanines are deposited on an electrode surface, only the outermost layer is active for the reduction of O_2 [402] and this is also true for other electrochemical reactions. This shows that multilayers of phthalocyanines or polymerized multilayers of phthalocyanines are rather compact and the inner layers are not accessible to O_2 molecules [368].

4.3. One-electron reduction catalysts for the reduction of molecular oxygen

Practically all reports on the catalytic reduction of O_2 on metallomacrocyclics in aqueous media have shown that the overall reaction involves two or four electron pathways or mixtures, depending on the nature of the central metal ion but to best of our knowledge there is only one report that shows evidence for the one-electron reduction of O_2 in alkaline media. A reversible one-electron reduction of O_2 to produce the stable superoxide ion was observed in an aqueous solution of 1 M NaOH. This process was catalyzed by $16(F)CoPc$ adsorbed on a graphite electrode [403]. The OH^- concentration has a very strong effect on the reduction process. Higher OH^- concentration could stabilize the superoxide ion [24]. What is curious is that $16(F)Co^{II}Pc$ is the most active catalyst for the two-electron reduction of O_2 in the correlations in Figs. 14, 16 and 17 so it is surprising that this catalyst is also active for the one-electron reduction of O_2 , which is thought to be an outer-sphere reaction.

4.4. Two to four-electron reduction catalysts for the reduction of molecular oxygen

Most mono-nuclear Co phthalocyanines catalyze the reduction of dioxygen via two electrons to give peroxide [13,14,16–19,23,361,397]. The activity of iron phthalocyanines in general is higher than those of cobalt phthalocyanines and the opposite is true for porphyrins, which reveals the importance of the nature of the ligand in determining the catalytic activity [27,404]. Theoretical calculations by Shi and Zhang corroborate this [379]. The opposite is observed for heat-treated materials [364,404]. Cobalt complexes are more stable than iron complexes and this trend is maintained after heat-treatment [405]. However, iron complexes tend to promote the four-electron reduction of dioxygen and this will be discussed further on.

Spectroscopic investigations of polymer-modified electrodes containing $4\beta(SO_3^-)CoPc$ using UV–visible differential reflectance spectroscopy allowed identifying Co(III)/Co(II) transition when varying the electrode potential [406,407]. Electron spin resonance on the Ppy (polypyrrole) and Ppy- $4\beta(SO_3^-)CoPc$ coated electrodes in deoxygenated and oxygen saturated solutions showed that the $4\beta(SO_3^-)Co(III)Pc$ species is effective in the electroreduction of oxygen and that this species is more stable in oxygen saturated medium than in deoxygenated medium because of its stabilization under Co(III)(O_2) form. In the case of Ppy- $4\beta(SO_3^-)CoPc$ film, the polypyrrole matrix undergoes strong interactions with oxygen species, and most likely, with hydrogen peroxide.

Phosphoric acid is one of the electrolytes used in fuel cells and very few reports have focused their attention on the activity of metallo macrocyclics in this electrolyte (without heat treatment). Phougat and Vasudevan [408] investigated the electrocatalytic activity of cobalt monophthalocyanines and polymers with imido and carboxylic group ends. The complexes were mixed with carbon powder and polyethylene powder. The activity of the monomeric compounds was higher than that of polymeric compounds.

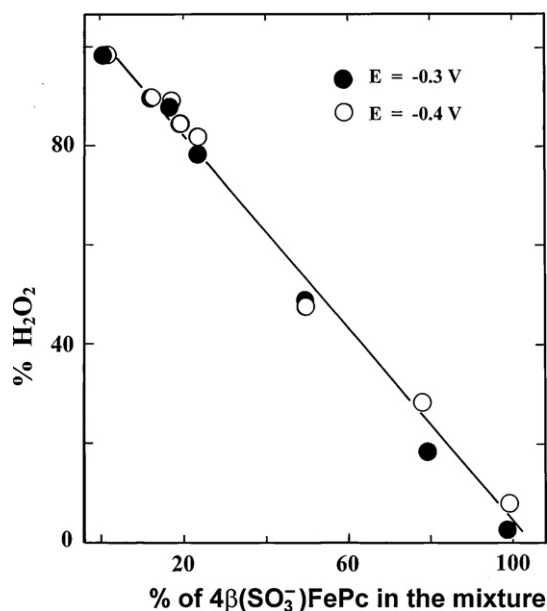


Fig. 20. Hydrogen peroxide yield as a function of surface composition of electrode with mixtures of $4\beta(\text{SO}_3^-)\text{CoPc}$ and $4\beta(\text{SO}_3^-)\text{FePc}$ coadsorbed on graphite. From reference [14] reproduced with permission of Elsevier.

Elzing et al. have proposed [409] that the presence of a basic axial ligand will lessen the charge transfer from the Fe(II) center to dioxygen:



In order to verify if $4\beta(\text{SO}_3^-)\text{CoPc}$ is active for the electroreduction of hydrogen peroxide a study was conducted on adsorbed mixtures of $4\beta(\text{SO}_3^-)\text{CoPc}$ and $4\beta(\text{SO}_3^-)\text{FePc}$ on graphite in different proportions. As $4\beta(\text{SO}_3^-)\text{CoPc}$ catalyzes the reduction of O_2 only to hydrogen peroxide, if $4\beta(\text{SO}_3^-)\text{FePc}$ had any catalytic activity it would reduce the hydrogen peroxide generated on the $4\beta(\text{SO}_3^-)\text{CoPc}$ sites. However this was not observed and both catalysts behave independently [410]. The amount of hydrogen peroxide generated was inversely proportional to the fraction of $4\beta(\text{SO}_3^-)\text{FePc}$ present on the surface (see Fig. 20). In spite of these results, it is possible for the Fe centers to form hydrogen peroxide and promote its decomposition since Fe(II) sites are known for their catalase activity [411]. Indeed for some metal chelates van Veen and van Baar have shown that their catalytic activity for hydrogen peroxide decomposition is directly proportional to their activity for O_2 reduction [412].

It was suggested for FePc and $4\beta(\text{SO}_3^-)\text{FePc}$ that dioxygen can bind to the Fe center and to a highly electronegative nitrogens in the ring, which will avoid the desorption of hydrogen peroxide before it is reduced [241,369,410,413]. This dual site mechanism would aid charge injection via back-bonding from the macrocycle into anti-bonding orbitals of O_2 or bound hydrogen peroxide, causing the destabilization and further rupture of the O–O bond [414]. At more negative potentials at which reduction of the ligand takes place, this mechanism becomes inoperative; the O_2 molecule only binds to the Fe center and hydrogen peroxide can desorb into the solution. In a study involving heat treated $4(\text{Ph})\text{FePc}$ [415] and deposited by thick layers on glassy carbon, the amount of hydrogen peroxide decomposed, compared to the amount of oxygen and hydrogen peroxide reduced, was so small that chemical decomposition was ruled out.

van den Brink et al. [413] have found that for vacuum deposited layers of FePc the first reduction wave scan was very different from subsequent scans, indicating that some reorganization of the deposited layers took place (this phenomenon is not observed on

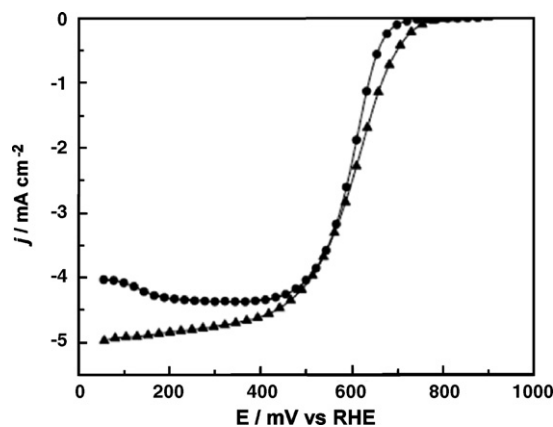


Fig. 21. Polarization curves for the oxygen reduction on a $\alpha\text{-FePc/C}$ (\blacktriangle) and a $\beta\text{-FePc}$ (\bullet) disk electrode recorded at 2500 rpm in O_2 -saturated 0.5 M H_2SO_4 electrolyte ($T = 20^\circ\text{C}$, $\nu = 5 \text{ mV s}^{-1}$). From ref. [414] with permission from Elsevier.

adsorbed layers of FePc). The effect of irreversible changes of FePc when treated under potential load with oxygen is only observed using vacuum deposited multilayers [394]. Léger and co-workers [414] have shown that the structure of FePc films affects their electrocatalytic activity. XRD studies have suggested that non-heat treated FePc is under the α -phase whereas heat-treated FePc is under the β -phase. Surprisingly, the α -phase shows higher activity than the β -phase (see Fig. 21). These authors have also shown using electrochemical quartz crystal microbalance (EQCM) technique that the α -phase FePc probably forms μ -oxo dimers at potentials higher than 700 mV versus RHE. These μ -oxo dimers are reduced at the same potential as the monomer of α -phase FePc [414].

Carbon supported iridium porphyrins are the only known mono-metal chelates that catalyze the direct four-electron reduction of O_2 in acid [415–418]. van Veen and co-workers [417] have report that the support affects the O_2 reduction selectivity. They used *in situ* Raman spectroscopy at adsorbed layers of iridium-octaethylporphyrin ($4(\text{C}_2\text{H}_5)\text{IrP}$), iridium-tetraphenylporphyrin ($4(\text{Ph})\text{IrP}$) and iridium phthalocyanine (IrPc). Raman spectra suggested that on both substrates, the molecules lie flat on the electrode surface. For $4(\text{C}_2\text{H}_5)\text{IrP}$ and $4(\text{Ph})\text{IrP}$ adsorbed on gold, reduction of O_2 gives only peroxide. However, for the same porphyrins adsorbed on pyrolytic graphite a four-electron reduction is observed. On both supports a peculiar, reversible deactivation is observed at low overpotentials. In contrast IrPc gives peroxide on both substrates and no deactivation. The oxygen reduction on iridium sites can be explained with a single site mechanism, taking into account redox transitions. It is thought to be active only in its II and III valence states, but inactive in its IV and I valence states. This is similar to the O_2 reduction mechanism on FePc and derivatives where the active site seems to be Fe in its II valence state. The III and I states in Fe phthalocyanines are inactive. The position of the iridium affects whether oxygen–oxygen bond cleavage is possible. For the out-of-plane iridium in porphyrins side on adsorption of oxygen occurs and its reduction gives water as the reduction product. In contrast, for the in-plane iridium in phthalocyanines (D_{4h} symmetry shown by Raman spectroscopy) only end-on adsorption of oxygen occurs, which leads to the peroxide reduction route. The Raman studies carried out by van Veen and co-workers [417] are consistent with the above observations but not necessarily conclusive. Since the nature of the adsorption of oxygen (side on, four electrons, water final product versus end-on two electrons, peroxide final product) seems to be extremely important in dictating the reduction mechanism, which, once again, is of crucial importance in fuel cells applications, some theoretical studies have been carried

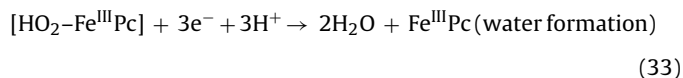
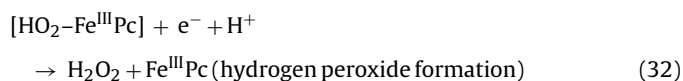
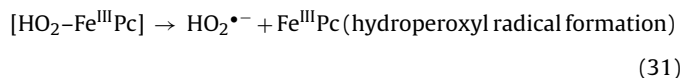
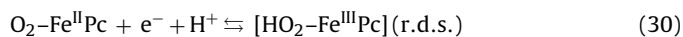
out by several authors in an effort to predict the type of interaction of the dioxygen molecule with an active site in a macrocyclic.

Anderson and Sidik [419] have carried out theoretical studies using spin-unrestricted hybrid gradient-corrected density functional calculations that have predicted that Fe(II) is the active site for four-electron reduction of oxygen by iron in the FeN4 systems. The calculations have suggested that Fe(II) is favored over Fe(III) because H₂O bonds strongly to the Fe(III) site, preventing O₂ adsorption and water does not bond strongly to Fe(II). On the first step, –OOH binds more strongly to Fe(II) than to Fe(III), which results in a more reversible potential for its formation over Fe(II). Calculations indicate that subsequent reduction steps have very reversible potentials over both centers (Fe(II) or Fe(III)). Calculations also show a hydrogen bonding interaction between –(OHOH) bonded to Fe(II) and to a nitrogen lone-pair orbital in the N4 chelate. This interaction prevents peroxide from desorbing as a two-electron reduction product. So essentially these studies show that adsorbed hydrogen peroxide is an intermediate formed from FeN4–OOH on Fe(II) sites and can be released into the solution at more negative potentials as found experimentally [366,413].

Phthalocyanines containing Fe and Co as metal centers are the most studied complexes. However, complexes of other metals have also been investigated. For example 4β(SO₃[–])CrPc and 4β(SO₃[–])MnPc were investigated [366] and they resemble somewhat the behavior of Fe complexes, mainly 4β(SO₃[–])MnPc in the sense that it shows a pre-wave where O₂ reduction proceeds entirely via four electrons to give water. Hydrogen peroxide was formed only at higher polarizations. The low activity of Cr and Mn can be attributed to their low redox potential, i.e. they are easily oxidized [14,385]. Most macrocyclic metal complexes increase their activity after heat treatment [361]. However, for manganese complexes heat treatment decreases their activity probably because the metal is lost from the N4 structure.

Complexes of Mo can only be used in alkaline solution since they are not stable in acid. MoNc shows less catalytic activity than FeNc [420].

In spite of the significant amount of work carried with metallophthalocyanines on the oxygen reduction reaction, the effect of temperature on the catalytic process has only been studied by very few authors [421]. Studies at temperatures well above room temperature in an acidic electrolyte are important in order to simulate the environment of an operating PEM fuel cell. Wilkinson and co-workers [421] have conducted experiments in the temperature range of 20–80 °C and using unsubstituted and substituted Fe phthalocyanines. The surface electrochemical responses of the FePc species were characterized with respect to their surface concentrations and adsorbed surface orientations. Depending on the type of substituent, the adsorption mode could be flat, edge-on, as a dimer, or as agglomerate, suggesting that the substituent has a strong effect on the FePc species' adsorption mode. Substitution also has a significant effect on stability. Of the four iron phthalocynine species tested, 16(F)FePc was the most stable in an acidic environment. With respect to their electrocatalytic activity, temperature, substitution and possibly mode of adsorption can significantly affect the mechanism. For example, the overall electron transfer number “*n*” observed can change from 1 to 3 depending on the type of substituent and the reaction temperature. Further research is required to determine if this change in *n* reflects a change in the reduction pathway, and/or a decrease in the stability of the adsorbed intermediates. Based on their experimental results, the various approaches found in the literature, and the current understanding, a mechanism was suggested as follows:



Wilkinson and co-workers [422] have also conducted studies at different temperatures using a Fe fluoroporphyrin and essentially found results similar to those obtained with FePc.

In conclusion, it can be said that in spite of the considerable amount of work published in the literature, there are still many questions that remain unsolved about the electrocatalytic reduction of O₂ mediated by metallo macrocyclics confined on electrode surfaces. However some clear trends do exist. It is now well established that Fe and Co macrocyclic complexes are by far the best catalysts for oxygen reduction even though recent studies suggested that co-facial Ir complexes are also very active. These complexes are characterized by exhibiting a reversible redox transition involving the M(III)/M(II) couple. Some authors have reported volcano-shaped correlations between activity (measured as current at constant potential or potential at constant current) versus M(III)/M(II) formal potential of the catalyst suggesting that an optimal M(III)/M(II) redox potential does exist for maximum activity. However other authors have shown only linear correlations between activity and M(III)/M(II) redox potential, which indicates that the more positive the redox potential the higher the activity. In the latter correlations the activity decreases with increasing the driving force of the catalyst. This finding is important since *a priori* one would expect that the more negative the M(III)/M(II) formal potential the higher the activity, since this could favor the partial reduction of O₂ upon interacting with the metal center, i.e. M(III)–O₂[–]. It is also possible that the linear correlations found are part of an “incomplete volcano”. However, in these correlations Cr, Mn, Fe and Co complexes, which exhibit a M(III)/M(II) transition give rise to two separated correlations or families of compounds. This is a reflection of the fact that the wave for O₂ reduction on for example Mn and Fe complexes starts at a potential very close to the M(III)/M(II) formal potential of the catalyst. In contrast, for Co-macrocyclics, the reduction wave starts at potentials far more negative than the Co(III)/Co(II) formal potentials. The proximity of the O₂ reduction wave to the M(III)/M(II) for some complexes is also reflected in the observation that a direct four-electron reduction process operates, as observed for Fe and Mn complexes. For most monomeric or monolayers of Co complexes the onset for O₂ reduction is far removed from the Co(III)/Co(II) transition and only the hydrogen peroxide pathway is observed. Ir porphyrins promote the four-electron reduction of O₂ in acid whereas Ir phthalocyanines only promote the two-electron reduction pathway.

Finally some of the advantages of MN4 macrocyclics over Pt catalysts is their tolerance to methanol cross over [16], which is a very critical problem in methanol–air fuel cells [361]. When methanol crossover from the anode through the electrolytic membrane to the cathode occurs, electroreduction of dioxygen and electrooxidation of methanol occur simultaneously and this is detrimental to the overall performance of the fuel cell. FePc and CoPc are highly tolerant to methanol [423,424] and in general MN4 macrocyclics are poor catalysts for the oxidation of methanol.

Table 9

A selection of peak potentials for the detection of nitrogen compounds on MPc modified electrodes versus Standard Calomel Electrode (SCE). Potentials reported versus Ag|AgCl have been corrected to versus SCE using -0.045 V conversion factor.

MPc ^a	Electrode ^b	Modification method	E_p (V versus SCE ^d)	Medium ^c	Reference
Nitric oxide oxidation					
4 β (SO ₃ ⁻)NiPc/o-PD	CF	Electrodeposition	+0.75	Aerobic PBS	[113]
4 β (SO ₃ ⁻)NiPc	GCE	Homogeneous	+1.16	pH 9	[115]
NiPc/CoPc CoPc	CF	Electrodeposition	+0.75	pH 7.4	[116]
	GCE	Adsorption	+0.90	pH 4	[118]
4 β (SO ₃ ⁻)CoPc	GCE	Electrodeposition	+1.04	pH 4	[117]
4 β (NH ₂)CoPc	GCE	polymerization	+0.66	pH 4.3	[119]
Nitric oxide reduction					
4 β (SO ₃ ⁻)CoPc	GCE	Electrodeposition	-1.01	pH 4	[117]
			-1.25	pH 7	[117]
CoPc	GCE	Adsorption	-0.98	pH 4	[118]
4 β (SO ₃ ⁻)CoPc/DDA	GCE	Adsorption	-0.77	pH 6	[275]
4 β (SO ₃ ⁻)CoPc/DTA			-0.51		
Nitrite					
CoTPy2,3-Pz	GCE	Electrodeposition	-1.4 (R)	0.5 M NaOH	[276]
CoPc	VCE	Adsorption	+0.87	pH 7.3	[277]
4 β (SCH ₂ Ph)NiPc	Au	Polymer	+0.75/	pH 7.4	[278]
4 β (SC ₁₂ H ₂₅)NiPc			+0.81		
4 β (SCH ₂ Ph)CoPc	Au	Electrodeposition	+0.62 to +0.75	pH 7.4	[279]
4 β (SC ₁₂ H ₂₅)CoPc					
4 β (SCH ₂ Ph)FePc					
4 β (SC ₁₂ H ₂₅)FePc					
4 β (SCH ₂ Ph)FePc	Au	SAM	+0.51, +0.63	pH 7.4	[280]
4 β (SCH ₂ Ph)CoPc					
4 β (NH ₂)OTiPc	Au	Polymerization	+0.63	pH 7.4	[281]
4 β (C(CH ₃) ₃ Ph)OTiPc	GCE	Adsorption	+0.66 to 0.73	pH 7.4	[281]
4 β (OPh)OTiPc					
4 β (NH ₂)OHMnPC	GCE	Polymer	0.65	pH 7.4	[89]
4 β (NH ₂)OTiPc	GCE	Polymer	0.63	pH 7.4	[89]
4 β (NH ₂)CrPc	GCE	Polymer	0.6	pH 7.4	[119]
(RuPc) ₂	RDE	Adsorption	-0.9 (R)	pH 5.8	[11]
4 β (NH ₂)NiPc	GCE	Polymer	0.86	0.1 M H ₂ SO ₄	[282]

^a o-PD: o-phenylenediamine; DDA: dodecyltrimethylammonium; DTA: dodecyltrimethylammonium.

^b GCE: glassy carbon electrode; CF: carbon fiber; RDE: rotating disk electrode; VCE: vitreous carbon electrode.

^c PBS: phosphate buffer solution.

^d R: reduction.

5. Catalytic properties of MPcs in electrochemical oxidation of nitric oxide NO

The design of modified electrode surfaces using metal complexes is very attractive for the electrochemical activation and measurement of nitric oxide NO in biological systems and/or models. Indeed, this is very difficult because of the low concentration and fleeting existence of NO, and the need to monitor *in situ* its release (in the submicromolar concentration range) has stimulated research in this area [425]. Surface electrode modification is needed to make it sensitive and selective for NO. Among the widely used catalysts, planar macrocyclic metal complexes such as porphyrin [426–430], phthalocyanine [113,116,431–436], vitamin B₁₂ [437] and related complexes [438] have been reported in the last few years. Table 9 recapitulates some significant examples of MPcs used for the electro-activation of NO.

In a recent work [436] using surface bound non-substituted MPcs, the reactivity for NO oxidation follows the trend:



The trend was found by studying the evolution of the kinetic current intensity versus NO concentration [436]. Fig. 22 illustrates the dependence of the kinetic currents I_k , calculated at $E=0.82$ V versus SCE, versus the redox potential of the catalyst. Two rather linear correlations are established: the first one is by using the potential values of the redox process that appears closer to the potential range where the oxidation of NO takes place (and noted as E_1) and the second one by using the potential value of the redox process that appears at far more negative potentials compared to that where the oxidation of NO takes place (and noted as E_2).

E_2 could involve Cr(II)-Pc(-2)/Cr(I)-Pc(-2), Mn(II)Pc(-2)/Mn(I)Pc(-2), Fe(II)Pc(-2)/Fe(I)Pc(-2), Co(II)Pc(-2)/Co(I)Pc(-2), and probably Ni(II)Pc(-2)/Ni(I)Pc(-3), Cu(II)Pc(-2)/Cu(I)Pc(-3) and Zn(II)Pc(-2)/Zn(I)Pc(-3) redox processes [21,433,434]. To a certain degree, these results agree with the previously reported trend observed by Vilakasi and Nyokong [116] using MPcs deposited on carbon microfibers ($\text{Fe} > \text{Ni} > \text{Co} > \text{Mn} > \text{Zn} > \text{Cu}$).

The effects of substituents on the periphery of the macrocycle ligand were also explored and discussed in terms of electron density located on the metal center and correlated with the formal potential of the corresponding involved redox couples. Tafel plots (with currents corrected for mass-transport) for the oxidation of NO on vitreous carbon modified electrode with adsorbed different substituted NiPcs showed that the activity of the considered complexes is affected by the presence of different groups on the periphery of the phthalocyanine ring. It decreases as follows: 4 β (SO₃⁻)NiPc > NiPc > 4 β (NH₂)NiPc > 4 β (OPhC(CH₃)₂Ph)NiPc > 4 β (OPh)NiPc > 4 β (NO₂)NiPc > NiPc. In other words, electron-withdrawing groups like -SO₃⁻ (in 4 β (SO₃⁻)NiPc) increase the rate of the reaction compared to electron-donating groups, such as the butoxy moiety in 8 α (OBu)NiPc. It was also noticed that the plot of log of the kinetic current, at constant potential, versus the redox potential of Ni phthalocyanines is linear, with a negative slope indicating that the activity of the adsorbed complex decreases as the redox potential becomes more positive.

The way the NO molecule interacts with the NiPcs is not fully established. It is plausible that NO interacts with the metal center as suggested by Bettelheim and co-workers [439] in the case of 4 β (SO₃⁻)NiPc dissolved in aqueous solution, or with other macrocyclic Ni complexes [440]. So electron-withdrawing groups could

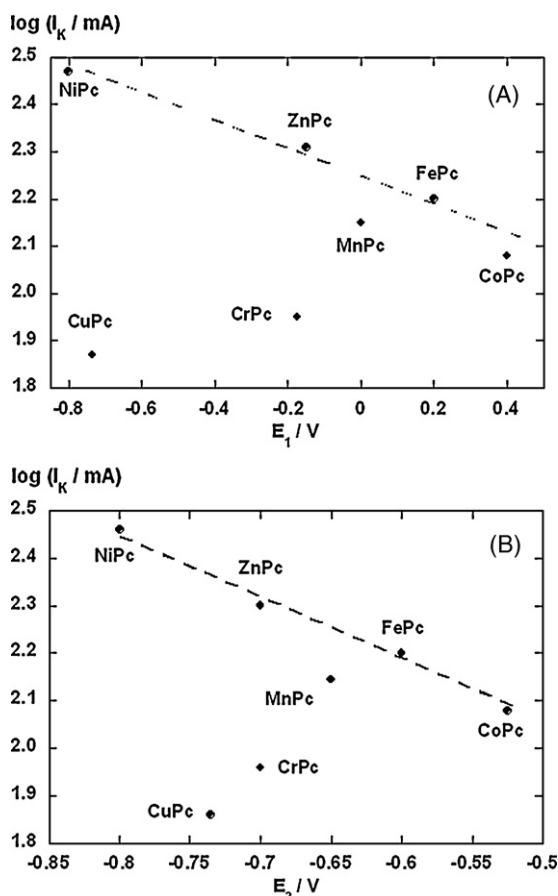
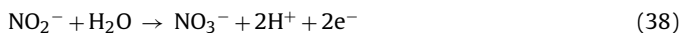
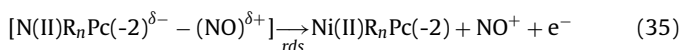
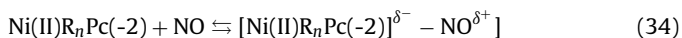


Fig. 22. (A) Plot of $\log I_k$ (at $E = 0.82 \text{ V}$) versus the most positive redox potential of the MPc, noted E_1 . (B) Plot of $\log I_k$ (at $E = 0.82 \text{ V}$) versus the most negative redox potential of the MPc, noted E_2 . Adapted from ref. [436].

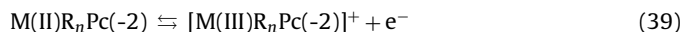
decrease the electron density on the Ni center and this will favor the oxidation of NO in the first step. From the kinetic analysis and from evidence provided in the literature, the following reaction scheme for NO electrocatalytic oxidation by adsorbed NiPcs can be proposed (R_n represents the n substituents on the phthalocyanine ligand). The symbol δ^- denotes a partial increase in electron density on the complex not necessarily located on the metal center:



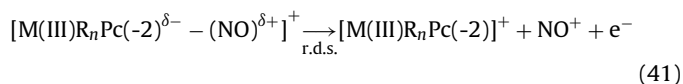
From experiments conducted by Bettelheim and co-workers [439] in 0.05 M Na_2HPO_4 aqueous solutions (pH 9) containing $4\beta(\text{SO}_3^-)\text{NiPc}$, these authors suggested the formation of an adduct involving the Ni(III) state, i.e. $[\text{Ni(III)}R_n\text{Pc}(-2)](\text{NO}^-)$ with an equilibrium constant of ca. $2.7 \times 10^5 \text{ M}^{-1}$. However, one should be reluctant to write a mechanism involving this adduct since it seems unlikely that a NO^- species could be formed at the high potentials at which oxidation currents are observed. Step 35 would be rate controlling and this agrees with the Tafel slopes of ca. 0.11 V/decade reported for the oxidation of NO on the NiPcs.

Different adducts could be formed between NO and MPcs depending on the nature of the central metal. For example, in the case of CrPc, MnPc, CoPc and FePc, a step involving the M(III) metal

center should be considered since the NO oxidation waves for these particular complexes occur at potentials more positive than the $[\text{M(III)}R_n\text{Pc}(-2)]^+ / [\text{M(II)}R_n\text{Pc}(-2)]$ redox process. So the following reaction scheme can be proposed:



followed by the rate determining step 41 where NO^+ is liberated, after the transfer of a single electron:



In these cases, one might argue that a low Tafel slope should be observed (0.040 V/decade for a symmetry factor equal to 0.5) since the rate determining step 41 is preceded by the fast one-electron transfer step 39. However, the potentials at which the NO oxidation currents are observed are more positive than the formal potential of the corresponding $[\text{M(III)}R_n\text{Pc}(-2)]^+ / [\text{M(II)}R_n\text{Pc}(-2)]$ couple. So the electrode surface is practically covered by $[\text{M(III)}R_n\text{Pc}(-2)]^+$ species at a concentration, for a given potential, that can be written according to the Nernst equation (applied to adsorbed species). If $[\text{MR}_n\text{Pc}]_{\text{ads}}$ is the total initial surface concentration of the complex, then:

$$[\text{M(III)}R_n\text{Pc}(-2)]_{\text{ads}}^+ = [\text{MR}_n\text{Pc}]_{\text{ads}} \theta \quad 0 < \theta < 1 \quad (42)$$

$$[\text{M(II)}R_n\text{Pc}(-2)]_{\text{ads}} = [\text{MR}_n\text{Pc}]_{\text{ads}} (1 - \theta). \quad (43)$$

Applying the Nernst equation and assuming ideal behavior of the adsorbed species give:

$$E = E^\circ + \frac{RT}{F} \ln \frac{\theta}{1 - \theta} \quad (44)$$

$$\theta = \exp \frac{(E - E^\circ)F/RT}{1 + \exp(E - E^\circ)F/RT} \quad (45)$$

where E is the applied potential and E° is the formal potential of the $[\text{M(III)}R_n\text{Pc}(-2)]^+ / [\text{M(II)}R_n\text{Pc}(-2)]$ couple. So, it can be easily demonstrated that as $(E - E^\circ) \gg RT/F$, $\theta \rightarrow 1$, i.e. $[\text{M(III)}R_n\text{Pc}(-2)]_{\text{ads}}^+ \rightarrow [\text{MR}_n\text{Pc}(-2)]_{\text{ads}}$ and $[\text{M(II)}R_n\text{Pc}(-2)]_{\text{ads}} \rightarrow 0$. The rate of the reaction expressed as a current would be:

$$I_k = nFAk_{41}[\text{M(III)}R_n\text{Pc}(-2)]^{\delta^-} - (\text{NO})^{\delta+} \exp \frac{\alpha\eta F}{RT} \quad (46)$$

where k_{41} is the rate constant of step 41, η is the overpotential of step 41, n the total number of electrons transferred and A the area of the electrode. All other terms have the usual meaning. The adduct surface concentration is then:

$$[\text{M(III)}R_n\text{Pc}(-2)]^{\delta^-} - (\text{NO})^{\delta+} \text{ads} = K_{34}[\text{M(III)}R_n\text{Pc}(-2)]_{\text{ads}} C_{\text{NO}} \quad (47)$$

where K_{34} is the equilibrium constant for step 34 and C_{NO} is the concentration of NO. Finally, the rate expression can be written as:

$$I_k = nFAk_{41}K_{34}[\text{M(III)}R_n\text{Pc}(-2)]_{\text{ads}} C_{\text{NO}} \exp \frac{\alpha\eta F}{RT} \quad (48)$$

and then, for $\alpha \approx 0.5$, the Tafel slope is $\approx 2.303 \times 2RT/F$ or 0.12 V/decade.

It is interesting to note from Eq. (48) that the rates of NO oxidation for each particular catalyst would be controlled by both the rate constant k_{41} of the rate determining step and the equilibrium constant K_{34} for adduct formation. Electron-withdrawing groups will favor K (since they will stabilize a more negatively charged complex) and electron-donating groups will favor k (since they will stabilize a more positively charged complex). This should be valid if adduct formation implies partial transfer of electron density from the NO molecule to the metallophthalocyanine.

So the role of the metal complexes is simply to bind the NO with probably partial charge transfer from NO to the MPc. This facilitates the electron transfer from the electrode to the bound NO molecule to form NO⁺ which undergoes further oxidation steps to finally give nitrate ions. In fact metal-free phthalocyanine (H₂Pc) adsorbed on vitreous carbon exhibits very little catalytic activity for NO oxidation. Finally, one can notice that Eq. (48) would also apply for phthalocyanines with no redox activity centered on the metal, but replacing [M(III)R_nPc(-2)]⁺ by [M(II)R_nPc(-2)].

In the case of CuPcs, the trend in activity increases as follows: 4β(NH₂)CuPc > 4β(NO₂)CuPc > 8α(OBu)CuPc > TPyr3,4CuPz > 4β(SO₃⁻)CuPc > 16(F)CuPc. Contrary to what is observed for the nickel derivatives, the activity decreases with an increase of the electron-withdrawing power of the substituents. In this case electron-withdrawing groups like -SO₃⁻ and -F have a detrimental effect in the activity of the Cu based phthalocyanines. This may be explained by the fact that the effect of substituents has a more profound effect on the rate constant *k* of the rate determining step than on the equilibrium constant *K* for adduct formation, as discussed above. So for Cu phthalocyanines, electron-donating substituents would favor the value of *k* more than their detrimental effect on the value of *K* in the rate expression (48).

Apart from the explanations given above, no other interpretation for the observation that the Cu complexes follow a trend that is opposite to what is observed for the Ni chelates is suggested in the literature. One could speculate that with the most active Ni complexes, the nature of the binding of the NO molecule with the Ni center is different to that with Cu. The participation of the ligand in the binding process for each group of complexes (NiPcs or CuPcs) cannot be ruled out.

6. Catalytic properties of MPcs in electrochemical oxidation of nitrite

The electrochemical activation of nitrite is frequently limited by slow electron transfer at conventional electrodes and complicated by irreversible passivation of the electrode surface. In order to avoid such limitations, several studies have reported on the use of chemically modified electrodes with phthalocyanines, porphyrins, hemoglobin, and myoglobin for the reduction of nitrite [150,276,441–447]. In spite of the fact that the anodic electrochemical determination of this anion offers several advantages, such as no interference from nitrate and from molecular oxygen, there are very few reports related to the oxidation of nitrite [277,448]. Table 9 recapitulates some significant examples of the several approaches described in the literature.

Regarding previous studies devoted to the study of the electrocatalytic activity of MPcs based molecular materials of potential interest for the activation of various species, a large variety of metallophthalocyanines (Co, Cr, Fe, Ni, Mn, Cu and Zn) were explored in order to get further insights into the catalytic electrooxidation process of nitrite [448]. The study was aimed at establishing the role of the metal center and that of the nature of the ligand on the electrocatalytic activity of the obtained modified electrodes and a short theoretical approach was achieved to provide a possible structure/reactivity correlation. Indeed, reactivity descriptors defined in the framework of the Density Functional Theory (DFT) such as the Fukui function [449] have been reported in the literature to characterize the activity of sites within transition metal MPcs [450–453]. These descriptors discriminate between reactivity of the metal center from that located on the ligand, in terms of the *soft* and *hard* local character in agreement with the global and local HSAB (hard soft acid base) principle [450–453].

Tafel plots obtained from polarization curves measured on a rotating disk electrode modified with the various examined MPcs

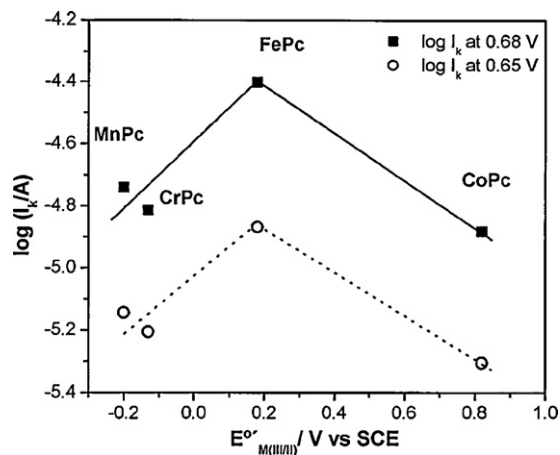


Fig. 23. Plot of $\log I_k$ (at $E = 0.65$ and 0.68 V) versus the M(III)/(II) formal redox potential of the MPc measured at pH 7.3. Adapted from ref. [451].

give almost parallel lines with slopes close to 0.059 V/decade [448] so it is possible to compare activities as currents at a constant potential. This comparison gives the following trend in reactivities:



In general, it appears that MPcs with redox active metal centers are catalytically more active than those having a redox inactive metal center. More precisely, FePc is the most active catalyst, while CuPc is the less active complex. The similarity in the Tafel slopes indicates a common rate-determining step for the reaction activated by different complexes regardless of the nature of the metal.

Fig. 23 illustrates the dependence of the kinetic currents I_k , measured at 0.65 and 0.68 V versus SCE, versus the M(III)/M(II) redox potential for the complexes that exhibit this process, namely Cr(III)Pc(-2)/Cr(II)Pc(-2), Mn(III)Pc(-2)/Mn(II)Pc(-2), Fe(III)Pc(-2)/Fe(II)Pc(-2) and Co(III)Pc(-2)/Co(II)Pc(-2) processes. The correlation is not linear. Indeed, a volcano plot is obtained as observed for other reactions discussed in this review. The data were plotted in such a way that the driving force or oxidizing power of the MPcs increases from left to right. Thus, it appears that $\log(I_k)$ increases with driving force, then it reaches a maximum and decreases as the oxidizing power of MPcs increases. This illustrates once more the concept that the redox potential of the catalyst needs to be located in a certain potential window to obtain maximum activity as discussed before for other reactions.

The theoretical calculations for the Fukui function f^+ showed the f^+_x values calculated for Cr and Mn, and $f^+_{\text{SOMO},x}$ values obtained for Fe and Co illustrate dramatic change when comparing the corresponding atoms of the ligand (C,N,H) with that of the metal center. For all these metals, it was observed that the metal center presents the highest value of the Fukui function. In contrast, the ligand atoms have the lowest f^+ values. These results indicate that the preferred site along the [M(III)Pc]⁺ molecule to receive one electron is the metallic center. Although the CrPc molecule is open shell, the $f^+_{\text{SOMO},x}$ index is not used because the calculated symmetry for the SOMO molecular orbital indicates that the SOMO will not be able to interact with the HOMO molecular orbital of nitrite. With the exception to NiPc, the f^+_x values obtained for atoms belonging to the ligand in the M(II)Pc set are much higher than the one calculated for the metal atom. Thus, one can conclude that for the CuPc and ZnPc molecules, the preferred sites to attract one electron are located on the ligand. In the case of NiPc, the calculation shows that both ligand atoms (C, N) and the metal atom center present similar f^+_x values suggesting that one electron can be captured by

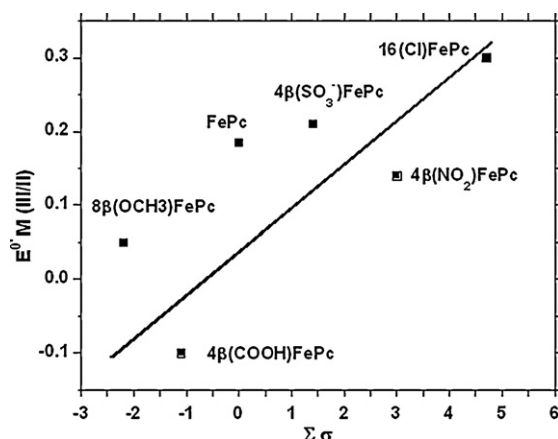


Fig. 24. Plot of the Fe(III)/(II) formal redox potential of the FePcs versus the Hammett parameters of the substituents. Adapted from ref. [448].

both sites. This reveals that for the M(II)Pc complexes, there is no unique preferred site, as it is the case for the [M(III)Pc]⁺ complexes, with each site having a minor probability of attack. These theoretical predictions are in agreement with the experimental results discussed above. Indeed, on the basis of the electronic structure calculated in the gas phase, for FePc there is one preferred site for a nucleophilic attack which corresponds to the iron center. However, in CuPc there are several sites for this kind of attack, mainly located on the ligand and therefore present a less electrophilic power than the metal center in FePc.

In order to get further insights on this behavior, the activity of various phthalocyanines bearing electron-donating and electron-withdrawing substituents on the ligand were explored. Particularly Fe and Cu derivatives since these metal-based complexes showed the highest and the lowest activity, respectively. For iron complexes, the reactivity decreases as follows: 4β(NO₂)FePc > 4β(COOH)FePc > FePc > Fe(Py)Pc > 8β(OCH₃)FePc > 16(Cl)FePc > 4β(SO₃[−])FePc and the most active complexes (4β(NO₂)FePc and 4β(COOH)FePc) show slightly higher Tafel slopes. For the copper complexes, the activity decreases as: 4β(NO₂)CuPc > 4β(NH₂)CuPc > 4α(N(CH₃)₂)₄β((CH₃)₃)CuPc > CuNc > 8α(OBu)CuPc > 4β(OBu)CuPc > 8α(OBu)CuNc > 4β(SO₃[−])CuPc > CuPc > 16(F)CuPc > TPyr3,4CuPz. In both cases, Fe and Cu, the most active complexes are those bearing four nitro substituents on the periphery of the phthalocyanine ligand.

Fig. 24 shows a linear correlation between the Fe(III)/Fe(II) redox potential and the sum of the Hammett parameters σ [367,454]. Even though FePc and 4β(NO₂)FePc exhibit similar formal potentials, their Σσ values are far apart. This could be an indication that the measured formal potential for 4β(NO₂)FePc might not be indicative of only the metal center redox activity but also that of another redox active group. The plot of log(*I_k*), at 0.65 and 0.68 V versus SCE, versus the redox potential of the Fe(III)/Fe(II) process of the examined FePcs is linear, with a negative slope (see Fig. 25a). The same happens with the plot of log(*I_k*), at 0.65 and 0.68 V versus SCE, versus the Hammett parameters σ (Fig. 25b). Such linear correlation is not surprising since the redox potentials of phthalocyanines are themselves linearly correlated with the sum of the Hammett parameters of the groups located on the periphery of the ligand (see Fig. 24). 4β(NO₂)FePc was not included as its activity is very high (log *I_k* = −3.8 at 0.68 V versus SCE) and falls well off the linear correlations. The nitro groups help in promoting a faster reaction than the redox potential can predict. This is probably due to some electronic effects of this group which are not well established. In general, with the exception of 4β(NO₂)FePc, these results

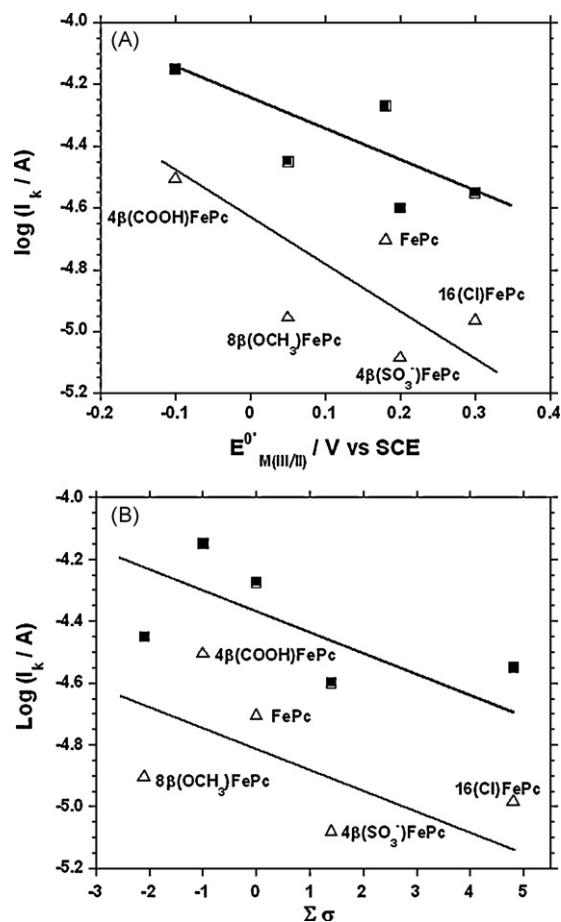
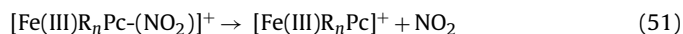


Fig. 25. (A) Plot of log(*I_k*) (at *E* = 0.65 and 0.68 V) versus the Fe(III)/(II) formal redox potential of the Fe-Pcs. (B) Plot of log(*I_k*) (at *E* = 0.65 and 0.68 V) versus the Hammett parameters of the substituents for Fe-Pcs. Adapted from ref. [448].

suggest that the activity of the adsorbed complex decreases as the Fe(III)/Fe(II) redox potential becomes more positive and this would correspond to the descending portion of the volcano plot of Fig. 23.

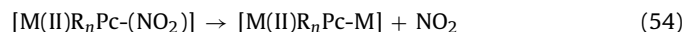
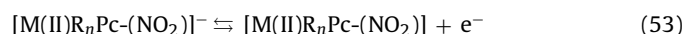
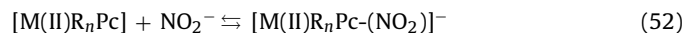
From this kinetic analysis and from other evidences provided in the literature, the following reaction scheme for nitrite electrocatalytic oxidation mediated by adsorbed FePcs was suggested (*R_n* represents the *n* substituents on the phthalocyanine ligand):



Step 51 can be rate controlling and this would agree with the Tafel slopes close to 0.060 V/decade reported for the oxidation of nitrite on the FePcs. However, for 4β(NO₂)FePc and 4β(COOH)FePc the slopes are 0.090 V/decade. This could be the value of slope if step 50 is rate controlling with an asymmetrical energy barrier (symmetry factor α = 0.65). However it seems unlikely that for those two catalysts the rate determining step is different from that for the other complexes. There could be other factors that increase the Tafel slope from 0.060 to 0.090 V and this requires further investigation. The decrease in activity with increasing driving force may be due to a decrease in the electronic coupling between the donor (nitrite) and the acceptor (metal center in the complex). Reaction 40 could explain the inverted correlations in Fig. 25. Indeed, the electron withdrawing groups should facilitate adduct formation through the pre-equilibrium of step 49 whereas electron-donating

groups would facilitate the release of one electron from the adduct in step 50. It is possible that the inverted correlation of Fig. 25 is part of a volcano correlation, where the ascending portion is missing since the range of redox potentials examined is not wide enough to show that region.

In the case of CuPcs there are also complexes that show Tafel slopes higher than 0.060 V/decade, namely $4\beta(\text{NO}_2)\text{CuPc}$, $4\beta(\text{NH}_2)\text{CuPc}$ and $4\beta(\text{OPhC}(\text{CH}_3)_2\text{Ph})\text{CuPc}$ that give slope in the range 0.080–0.090 V/decade. In a general manner, in the case of NiPc, CuPc and ZnPc, the adduct that could be formed between nitrite and these MPcs is probably different from that involving the iron-based phthalocyanines since it does not involve the redox activity at the metal center. The mechanism may be as follows:



So the role of the metal complexes is to bind the NO_2^- molecule and this facilitates the electron transfer from the electrode to the bound nitrite to form intermediates or products. Finally, Tafel slopes close to 0.060 V/decade indicate that the transfer of the first electron is fast, followed by a slow chemical rate determining (step 54). Both mechanisms written above are hypothetical assuming NO_2 is the final product of the reaction but it is likely that at high potentials nitrate ions are also formed.

7. Catalytic properties of MPcs in electrochemical oxidation of hydrazine and hydroxylamine

7.1. Electrooxidation of hydrazine

Hydrazine (N_2H_4) is a very important organic compound because of its wide application in industrial, pharmaceutical, fuel cell, and biological fields due to its high reactivity [455]. Thus, the oxidation of hydrazine to molecular nitrogen has been extensively studied over the past years [79,84,387,456–459], and the mechanism and kinetics of hydrazine oxidation have been analyzed under a wide range of conditions, in solution and with several electrodes [460]. Because of the large overpotential of hydrazine at conventional electrodes, one promising approach to minimize overvoltage effects is through the use of an electrocatalytic process at chemically modified electrodes with phthalocyanines [75,80,96,461–463]. As expected, as seen for other reactions discussed in this review, the catalytic activity of MPc is dependent on the nature of central metal in the phthalocyanine [84]. Amongst phthalocyanines, cobalt phthalocyanine (CoPc) and substituted CoPc exhibit relatively high catalytic activity [387,456,460–463]. Any molecule or species that requires an interaction with an active site to undergo an electron transfer process could react catalytically in the presence of a metal phthalocyanine.

Hydrazine is a highly reactive molecule that can be oxidized via four electrons to give molecular nitrogen ($E^\circ = 1.16 \text{ V}$ versus NHE). It has been used in the anode of fuel cells [464]. Hydrazine is known to interact with transition metal phthalocyanines [465] and this has been confirmed by several spectroscopic studies including IR [466] and EPR. [467]. Oxidation of hydrazine by air is also catalyzed by MPc and $4\beta(\text{SO}_3^-)\text{MPc}$ [466,469]. Several studies have shown that the electrooxidation of hydrazine to molecular nitrogen is catalyzed by phthalocyanines of several transition metals [2,3,6–8,75,77,79,80,84,387,416,460,461,470,471].

The redox catalysis concept can also be applied to the oxidation of hydrazine and the mechanisms proposed [70–75] take into account the $\text{M}(\text{II})/\text{M}(\text{I})$ reversible couple of the metal in the phthalocyanine

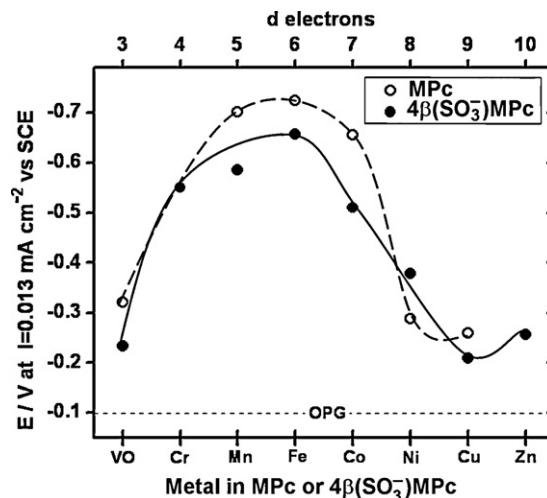
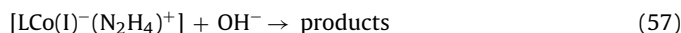
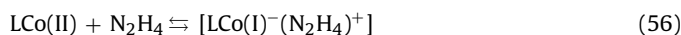


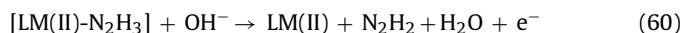
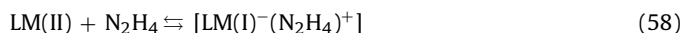
Fig. 26. Electrocatalytic activity of different metallophthalocyanines for the oxidation of hydrazine in 0.1 M NaOH as a function of the number of d electrons. Adapted from ref. [75].

cyanine



where $\text{L} = \text{Pc}$,

Or in general,



where $\text{L} = \text{Pc}$, and $\text{M} = \text{Fe}$, Mn and Cr .

The hydrazine non-bonding orbitals responsible for the oxidation of this molecule results from the $\pi-\sigma^*$ and $\pi^*-\sigma$ orbital mixing due to the pyramidalization at each N center. This hybridization changes the original π^* character of the HOMO to a non-bonding orbital similar to the $3a_1$ lone-pair of ammonia [472]. The resulting MO's are ideally polarized for a σ interaction with a d_{z^2} -like metal orbital. In contrast to the O_2 activation, in this case electron donation is in one direction, from N_2H_4 to the metal.

Cardenas-Jirón and co-workers [473,474] have proposed two quantum chemistry theoretical models in the gas phase at the density functional theory B3LYP/LACVP(d) level of calculation to rationalize the hydrazine oxidation catalyzed by $\text{Co}(\text{II})\text{Pc}$. These theoretical models that are described in terms of energy profiles include a *through-space* mechanism for the transfer of the first electron of the hydrazine and a *through-bond* mechanism proposed for the transfer of the three electrons remaining. The main difference between both models arises from a one-electron and one-proton alternate transfer for model 1 and a two-electron and two-proton alternate transfer for model 2. They conclude that model 1 is more reasonable than model 2 because the whole oxidation process is always exergonic.

Fig. 26 shows a volcano curve in which the activity is plotted versus the number of d-electrons in the metallophthalocyanine. Again, as observed for O_2 reduction, the iron complexes show the highest activity. This strongly suggests that the best match of energies between the metal d orbitals and the hydrazine HOMO occurs for iron phthalocyanines. This seems to indicate that the energies of the O_2 and N_2H_4 HOMOs are not far from each other. In fact if one plots overpotential for O_2 reduction versus overpotential for N_2H_4 oxidation for each metallophthalocyanine a linear correlation is obtained [14].

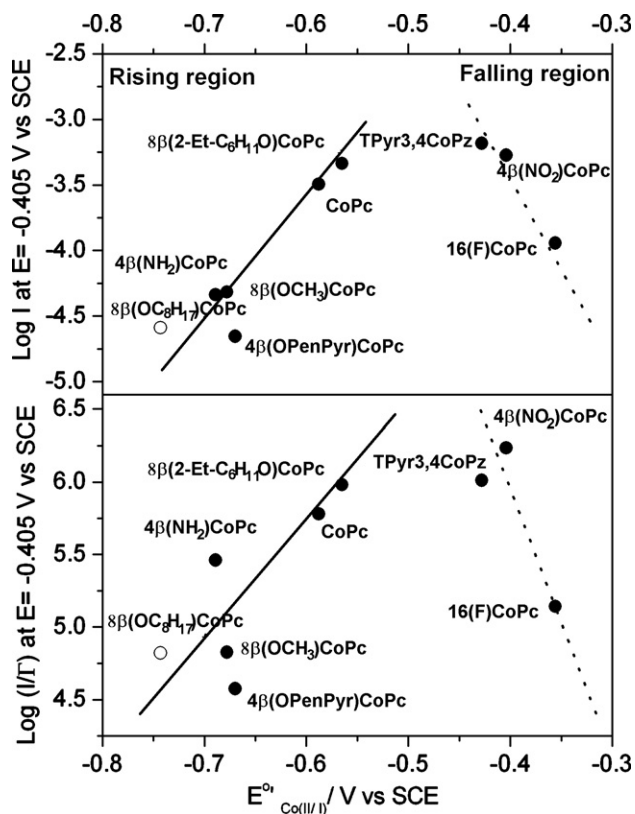


Fig. 27. Variation of $\log(I/I^\circ)$ complex (currents normalized for the surface concentration of the catalyst) versus formal potential of the catalyst for the electrooxidation of hydrazine on CoPcs with different substituents. Adapted from ref. [83].

A correlation between electrocatalytic activity (as current normalized by the number of Pcs molecules per unit of area) for the oxidation of hydrazine in alkaline media gives non-linear correlations (Figs. 27 and 28) when the activity is plotted versus the $M(II)/M(I)$ redox potential of CoPcs and FePcs. This illustrates again the concept “tuning” the redox potential of the catalyst to a desired value, using appropriate groups on the phthalocyanine ligand to obtain the highest activity. It is important to point out here that macrocyclic complexes that are not phthalocyanines do fit in this volcano correlation indicating that the redox potential of the cata-

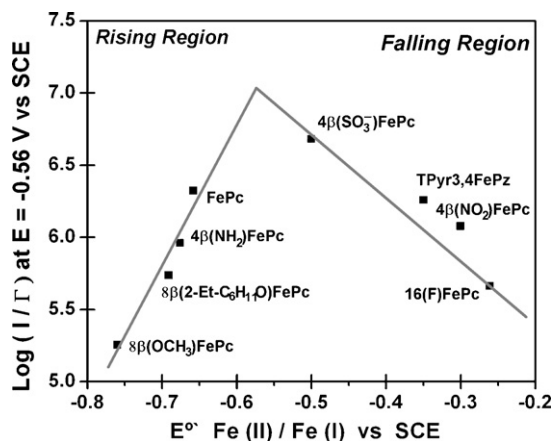


Fig. 28. Variation of $\log(I/I^\circ)$ complex (currents normalized for the surface concentration of the catalyst) versus the formal potential of the catalyst for the electrooxidation of hydrazine on FePcs with different substituents. Adapted from ref. [475].

lyst is a good reactivity index and seems to be independent of the nature of the ligand in the complex [85,475].

As shown for other reactions, the electrocatalytic activity of electrodes modified with MPcs can be enhanced, sometimes by two orders or magnitude or more if carbon nanotubes are incorporated on the electrode surface [476]. Geraldo et al. have shown [86] that single-walled carbon nanotubes (SWCNT) functionalized with CoPc enhances the catalytic activity of the complex itself without any change in the reaction mechanism. A synergistic effect, in terms of reactivity when the new nanocomposite material is adsorbed on the glassy carbon (GC) electrode, is observed. The obtained hybrid electrodes were tested under hydrodynamic conditions, showing two different oxidation processes, which suggest the presence of two different types of active sites on the electrode surface catalyzing the reaction. Atomic force microscopy (AFM) images (Fig. 29) showed the clear differences in surface roughness for each film, confirming the different compositions of the hybrid electrodes [86].

One important application of electrodes modified with phthalocyanines in relation to hydrazine oxidation is the possibility to make electrochemical sensors using this molecule. Kubota and co-workers [477] have reported that $4\beta(\text{SO}_3^-)\text{NiPc}$ immobilized onto titanized silica gel shows high stability and catalytic activity for hydrazine oxidation. The process is controlled by the electron transfer step and no diffusion limitation was observed. The modified electrode was very sensitive for hydrazine, giving a detection limit of $1.0 \times 10^{-5} \text{ mol L}^{-1}$, for an applied potential of 450 mV versus SCE. Ozoemena [478] has described the electrocatalytic behavior of a GC modified with CoPc peripherally tetrasubstituted with cobalt(II)tetraphenylporphyrin ($4(\text{Ph})\text{CoP}$) complexes via ether linkages (i.e., $\text{CoPc}-(4(\text{Ph})\text{CoP})_4$, see Fig. 1). The viability of this supramolecular complex as a redox mediator for the anodic oxidation and sensitive amperometric determination of hydrazine in alkaline conditions was tested. The proposed amperometric sensor displays excellent characteristics for the determination of hydrazine in 0.2 M NaOH; such as low overpotentials (+100 mV versus Ag/AgCl), very fast amperometric response time (1 s), linear concentration range of up to 230 μM , with micromolar detection limit, high sensitivity and stability. Also Ozoemena and Nyokong [82] have studied the electrocatalytic oxidation and detection of hydrazine in pH 7.0 by using gold electrode modified with SAM films of FePc axially ligated to a preformed 4-mercaptopyridine SAMs. The mechanism for the interaction of hydrazine with the FePc–SAM is proposed to involve the $\text{Fe(III)Pc}/\text{Fe(II)Pc}$ redox process. Using cyclic voltammetry and Osteryoung square wave voltammetry, hydrazine was detected over a linear concentration range of 1.3×10^{-5} to $9.2 \times 10^{-5} \text{ mol L}^{-1}$ with limits of detection as low as 5 and 11 μM , respectively. Finally, Li et al. have fabricated covalently attached multilayer film electrode containing CoPc which show electrocatalytic activity oxidation of hydrazine [455].

7.2. Electrooxidation of hydroxylamine

In connection with phthalocyanines, hydroxylamine has been much less studied than hydrazine. Hydroxylamine, NH_2OH , is a strong reducing agent. It is used as an anti-oxidant in soaps and fatty acids and as an intermediate in the production of pesticides and pharmaceutical drugs. It induces highly specific mutations and is very toxic for aquatic organisms. EPR spectroscopic studies conducted at low temperature have indicated that hydroxylamine forms stable adducts with Co and $4\beta(\text{SO}_3^-)\text{FePcs}$ [467]. It has also been shown that hydroxylamine is catalytically oxidized by molecular oxygen in the presence of $4\beta(\text{SO}_3^-)\text{MPcs}$ in aqueous solutions [467–469]. From these results, one would expect that phthalocyanines, when adsorbed on a graphite electrode surface would catalyze the electrochemical oxidation of NH_2OH . This is indeed the case: $4\beta(\text{SO}_3^-)\text{FePc}$ possesses some catalytic activity for the

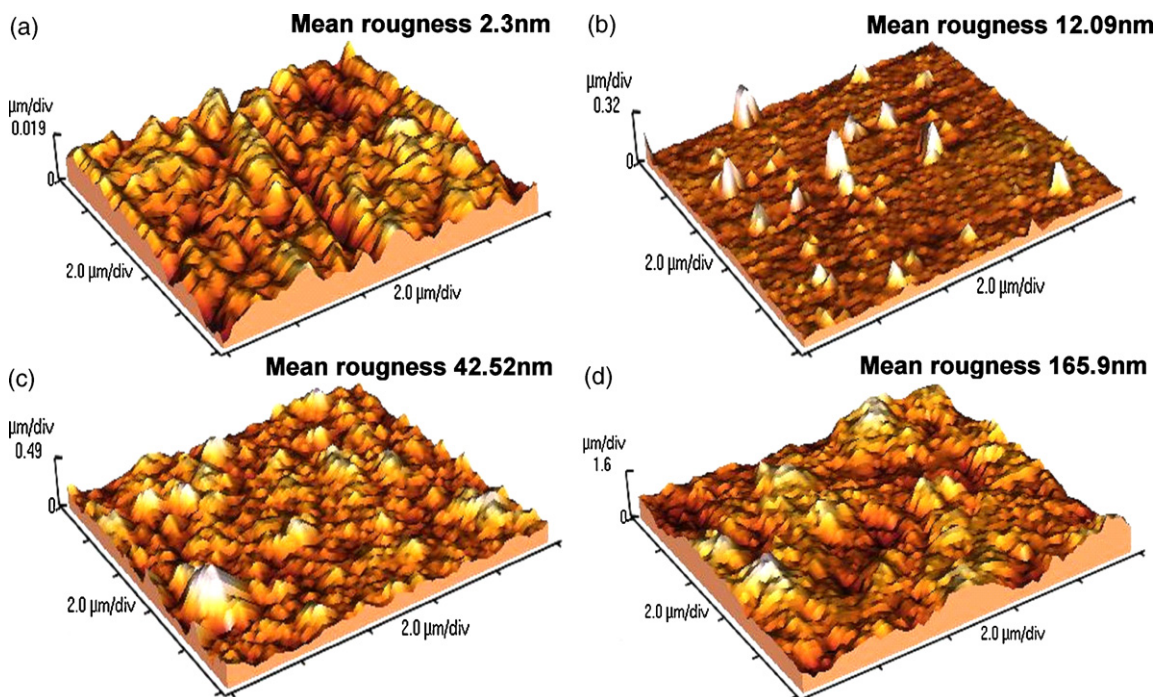


Fig. 29. AFM images of the surface of: bare GC electrode (A); GC/CoPcads (B); GC/SWCNT (C) and GC/SWCNT + CoPc (D). From ref. [86] (Reproduced with permission of Elsevier.).

reaction [110] but the catalytic effects are not as pronounced as those observed for other reactions like O_2 reduction and hydrazine oxidation. This has been attributed to the formation of a “stable adduct” where NH_2OH binds to the $4\beta(SO_3^-)FePc$ preventing new molecules of hydroxylamine to interact with Fe and react. To have pronounced catalytic effects, the adducts or intermediates need to be labile and decompose fast to maintain the catalytic cycle functioning. As discussed for other reactions, the interaction of the reacting molecule needs to be not too weak, not too strong, as indicated by the volcano correlations. For the particular case of hydroxylamine, its interaction with the Fe sites is too strong. Electrochemical evidence was reported for the formation of Fe–hydroxylamine adduct as the cyclic voltammogram of adsorbed $4\beta(SO_3^-)FePc$ is modified in the presence of small amounts of hydroxylamine [110]. The catalytic effects are small as the reaction rates for the most active $4\beta(SO_3^-)MPcs$ are only 7 times greater than the least active ones. Evidence for the formation of these adducts has also been found electrochemically for $4\beta(SO_3^-)CoPc$ [110]. From the kinetic parameters determined electrochemically, the following mechanism has been proposed [14,110]:



$L = Pc$, which agrees with a -1 order in protons.

The donor–acceptor intermolecular hardness concept (η_{DA}) associated with the interaction between substituted cobalt phthalocyanines ($Co(X)_nPc$) acceptor species such as hydrazine and hydroxylamine has been used to explain the relative reactivity of the different Co phthalocyanines for the oxidation of these molecules. Semiempirical (PM3) and *ab initio* (ROHF: CEP-31G and ROHF: 6-31G) theoretical methods were used to determine η_{DA} for the four charge transfer interactions. Theoretical results of η_{DA} correlate well with rate constants for electrooxidation of hydrazine and hydroxylamine and for electroreduction of O_2 for processes occurring on phthalocyanines confined on a graphite electrode. The lower η_{DA} the higher is the reactivity. The molecular hardness

(η) was also calculated as defined in density functional theory, of $Co(X)_nPc$. Other macrocyclic compounds NNNNtetramethyltetra-3,4-pyridoporphyrzinocobalt(II) [88] and vitamin B_{12} [479] also show high activity for the oxidation of hydroxylamine.

8. Catalytic properties of MPcs in electrochemical reactions involving other biologically and environmentally relevant compounds

8.1. Phenols and organohalides

Phenols are widespread in nature. They are released into the environment in a number of ways such as during the manufacture of industrial products like plastics, pharmaceuticals, dyes and pesticides (e.g. pentachlorophenol) and they accumulate in the environment as recalcitrant contaminants [480,481]. Organohalides are also recognized as important environmental pollutants arising from industrial as well as biological sources. Indeed, halogenated methanes and ethanes are often used as solvents. Trichloroacetic acid is for example used as plaguicide in some countries, although it is known to be toxic.

Electrochemical methods are preferred in analysis of phenols and halogenated organics since often traditional methods require extensive separation. However, direct determination using noble metal electrodes is not favored due to high overpotentials. Electrochemical oxidation of phenols readily occurs on unmodified electrodes, but oxidation results in the formation of dimers which poison the electrodes, decreasing the oxidation currents [482]. In order to improve the sensitivity and selectivity, chemically modified electrodes are employed. In this regard, MPcs have shown catalytic activity towards the detection of phenols and other species when they are employed as homogeneous catalysts or when they are adsorbed to electrodes (Table 10).

Bedioui and co-workers have studied the electrocatalytic reduction of trichloroacetic acid (TCA) on electrodes modified with heme proteins [483,484] or porphyrins [485], but very little work has been done for the reduction of TCA using electrodes modified

Table 10

A selection of peak potentials for the detection of neurotransmitters and phenols on MPc modified electrodes versus standard calomel electrode (SCE).

MPc ^a	Electrode ^b	Modification method ^b	Analyte ^c	<i>E</i> _p (versus SCE)	Medium	References
Phenols						
CoPc	GCE	Adsorption	Phenol, 2-CP, 4-CP	+1.01 to +1.02	0.05 M H ₂ SO ₄	[266,314]
CoPc	GCE	Adsorption	<i>o</i> -, <i>m</i> -, <i>p</i> -cresol	+0.87 to 0.94	0.05 M H ₂ SO ₄	[266]
CoPc + lactate dehydrogenase	C	Screen printed	PCP	+0.3	pH 7.4	[267]
CoPc/polyphenol oxidase	C	CPE	Phenol, catechol, dopamine	+0.2	pH 7.4	[265]
4β(PhPy)Ni(OH)Pc	VCE	Polymer	4-CP, phenol, NP	0.33	1 M NaOH	[126]
Neurotransmitters						
4β(SO ₃ ⁻)FePc	C	CPE	Dopamine	+0.18 to 0.28	pH 4 to 7.4	[268,269]
4β(SO ₃ ⁻)NiPc	CF	Polymer	Serotonin, noradrenaline dopamine adrenaline	0.35, 0.28	pH 7.4	[268,312]
				0.15		
				0.17		
				0.16		
4β(NH ₂)Ni(OH)Pc	GCE	Polymer	Dopamine	0.08	PBS	[121]
4β(NH ₂)NiPc	GCE	Polymer	Dopamine	-0.19	pH 7.4	[270]
4β(NH ₂)CoPc-SWCNT	Au	Preformed SAM	Dopamine	0.13	pH 7.4	[316]
4β(SO ₃ ⁻)NiPc/gum	ITO	Adsorption	Dopamine	0.68	0.1 M HCl	[272]
4β(SO ₃ ⁻)FePc/PAH	GCE	Adsorption	Dopamine	0.16	LiClO ₄ in acetonitrile	[273]
CoPc/polyphenol oxidase	C	CPE	Dopamine	+0.2	pH 7.4	[265]

Potentials reported versus Ag/AgCl have been corrected to versus SCE using -0.045 V conversion factor.

^a PAH: poly(allylamine hydrochloride), SWCNT: single walled carbon nanotube.^b ITO: indium tin oxide. VCE: vitreous carbon electrode, SAM: self-assembled monolayer, CF: carbon fiber, GCE: glassy carbon electrode, CPE: carbon paste electrode.^c CP: chlorophenol, NP: nitrophenol, PCP: pentachlorophenol.

with MPc complexes. Jiang et al. [486] studied β(SO₃⁻)CoPc/DDAB (DDAB = didodecylmethylammonium bromide) films for catalyzing the reduction of TCA and other organohalides. The catalytic reduction of TCA is more efficient in the acetonitrile/water solvent mixture than in the microemulsions [486].

CoPc modified carbon paste electrodes show good catalytic activity towards the measurement of triazolic herbicides such as amitrole at low oxidation potentials in basic media, a detection limit of 0.04 μg mL⁻¹ was obtained using an injection system [487]. 4β(SO₃⁻)CuPc was used as component of the microemulsion and lowered the overpotential for the reduction of *o*-chlorophenol by 1 V, hence showing promise for the catalytic decomposition of 1,1-bis(4-chlorophenyl)-2,2,2-trichloroethane [488].

Biosensors based on enzymes have been developed for many electrochemical analyses. The use of MPc complexes as part of the catalytic system improves the sensitivities of the biosensors. On screen-printed CoPc electrodes containing lactate dehydrogenase, oxidation of pentachlorophenol occurred at a low potential of 0.3 V [267].

The catalytic activity of NiPc complexes for the oxidation of phenols has been studied by Ureta-Zañartu and co-workers [125,489]. Electrooxidation of 2-chlorophenol takes place on electropolymerized 4β(SO₃⁻)NiPc [125,489]. The electrochemical oxidation of phenol, 4-chlorophenol and nitrophenol using electropolymerized NiPc (nickel hydroxy tetraphenoxy pyrrole phthalocyanine (*poly*-4β(PhPy)Ni(OH)Pc)) modified vitreous carbon electrodes has also been reported [126]. The films were formed by electropolymerizing pyrrole-substituted phenoxyphthalocyanine *poly*-4β(PhPy)NiPc in aqueous 0.1 M NaOH solution. The *poly*-4β(PhPy)Ni(OH)Pc films show better stability and resistance to electrode fouling compared to *poly*-4β(PhPy)NiPc and unmodified electrodes. The resistance to surface fouling and stability can be attributed to the structure of the ring substituent on the phthalocyanine macrocycle and to the particular O–Ni–O bridged architecture of the nickel phthalocyanine film [126]. Ureta-Zañartu and co-workers [490,491] have characterized films formed on glassy carbon electrodes modified by electropolymerization of two water-soluble compounds, Ni(II)tetrakisulfophthalocyanine (4β(SO₃⁻)NiPc) and Ni(II)tetrakisulfophenylporphyrin (4(PhSO₃⁻)NiP), and of two water-insoluble compounds, Ni(II)tetraaminophthalocyanine (4β(NH₂)NiPc) and Ni(II)tetraaminophenylporphyrin

(4(PhNH₂)NiP), using impedance measurements. The Nyquist plots of all these films shown in the potential range of the Ni(II)/Ni(III) process showed the semicircle typical of a charge transfer, the charge-transfer resistance decreasing very much with increasing potential. The uncompensated resistance of the GC electrode is barely affected by the films, showing that they are very porous. This is in contrast to polymeric films formed by 4β(NH₂)CoPc (Co tetraaminophthalocyanine) where only the external layer is accessible to reacting molecules. The IR spectra of the *poly*-4(PhSO₃⁻)NiP and the *poly*-4β(SO₃⁻)NiPc films shows bands at 3628 cm⁻¹ and 3500 cm⁻¹, respectively, which could be due to interstitial water molecules occluded during the polymerization. The Ni 2p XP spectra indicate that the magnetic character of the Ni(II) ions in 4(PhSO₃⁻)NiP is dramatically changed by the polymerization, from diamagnetic in the monomer to paramagnetic in the polymeric film, indicating the formation of Ni–O–Ni bridges or of clusters of Ni(OH)₂. On the contrary, the Ni 2p XP spectra of the unactivated 4(PhNH₂)NiP, film, in which the Ni(II)/Ni(III) process was absent, showed only diamagnetic Ni(II). Therefore, it is concluded that only paramagnetic Ni(II) ions can be electrooxidized to Ni(III) [491].

8.2. Catecholamines

Dopamine (DA), epinephrine (EP) and serotonin (5-hydroxytryptamine, 5-HT) are important catecholamine neurotransmitters in biological systems. Serotonin regulates mood and sleep and is a target for pharmaceutical treatment of depression. Dopamine is implicated in locomotion. Deficiencies in DA can result in some neurological disorders such as Parkinson's disease.

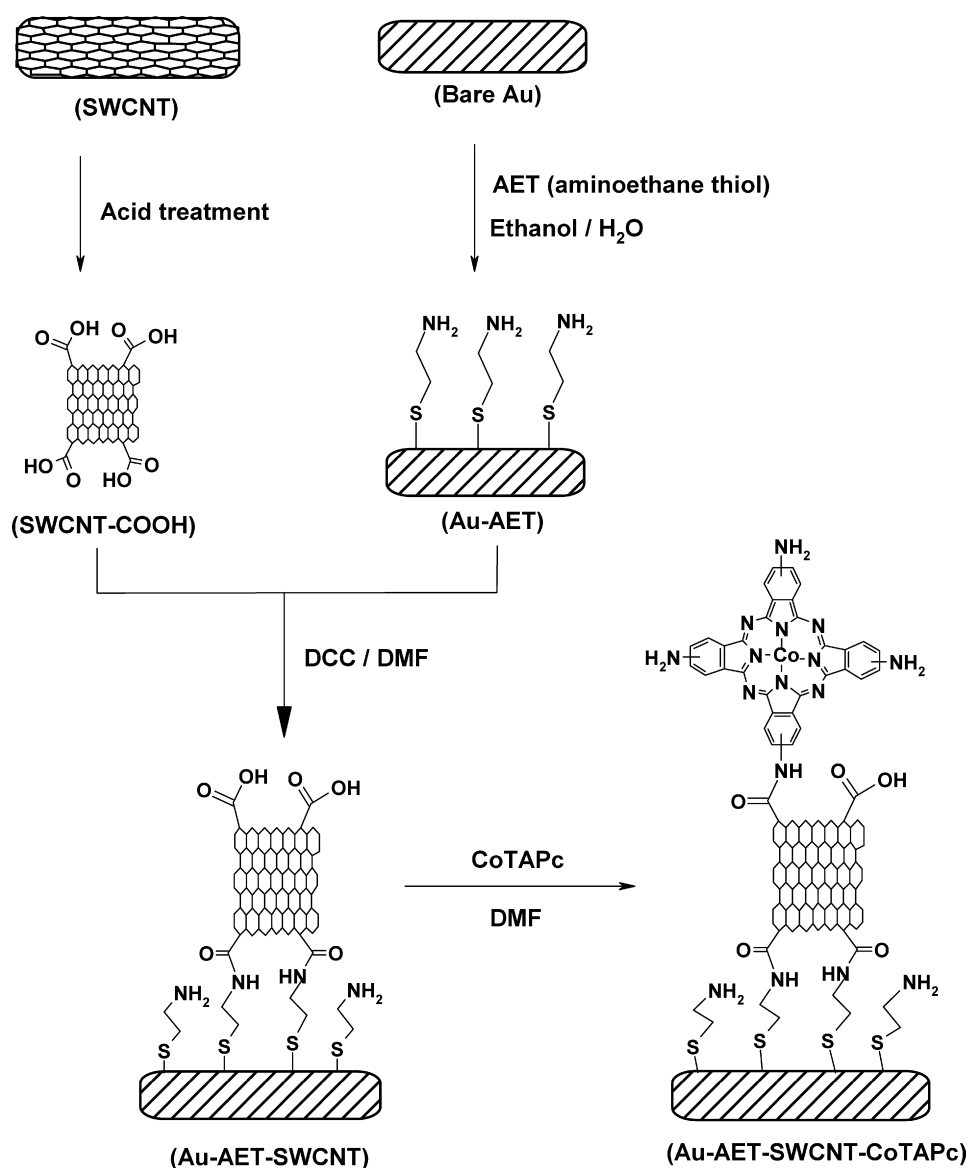
Electrochemical techniques show promise for the analysis of neurotransmitters in general because of the possibility of direct measurement of the analytes *in vivo* [492–498] and phthalocyanines play an important role in the development of electrodes for sensing purposes. Non-electrochemical techniques involve withdrawing samples from the subject followed by rigorous separation, conditioning and other forms of sample pretreatment methods prior to analysis. Advantages of electrochemical methods include high selectivity, good sensitivity and very low detection limits [494,495]. Simultaneous detection of neurotransmitters (such as

serotonin and dopamine) is important since they coexist in biological systems. The detection of the neurotransmitters on solid electrodes often suffers from fouling due to the accumulation of the oxidation products on the electrodes, resulting in poor selectivity and sensitivity. Thus the development of electrode modifiers which can improve the detection of neurotransmitters is of continuing interest (Table 10). The catecholamines also show potentials very close to one another, for example noradrenaline, dopamine and adrenaline show peaks at 0.15, 0.17 and 0.16 V versus SCE [312] and DA at 0.35 V versus SCE. Thus simultaneous detection of the catecholamines is difficult and the use of electrocatalysts to improve potential separation is an active area of research.

The other challenge in the detection of these neurotransmitters is the presence of a large excess of ascorbic acid that is always present in extra-cellular fluid and frequently interferes with the current signals obtained for the detection of neurotransmitters due to the closeness of their oxidation potentials to that of ascorbic acid. There have been many approaches towards overcoming this problem of interference posed by ascorbic acid. One of the most frequently used approach is to pre-coat the electrode surface

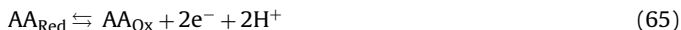
with a perm-selective layer of negatively charged polymer, such as Nafion[®], which repels all kinds of negatively charged species, in particular ascorbate, away from the electrode surface thereby preventing their oxido-reduction. In many other cases a modifier (such as an MPc molecule) that exhibits electrocatalytic activity towards the oxidation of the neurotransmitters is first applied to the electrode surface before finally coating the electrode with the negatively charged polymer. The use of Nafion[®] often results in the loss of sensitivity. A carbon paste electrode containing the negatively charged $4\beta(\text{SO}_3^-)\text{MPc}$ complexes ($\text{M} = \text{Co(II)}$ and Ni(II)) eliminates the effects of ascorbic acid by acting in the same manner as Nafion[®] without the loss of sensitivity observed for the latter [268]. The oxidation peak for DA was obtained at 0.18 V on $4\beta(\text{SO}_3^-)\text{FePc}$ modified electrode. The $4\beta(\text{SO}_3^-)\text{FePc}$ modified electrode allowed for the determination of DA, nitric oxide and 5-HT in the presence of large concentrations of ascorbic acid.

The reduction of the oxidation product of dopamine (DA_{ox}) by ascorbic acid in solution (Eqs. (63)–(65)), has been shown [269] to induce a shift of the DA potential as a function of ratio of concentration of dopamine to ascorbic acid, making it possible to determine



Scheme 1. Formation of preformed SAM using aminoethanethiol (AET), single walled carbon nanotubes (SWCNT) and $4\beta(\text{NH}_2)\text{CoPc}$. Adapted from reference [499].

both ascorbic acid (AA) and DA from the potential shift and the experimental peak current, using Eqs. (66) and (67).



where DA_{Red} is reduced DA, DA_{Ox} is oxidized DA and similarly for AA, AA_{Red} is reduced AA, AA_{Ox} is oxidized AA.

$$c_{\text{AA}} = \frac{-582(I_p - 2I_{\text{bg}})}{k(1.6E_{1/2} - 918)} \quad (66)$$

$$c_{\text{DA}} = \frac{(I_p - kc_{\text{AA}} - I_{\text{bg}})}{k'} \quad (67)$$

where I_{DA} and I_{AA} are the currents of dopamine and ascorbic acid, respectively, k and k' are the slopes of calibration plots of ascorbic acid and DA, respectively, I_{bg} is the background current, c_{AA} and c_{DA} are the concentrations of AA and DA, respectively. Using these equations and an $4\beta(\text{SO}_3^-)\text{FePc}$ modified carbon paste electrode, the detection limits of $4.5 \pm 0.2 \times 10^{-7}$ and $7.5 \pm 0.5 \times 10^{-7} \text{ mol L}^{-1}$ were obtained respectively for dopamine and ascorbic acid for $c_{\text{DA}}/c_{\text{AA}} > 0.01$ [269].

Finally, one can cite the following significant examples (Table 10):

- (i) Carbon paste electrodes modified with nanosized CoPc particles with good catalytic behavior for the detection of DA and AA [271]. The anodic peak potentials of DA and AA appear well separated with good sensitivity in the presence of cetyltrimethylammonium bromide (CTAB), thus allowing their simultaneous detection.
- (ii) Electropolymerized $4\beta(\text{SO}_3^-)\text{NiPc}$ that improves the response time towards serotonin [312]. The sensor can be used to determine serotonin in urine, requiring some pretreatment of the sample before analysis. The detection limit is $0.8 \mu\text{g L}^{-1}$. The $4\beta(\text{NH}_2)\text{Ni}(\text{OH})\text{Pc}$ (containing O–Ni–O bridges) shows high catalytic activity for the detection of DA via its oxidation, which is much better than for poly- $4\beta(\text{NH}_2)\text{NiPc}$ without the O–Ni–O oxo bridges [121].
- (iii) Nanoparticles of $4\beta(\text{SO}_3^-)\text{NiPc}$ and the Chichá gum [272] in a tetralayer with poly(allylamine hydrochloride) interposed between the layers allows the detection of DA with a detection limit of $1 \times 10^{-5} \text{ M}$.
- (iv) Indium tin oxide coated glass substrates modified with layer by layer films of polyaniline alternated with $4\beta(\text{SO}_3^-)\text{FePc}$ show catalytic activity for the oxidation of DA. The activity is explained in terms of a coordination between the two and the formation of a $(\text{DA}^+)4\beta(\text{SO}_3^-)\text{FePc}$ species via internal electron transfer [273].
- (v) Single-walled carbon nanotube SWCNT co-ordinated to $4\beta(\text{NH}_2)\text{CoPc}$ and assembled onto a preformed aminoethanethiol SAM on gold electrode (Scheme 1) can be used for the electrochemical detection of DA in pH 7.4 PBS [499]. These studies prove that SWCNT greatly improves the electronic communication between $4\beta(\text{NH}_2)\text{CoPc}$ and the Au electrode surface.

9. Oxidation of glucose and other sugars at molecular phthalocyanine electrodes

Future sensors, pacemakers, communication devices and other microelectronics technology may be powered by bio fuel cells, i.e. powered by sugars obtained from living systems that can include human or plant living tissue. On the other hand, monitoring glucose levels in human or animal fluids is important from the medical point

of view. So the electrocatalytic oxidation of glucose is a subject of current interest. The electrochemical oxidation of glucose can also be used for its detection using appropriate electrodes. MPCs show catalytic activity for the oxidation of glucose. Santos and Baldwin [500] were the first to report that chemically modified electrodes containing CoPc are active for the electrooxidation several sugars including glucose, galactose, maltose, lactose, ribose, fructose and sucrose in alkaline media. Sun et al. [501] used self-assembled molecular layer-based process on gold electrodes to allow the fixation of cobalt tetrasulfonated phthalocyanine to detect glucose. Several authors have proposed the use of Co phthalocyanine derivatives [55,502–504] as mediators of glucose oxidation, in conjunction with glucose oxidase (GOX). Along these lines Hart and co-workers have developed screen-printed electrodes which are fabricated using water-based carbon ink [505] containing GOX and CoPc. With this last approach it is possible to obtain low-cost electrodes for sensor applications.

Zagal and co-workers [59,60] have studied the role of the Co(II)/Co(I) formal potential of the catalyst on the electrocatalytic activity for glucose oxidation and have found volcano correlations, as reported for other reactions discussed in this article. The activity of the different modified electrodes was tested by linear voltammetry under hydrodynamic conditions using the rotating disk technique. Tafel plots constructed from mass-transport corrected currents gave slopes ranging from 0.080 to 0.160 V/decade for the different catalysts which suggests that the first-one electron step is rate controlling with the symmetry of the energy barrier depending on the nature of the ligand of the Co complex. A plot of $\log I$ versus the Co(II)/(I) formal potential gives a volcano curve (see Fig. 30) with a slope close to 0.118 V for the ascending portion and -0.20 V for the falling region. This is an “unsymmetrical” volcano, which is a common observation for other reactions discussed in this review. This illustrates once more the concept that the formal potential of the catalyst needs to be tuned to a certain value for achieving maximum activity not only for this reaction but probably for most reactions catalyzed by phthalocyanines, porphyrins and by macrocyclic complexes in general. A theoretical interpretation of these results has been given in terms of Langmuir isotherms [60] for the adsorption of glucose on the Co sites of the surface-confined metal complexes, as discussed before for the oxidation of thiols and for other reactions. These electrodes modified with metal complexes and with any reactive species present a great advantage over conventional electrodes in the sense that their reactivity can be

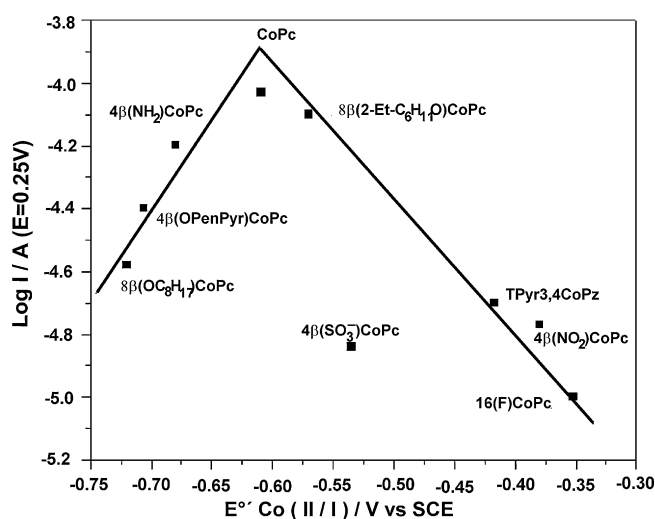


Fig. 30. Plot of $\log I$ versus redox potential of CoPcs for the electrooxidation of glucose in deaerated 0.15 M NaOH on OPG modified with the different Co complexes. From ref. [60] (Reproduced with permission of Elsevier.).

controlled by manipulating the structure of the complex or reactive molecule to be confined on the surface of the electrode.

10. Conclusion and perspectives

MPcs are active catalysts for a large variety of electrochemical reactions. Electrodes containing these complexes confined on their surfaces can be obtained by simple adsorption on graphite and carbon electrodes. However, more stable electrodes can be achieved by coating their surfaces with electropolymerized complexes which show similar activity than their monomer counterparts. Modified electrodes can also be obtained on Au and Ag surfaces by using self-assembled monolayers of thiols that can act as anchors of macrocyclic complexes or by using complexes with thiol functionalities located on the periphery of the ligand, also serving as anchors. Electrodes modified by this method show catalytic activity for several electrochemical reactions so essentially, the activity of MPcs is almost independent of the method employed for electrode modification and seems to be independent of the orientation of the macrocyclic molecule on the electrode.

Fundamental studies carried out at adsorbed layers of these complexes on graphite and carbon surfaces have demonstrated that the redox potential is a very good reactivity index for predicting catalytic activities for many reactions. Volcano-shaped correlations have been reported between the electrocatalytic activity (as $\log I$ at constant E) versus the Co(II)/(I) formal potential of Co-macrocyclics for the oxidation of several thiols, hydrazine and glucose. For the electroreduction of O_2 only linear correlations between the electrocatalytic activity versus M(III)/M(II) redox potential have been found using Cr, Mn, Fe and Co phthalocyanines. It is very likely that these linear correlations are part of “incomplete” volcano correlations as found with earlier studies with thiol oxidation. The volcano correlations strongly suggest that intermediate values of E° , the formal potential of the complex, are optimum for achieving maximum activity, probably corresponding to surface coverages of an M-molecule adduct equal to 0.5 and to standard free energies of adsorption equal to zero. All these results indicate that the catalytic activity of MPcs for the oxidation of several molecules can be “tuned” by manipulating the E° formal potential, using the proper groups on the ligand. “Tuning” the redox potential can be achieved by knowing the Hammett parameters of substituents that can be located on the ligand for families bearing the same ligand. These results are probably valid for the different methods of modification of the electrode and point out to the right direction in designing better catalysts for many electrochemical reactions.

Finally, it is necessary to emphasize once more that MPcs are extremely versatile materials with many applications in electrocatalysis, and they provide very good models for testing their catalytic activity for many reactions in terms of simple parameters, such as the redox potential of these molecules. The redox potential can be easily modulated by placing the appropriate substituents on peripheral or non-peripheral positions of the phthalocyanine ligand. This is obviously valid for other macrocyclics like porphyrins. Even though the earlier applications of these complexes were focused on providing active materials for electroreduction of O_2 , for making active cathodes for fuel cells, the main trend in the literature nowadays is to use these complexes for making active electrodes for electrochemical sensors.

Acknowledgements

J.H.Z. thanks financial support by Fondecyt Projects 1060030 and 1100773 Chile, and to Nucleo Milenio de Ingenieria Molecular P07-006-F, Chile. J.F.S. is grateful to Proyecto Bicentenario PDA23 for support. T.N. thanks Department of Science and Technology (DST)

and National Research Foundation (NRF) of South Africa through DST/NRF South African Research Chairs Initiative for Professor of Medicinal Chemistry and Nanotechnology and Rhodes University. FB, SG and TN knowlegge finacial support from PROTEA project 07 F 10/SA (France-South Africa). Co-workers whose names appear in the references of this review are acknowledged for their highly significant contributions.

References

- [1] F.H. Moser, A.L. Thomas, The Phthalocyanines, vols. 1 and 2, CRC Press, Boca Raton, FL, 1983.
- [2] Katalyse und Phthalocyaninen, M. Kropf, F. Steinbach (Eds.), Georg Thieme, Verlag Stuttgart, 1973.
- [3] J. Manassen, Catal. Rev. Sci. Eng. 9 (1974) 223.
- [4] L.J. Bocler, in: G.A. Melson (Ed.), Coordination Chemistry of Macrocyclic Compounds, Plenum Press, New York, 1979.
- [5] C.C. Leznoff, A.B.P. Lever, Phthalocyanines, Properties and Applications, vols. 1–4, VCH Publishers Inc., New York, 1989.
- [6] R. Jasinski, Nature 201 (1964) 1212.
- [7] R. Jasinski, J. Electrochem. Soc. 112 (1965) 526.
- [8] H. Jahnke, M. Schönborn, G. Zimmermann, Topics Curr. Chem. 61 (1976) 133.
- [9] F. van den Brink, E. Barendrecht, W. Visscher, Rec. J. Roy. Neth. Chem. Soc. 99 (1980) 253.
- [10] M.R. Tarasevich, K.A. Radyushkina, Russ. Chem. Rev. 49 (1980) 718.
- [11] M.R. Tarasevich, A. Sadkowsky, E. Yeager, in: B. Conway, J. Bockris, E. Yeager, S. Khan, R. White (Eds.), Comprehensive Treatise of Electrochemistry Volume 7: Kinetics and Mechanisms of Electrode Processes, Plenum Press, New York, 1983, p. 301 (Chapter 6).
- [12] K. Wiesener, D. Ohms, V. Neumann, R. Franke, Mater. Chem. Phys. 22 (1989) 457.
- [13] P. Vasudevan, Santosh, N. Mann, S. Tyagi, Trans. Met. Chem. 15 (1990) 81.
- [14] J.H. Zagal, Coord. Chem. Rev. 119 (1992) 89.
- [15] R. Adzic, in: J. Lipkowski, P.N. Ross (Eds.), Electrocatalysis, Frontiers in Science, Wiley-VCH, 1998, p. 197.
- [16] J.H. Zagal, in: W. Vielstich, A. Lamm, H. Gasteiger (Eds.), Handbook of Fuel Cells-Fundamentals, Technology and Applications, vol. 2 Part 5, John Wiley & Sons, Ltd., Chichester, 2003, p. 544.
- [17] J.P. Dodelet, in: J.H. Zagal, F. Bedioui, J.P. Dodelet (Eds.), N4 Macrocyclic Metal Complexes, Springer, New York, 2006, p. 83.
- [18] J.H. Zagal, F. Silva, M. Páez, in: J.H. Zagal, F. Bedioui, J.P. Dodelet (Eds.), N4 Macrocyclic Metal Complexes, Springer, New York, 2006, p. 41.
- [19] D.A. Scherson, A. Palencsar, Y. Tolmochov, I. Stefan, in: R. Alkire, D. Kolb, J. Lipkowski, P. Ross (Eds.), Electrochemical Surface Modification, vol. 10, Wiley VCH, 2008, p. 191.
- [20] H. Li, T.F. Guarr, J. Chem. Soc. Chem. Commun. (1989) 832.
- [21] A.B.P. Lever, J. Porph. Phthal. 3 (1999) 488.
- [22] F. D'Souza, J. Porph. Phthal. 6 (2002) 285.
- [23] F. van den Brink, E. Barendrecht, W. Visscher, Recl. Trav. Chim. Pays-Bas 99 (1980) 253.
- [24] K.A. Rayushkina, M.R. Tarasevich, Elektrokhimiya 22 (1986) 1155.
- [25] E. Yeager, Electrochim. Acta 29 (1984) 1527.
- [26] N. Kobayashi, W.A. Nevin, Appl. Organomet. Chem. 10 (1996) 579.
- [27] P. Vasudevan, N. Phougat, A.K. Shukla, Appl. Organomet. Chem. 10 (1996) 591.
- [28] A.B.P. Lever, Y. Ma, in: A.J.L. Pombeiro, C. Amatore (Eds.), New Trends in Molecular Electrochemistry, Fontismedia/Marcel Dekker, Lausanne, Switzerland, 2004, p. 99.
- [29] J. Ma, Y. Liu, P. Zhang, J. Wang, Electrochem. Commun. 10 (2008) 100.
- [30] R.D. Patent, 2,128,842 (1972); Chem. Abs. 78 (1973) 79028.
- [31] J.A.R. van Veen, Ph.D. Thesis, Rijks Universiteit, Holland, 1981.
- [32] J.T. van Baar, J.A.R. van Veen, N. de Wit, Electrochim. Acta 27 (1982) 57.
- [33] J.F. van Baar, J.A.R. van Veen, J.M. van der Eijk, Th.J. Peters, N. de Wit, Electrochim. Acta 27 (1982) 1315.
- [34] K.A. Radyushkina, M.R. Tarasevich, E.A. Akhundov, Elektrokhimiya 15 (1979) 1884.
- [35] E.A. Akhundov, Mater. Konf. Molodykh Uch. Aspir. (1979) 46.
- [36] V.V. Zvezdina, L.V. Oparin, E.A. Vinogradova, V.P. Bochin, B.D. Berezin, D.A. Golubchikov, Vopr. At. Nanki i Tekhn. Atom-vodorov. Energ. i Tekhnol. (Moskba) 2–9 (1981) 10.
- [37] S. Meshitzuka, K. Tamaru, J. Chem. Soc. Faraday Trans. 73 (1977) 236.
- [38] A.R. Ramos, J. Arguello, H.A. Magosso, Y. Gushikem, J. Braz. Chem. Soc. 19 (2008) 755.
- [39] J. Arguello, H.A. Magosso, R. Landers, Y. Gushikem, J. Electroanal. Chem. 617 (2008) 45.
- [40] T.C. Canevari, J. Arguello, M.S.P. Francisco, Y. Gushikem, J. Electroanal. Chem. 609 (2007) 61.
- [41] M. Toledo, A.M.S. Lucho, Y. Gushikem, J. Mater. Sci. 39 (2004) 6851.
- [42] S.T. Fujiwara, Y. Gushikem, J. Braz. Chem. Soc. 10 (1999) 389.
- [43] J. Wang, P.V.A. Pamidi, C. Parrado, D.S. Park, J. Pingarron, Electroanalysis 9 (1997) 908.
- [44] G. Dong, J. Li, R. Zhuang, Fenzi Cuihua 10 (1996) 387.
- [45] H. Li, T.F. Guarr, J. Electroanal. Chem. 317 (1991) 189.
- [46] J. Wang, T. Golden, K. Varughese, I. El-Rayes, Anal. Chem. 61 (1989) 508.

- [47] J. Wang, T. Golden, R. Li, *Anal. Chem.* 60 (1988) 1642.
- [48] L.M. Santos, R.P. Baldwin, *Anal. Chem.* 58 (1986) 848.
- [49] Y.B. Vasil'ev, O.A. Khazova, N.N. Nikolaeva, *J. Electroanal. Chem.* 196 (1985) 127.
- [50] H. Sun, H. Tachikawa, *Anal. Chem.* 64 (1992) 1112.
- [51] I. Rosen-Margalit, A. Bettelheim, J. Rishpon, *Anal. Chim. Acta* 281 (1993) 327.
- [52] T.J. O'Shea, S.M. Lunte, *Anal. Chem.* 66 (1994) 307.
- [53] F. Mizutani, S. Yabuki, S. Iijima, *Anal. Chim. Acta* 300 (1995) 59.
- [54] J.P. Hart, S.A. Wring, *Trends Anal. Chem.* 16 (1997) 89.
- [55] K.I. Ozoemena, T. Nyokong, *Electrochim. Acta* 51 (2006) 5131.
- [56] R. Fogel, P. Mashazi, T. Nyokong, J. Limson, *Biosens. Bioelectron.* 23 (2007) 95.
- [57] P.N. Mashazi, K.I. Ozoemena, D.M. Maree, T. Nyokong, *Electrochim. Acta* 51 (2006) 3489.
- [58] P.N. Mashazi, K.I. Ozoemena, T. Nyokong, *Electrochim. Acta* 52 (2006) 177.
- [59] C. Barrera, I. Zhukov, E. Villagra, F. Bedioui, M.A. Páez, J. Costamagna, J.H. Zagal, *J. Electroanal. Chem.* 589 (2006) 212.
- [60] E. Villagra, F. Bedioui, T. Nyokong, J.C. Canales, M.A. Páez, J. Costamagna, J.H. Zagal, *Electrochim. Acta* 53 (2008) 4883.
- [61] C. Sun, X. Zhang, D. Jiang, Q. Gao, H. Xu, Y. Sun, X. Zhang, J. Shen, *J. Electroanal. Chem.* 411 (1996) 73.
- [62] G. Turdean, I.C. Popescu, L. Oniciu, *Revue Roumaine de Chimie* 43 (1998) 203.
- [63] K. Wang, J.-J. Xu, H.-Y. Chen, *Biosens. Bioelectron.* 20 (2005) 1388.
- [64] U.S. Patent 5,585,079 (1971).
- [65] U.S. Patent 3,617,388 (1971).
- [66] O.A. Osmanbas, A. Koca, M. Kandaz, F. Karaca, *Int. J. Hydrogen Energy* 33 (2008) 3281.
- [67] F.J. Rawson, W.M. Purcell, J. Xu, D.C. Cowell, P.R. Fielden, N. Biddle, J.P. Hart, *Electrochim. Acta* 52 (2007) 7248.
- [68] A. Koca, S.M. Kasim, M.B. Kocak, A. Guel, *Int. J. Hydrogen Energy* 31 (2006) 2211.
- [69] K.I. Ozoemena, Z. Zhao, T. Nyokong, *Electrochim. Commun.* 7 (2005) 679.
- [70] J.H. Zagal, *J. Electroanal. Chem.* 109 (1980) 389.
- [71] J.H. Zagal, C. Fierro, E. Muñoz, R. Rozas, S. Ureta, in: W.E. O'Grady, P.N. Ross Jr., F.G. Will (Eds.), *Electrocatalysis, The Electrochemical Society Symposium Series*, 1982, p. 389.
- [72] J. Zagal, S. Ureta-Zañartu, *J. Electrochem. Soc.* 129 (1982) 2242.
- [73] J. Zagal, E. Muñoz, S. Ureta-Zañartu, *Electrochim. Acta* 27 (1982) 1373.
- [74] J. Zagal, P. Herrera, K. Brinck, S. Ureta-Zañartu, *Proc. Electrochem. Soc.* 84 (1984) 602.
- [75] J. Zagal, S. Lira, S. Ureta-Zañartu, *J. Electroanal. Chem.* 210 (1986) 95.
- [76] Q.-Y. Peng, T.F. Guarr, *Electrochim. Acta* 39 (1994) 2629.
- [77] E. Trollund, P. Ardiles, M.J. Aguirre, S. Xe, R. Biaggio, R.C. Rocha-Filho, *Polyhedron* 19 (2000) 2303.
- [78] M. Ebadi, *Can. J. Chem.* 81 (2003) 161.
- [79] M. Isaacs, M.J. Aguirre, A. Toro-Labbé, J. Costamagna, M. Paez, J.H. Zagal, *Electrochim. Acta* 43 (1998) 1821.
- [80] K.M. Korfhage, K. Ravichandran, R.P. Baldwin, *Anal. Chem.* 56 (1984) 1514.
- [81] M.P. Vinod Kr, T. Das, A.J. Chadawadkar, K. Vijayamohan, J.G. Chandawadkar, *Mater. Chem. Phys.* 58 (1999) 37.
- [82] K. Ozoemena, T. Nyokong, *Talanta* 67 (2005) 162.
- [83] D. Geraldo, C. Linares, Y.-Y. Chen, S. Ureta-Zañartu, J.H. Zagal, *Electrochim. Commun.* 4 (2002) 182.
- [84] C. Linares, D. Geraldo, M. Paez, J.H. Zagal, *J. Solid State Electrochem.* 7 (2003) 626.
- [85] L.M.F. Dantas, A.P. dos Reis, S.M.C.N. Tanaka, J.H. Zagal, Y.-Y. Chen, A.-A. Tanaka, *J. Braz. Chem. Soc.* 19 (2008) 720.
- [86] D.A. Geraldo, C.A. Togo, J. Limson, T. Nyokong, *Electrochim. Acta* 53 (2008) 8051.
- [87] C. das, D. Conceicao, R.C. Faria, O. Fatibello-Filho, A.A. Tanaka, *Braz. Anal. Lett.* 41 (2008) 1010.
- [88] J. Zhang, Y.-H. Tse, W.J. Pietro, A.B.P. Lever, *J. Electroanal. Chem.* 406 (1996) 203.
- [89] N. Nombona, P. Tau, N. Sehloho, T. Nyokong, *Electrochim. Acta* 53 (2008) 3139.
- [90] P. Tau, T. Nyokong, *Electrochim. Acta* 52 (2007) 4547.
- [91] J.H. Zagal, C. Páez, *Electrochim. Acta* 34 (1989) 243.
- [92] F. Bedioui, S. Griveau, T. Nyokong, A.J. Appleby, C.A. Caro, M. Gulppi, G. Ochoa, J.H. Zagal, *Phys. Chem. Chem. Phys.* 9 (2007) 3383.
- [93] N. Sehloho, S. Griveau, N. Ruillé, M. Boujtita, T. Nyokong, F. Bedioui, *Mater. Sci. Eng. C* 28 (2008) 606.
- [94] J. Zagal, C. Fierro, R. Rozas, *J. Electroanal. Chem.* 119 (1981) 403.
- [95] J. Zagal, P. Herrera, *Electrochim. Acta* 30 (1985) 449.
- [96] M.K. Halbert, R.P. Baldwin, *Anal. Chem.* 57 (1985) 591.
- [97] P.N. Mashazi, P. Westbroek, K.I. Ozoemena, T. Nyokong, *Electrochim. Acta* 53 (2007) 858.
- [98] J.C. Obirai, T. Nyokong, *J. Electroanal. Chem.* 600 (2007) 251.
- [99] R.C.S. Luz, A.B. Moreira, F.S. Damos, A.A. Tanaka, L.T. Kubota, *J. Pharm. Biomed. Anal.* 42 (2006) 184.
- [100] N. Sehloho, T. Nyokong, J.H. Zagal, F. Bedioui, *Electrochim. Acta* 51 (2006) 5125.
- [101] N. Sehloho, T. Nyokong, *Electrochim. Acta* 51 (2006) 4463.
- [102] K.I. Ozoemena, T. Nyokong, *Electrochim. Acta* 51 (2006) 2669.
- [103] C.D. Kuhnline, M.G. Gangel, M.K. Hulvey, R.S. Martin, *Analyst* 131 (2006) 202.
- [104] J.C. Obirai, T. Nyokong, *Electrochim. Acta* 50 (2005) 5427.
- [105] S.S. Khaloo, M.K. Amini, S. Tangestaninejad, S.K. Shahrokhian, *J. Iran. Chem. Soc.* 1 (2004) 128.
- [106] S. Griveau, M. Gulppi, J. Pavez, J.H. Zagal, F. Bedioui, *Electroanalysis* 15 (2003) 779.
- [107] S. Komorsky-Lovric, M. Lovric, F. Scholz, *Mikrochim. Acta* 127 (1997) 95.
- [108] K.I. Ozoemena, T. Nyokong, P. Westbroek, *Electroanalysis* 15 (2003) 1762.
- [109] K. Ozoemena, T. Nyokong, *J. Electroanal. Chem.* 579 (2005) 283.
- [110] J. Zagal, E. Villar, S. Ureta-Zañartu, *J. Electroanal. Chem.* 135 (1982) 343.
- [111] M. Ebadi, A.B.P. Lever, *J. Porph. Phthal.* 7 (2003) 529.
- [112] M. Ebadi, *Electrochim. Acta* 48 (2003) 4233.
- [113] M. Pontie, C. Gobin, T. Pauporté, F. Bedioui, J. Devynck, *Anal. Chim. Acta* 411 (2000) 175.
- [114] P. Ascenzi, R. Fruttero, C.I. Ercolani, F. Monacelli, *Analisis* 24 (1996) 316.
- [115] I. Zilbermann, J. Hayon, T. Katchalski, O. Raveh, J. Rishpon, A.I. Shames, E. Korin, A. Bettelheim, *J. Electrochem. Soc.* 144 (1997) L228.
- [116] S.L. Vilakazi, T. Nyokong, *J. Electroanal. Chem.* 512 (2001) 56.
- [117] S.L. Vilakazi, T. Nyokong, *Polyhedron* 19 (2000) 229.
- [118] S.L. Vilakazi, T. Nyokong, *Polyhedron* 17 (1998) 4415.
- [119] J. Obirai, T. Nyokong, *J. Electroanal. Chem.* 573 (2004) 77.
- [120] F.C. Moraes, M.F. Cabral, S.A.S. Machado, L.H. Mascaro, *Electroanalysis* 20 (2008) 851.
- [121] A. Goux, F. Bedioui, L. Robbiola, M. Pontie, *Electroanalysis* 15 (2003) 969.
- [122] T.-F. Kang, G.-L. Shen, R.-Q. Yu, *Anal. Chim. Acta* 354 (1997) 343.
- [123] M. Dieng, O. Contamin, M. Savy, *Electrochim. Acta* 33 (1988) 121.
- [124] K. De Wael, A. Adriaens, *Talanta* 74 (2008) 1562.
- [125] M.S. Ureta-Zañartu, C. Berrios, J. Pavez, J. Zagal, C. Gutierrez, J.F. Marco, *J. Electroanal. Chem.* 553 (2003) 147.
- [126] J. Obirai, F. Bedioui, T. Nyokong, *J. Electroanal. Chem.* 576 (2005) 323.
- [127] B. Agboola, T. Nyokong, *Electrochim. Acta* 52 (2007) 5039.
- [128] A. Alatorre Ordaz, F. Bedioui, S. Gutierrez Granados, *Boletín de la Sociedad Chilena de Química* 43 (1998) 375.
- [129] R. Jiang, S. Dong, *Electrochim. Acta* 35 (1990) 1227.
- [130] M. Ebadi, C. Alexiou, A.B.P. Lever, *Can. J. Chem.* 79 (2001) 992.
- [131] F. Zhao, J. Zhang, T. Abe, D. Wohrle, M. Kaneko, *J. Mol. Catal. A: Chem.* 145 (1990) 245.
- [132] S. Meshitsuka, M. Ichikawa, K. Tamaru, *J. Chem. Soc. Chem. Commun.* (1974) 158.
- [133] H. Tanabe, K. Ohno, *Electrochim. Acta* 32 (1987) 1121.
- [134] P.A. Christensen, A. Hammett, A.V.G. Muir, *J. Electroanal. Chem.* 241 (1988) 361.
- [135] S. Kapusta, N. Hackerman, *J. Electrochem. Soc.* 131 (1984) 1511.
- [136] T.V. Magdesieva, K.P. Butin, T. Yamamoto, D.A. Tryk, A. Fujishima, *J. Electrochem. Soc.* 150 (2003) E608.
- [137] T.V. Magdesieva, I.V. Zhukov, D.N. Kravchuk, O.A. Semenikhin, L.G. Tomilova, K.P. Butin, *Russ. Chem. Bull.* 51 (2002) 805.
- [138] T. Abe, F. Taguchi, T. Yoshida, S. Tokita, G. Schnurpfeil, D. Woehrle, M. Kaneko, *J. Mol. Catal. A: Chem.* 112 (1996) 55.
- [139] T. Abe, T. Yoshida, S. Tokita, F. Taguchi, H. Imai, M. Kaneko, *J. Electroanal. Chem.* 412 (1996) 125.
- [140] T. Yoshida, K. Kamato, M. Tsukamoto, T. Iida, D. Schlettwein, D. Woehrle, M. Kaneko, *J. Electroanal. Chem.* 385 (1995) 209.
- [141] D. Lexa, J.M. Saveant, J.P. Soufflet, *J. Electroanal. Chem.* 100 (1979) 159.
- [142] C.M. Elliot, C.A. Marrese, *J. Electroanal. Chem.* 119 (1981) 395.
- [143] Z. Wang, D. Pang, *J. Electroanal. Chem.* 283 (1990) 349.
- [144] N. Furuya, L.H. Yoshida, *J. Electroanal. Chem.* 263 (1989) 171.
- [145] J.P. Collman, N. Marrocco, C.M. Elliot, M.L. Her, *J. Electroanal. Chem.* 124 (1981) 113.
- [146] J. Zhang, Y.-H. Tse, W.J. Pietro, A.B.P. Lever, *J. Porph. Phthal.* 1 (1997) 323.
- [147] X.K. Xing, A.A. Tanaka, C. Fierro, D. Scherson, 170th Meeting of The Electrochemical Society, San Diego, 1986, p. 1071 (Abstract 727).
- [148] H.L. Li, J.Q. Chambers, D.T. Hobbs, *J. Appl. Electrochem.* 18 (1988) 454.
- [149] M. Shibata, N. Furuya, *Electrochim. Acta* 48 (2003) 3953.
- [150] N. Chebotareva, T. Nyokong, *J. Appl. Electrochem.* 27 (1997) 975.
- [151] N. Doddapaneni, Spring Meeting, The Electrochem. Soc., Minneapolis, 1981 (Abstract 83).
- [152] N. Doddapaneni, Proceedings of the 30th Power Sources Symposium, 1982, p. 169.
- [153] N. Doddapaneni, Fall Meeting, The Electrochemical Society, Detroit, 1982 (Abstract 360).
- [154] N. Doddapaneni, in: J.D. McIntyre, M.J. Weaver, E.B. Yeager (Eds.), *The Chemistry and Physics of Electrocatalysis, The Electrochemical Society Softbound Proceeding Series*, 84-12, 1984, p. 618.
- [155] M.J. Madou, K. Kinoshita, M.C.M. Mc Kubre, S. Szpak, *J. Electrochem. Soc.* 130 (1983) C126.
- [156] M.J. Madou, J.J. Smith, S. Szpak, *J. Electrochem. Soc.* 34 (1987) 2794.
- [157] N. Doddapaneni, U.S. Patent 4,405,693 (1983).
- [158] W.P. Kilroy, M. Alingir, E.B. Willstaed, K.M. Abraham, in: K.M. Abrahams, M. Salomon (Eds.), *Primary and Secondary Lithium Batteries, The Electrochem. Soc.*, 91-3 1991, p. 12.
- [159] N. Doddapaneni, U.S. Patent 4,439,503 (1984).
- [160] A.J. Hills, N.A. Hampson, *J. Electrochem. Soc.* 135 (1988) 1861.
- [161] R.J. Nowak, D.R. Rolison, J.J. Smith, S. Szpak, *Electrochim. Acta* 33 (1988) 1313.
- [162] J.H. Zagal, C. Páez, S. Barbato, in: S. Srinivasan, S. Wagner, H. Wroblowa (Eds.), *Electrode Materials and Processes for Energy Conversion and Storage, The Electrochem. Soc.* 87-12, 1987, p. 211.
- [163] J.H. Zagal, J. de la Fuente, G. Lagos, *Bol. Soc. Chil. Quím.* 34 (1989) 301.
- [164] P.A. Bernstein, A.B.P. Lever, *Inorg. Chem.* 29 (1990) 608.
- [165] N. Sonoyama, H. Fujii, T. Sakata, *J. Electrochem. Soc.* 149 (2002) D182.

- [166] J.H. Sharp, M. Lardon, *J. Chem. Phys.* 72 (1968) 3230.
- [167] J.I. Yamaki, A. Yamaji, *J. Electrochem. Soc.* 129 (1982) 5.
- [168] D. Wöhrle, M. Kirschmann, N.I. Jaeger, *J. Electrochem. Soc.* 132 (1985) 1150.
- [169] M. Tachikawa, L.R. Faulkner, *J. Am. Chem. Soc.* 100 (1978) 4379.
- [170] N. Minami, T. Watanabe, A. Fujishima, K. Honda, B. Bunsenges, *Phys. Chem.* 83 (1976) 476.
- [171] F.F. Fan, A.J. Bard, *J. Am. Chem. Soc.* 101 (1979) 6139.
- [172] Y.S. Shuov, S.S. Chakhmakchyan, V.I. Ityaev, G.G. Komissarov, *Zh. Fiz. Khim.* 53 (1979) 1834.
- [173] V.R. Shepard Jr., N.R. Armstrong, *J. Phys. Chem.* 83 (1979) 1268.
- [174] F. Fan, L.R. Faulkner, *J. Am. Chem. Soc.* 101 (1979) 4779.
- [175] W.M. Ayers, *Faraday Disc* 70 (1980) 247.
- [176] N. Minami, *J. Chem. Phys.* 72 (1980) 6317.
- [177] C.D. Jaeger, F.F. Fan, A.J. Bard, *J. Am. Chem. Soc.* 102 (1980) 2592.
- [178] A. Giraudeau, F.F. Fan, A.J. Bard, *J. Am. Chem. Soc.* 102 (1980) 5137.
- [179] Y. Nakato, M. Shioji, M. Tsuboura, *J. Phys. Chem.* 85 (1981) 1670.
- [180] T. Mezza, C.L. Linkous, V.R. Shepard, N.R. Armstrong, R. Nohr, M. Kenney, *J. Electroanal. Chem.* 124 (1981) 311.
- [181] N.R. Armstrong, T. Mezza, C.L. Linkous, B. Thacker, T. Klofta, R. Cielinski, in: J.S. Miller (Ed.), *Chemically Modified Surfaces in Catalysis and Electrocatalysis*, ACS Symposium Series 192, 1982, p. 205.
- [182] T. Klofta, C. Linkous, N.R. Armstrong, *J. Electrochem. Soc.* 185 (1985) 73.
- [183] P. Loempoel, A. Castro-Acuña, F.R.F. Dan, A.J. Bard, *J. Phys. Chem.* 86 (1982) 1396.
- [184] P. Loempoel, F.R. Fan, A.J. Bard, *J. Phys. Chem.* 87 (1983) 2948.
- [185] C.A. Melendres, X. Feng, *J. Electrochem. Soc.* 130 (1983) 811.
- [186] K. Murata, S. Ito, K. Takahashi, B.M. Hoffman, *Appl. Phys. Lett.* 71 (1997) 674.
- [187] D. Schlottwein, in: J.H. Zagal, F. Bedioui, J.P. Dodelet (Eds.), *N₄ Macrocyclic Metal Complexes*, Springer, New York, 2006, p. 467.
- [188] W.H. Flora, H.K. Hall, N.R. Armstrong, *J. Phys. Chem. B* 107 (2003) 1142.
- [189] P.N. Moskalev, S. Kirin, Russ. *J. Phys. Chem.* 46 (1972) 1019.
- [190] M.M. Nicholson, F.A. Pizzarello, *J. Electrochem. Soc.* 127 (1980) 821.
- [191] H. Djellab, F. Dalard, *J. Electroanal. Chem.* 221 (1987) 105.
- [192] M.M. Nicholson, R.V. Galiardi, Final Report, Contract N 62269-76-C0574, AD-A039596, May 1977, (1977) 144073v (Che. Abstr. 87).
- [193] M.H. Nicholson, T.P. Weissmiller, Report C82-268/201, NTIS Order NAD-A120483, Rockwell, Anaheim, California, 1982.
- [194] J.L. Kahl, L.R. Faulkner, K. Dwarkanath, H. Tachikawa, *J. Am. Chem. Soc.* 108 (1986) 5434.
- [195] J.E. Hutchison, T.A. Postlethwaite, R.W. Murray, *Langmuir* 9 (1993) 3277.
- [196] J. Zak, H. Yuan, M. Ho, L.K. Woo, M.D. Porter, *Langmuir* 9 (1993) 2772.
- [197] T.A. Postlethwaite, J.E. Hutchison, K.W. Hathcock, R.W. Murray, *Langmuir* 11 (1995) 4109.
- [198] M.J. Cook, *Pure Appl. Chem.* 71 (1999) 2145.
- [199] M.P. Somashekarappa, J. Keshavayya, S. Sampath, *Pure Appl. Chem.* 74 (2002) 1609.
- [200] M.P. Somashekarappa, S. Sampath, *Chem. Commun.* (2002) 1262.
- [201] M.J. Cook, R. Hersans, J. McMurdo, D.A. Russell, *J. Mater. Chem.* 6 (1996) 149.
- [202] Z. Li, M. Lieberman, in: J.P. Blitz, C.B. Little (Eds.), *Fundamental and Applied Aspects of Chemically Modified Surfaces*, Royal Society of Chemistry, Lettchworth, 1999, p. 24.
- [203] Z. Li, M. Lieberman, W. Hill, *Langmuir* 17 (2001) 4887.
- [204] T. Nyokong, F. Bedioui, *J. Porph. Phthal.* 10 (2006) 1101.
- [205] H.O. Finklea, in: R.A. Meyers (Ed.), *Encyclopedia of Analytical Chemistry: Applications, Theory and Instrumentations*, Wiley, 2000, p. 10090 (Chapter 11).
- [206] E. Salomon, T. Angot, N. Papageorgiou, J.-M. Layet, *Surf. Sci.* 596 (2005) 74.
- [207] M. Lackinger, T. Müller, T.G. Gopakumar, F. Müller, M. Hietschold, G.W. Flynn, *J. Phys. Chem. B* 108 (2004) 2279.
- [208] G. Kalyuzhny, A. Vaskevich, G. Ashkenasy, A. Shanzer, I. Rubinstein, *J. Phys. Chem. B* 104 (2000) 8238.
- [209] J.B. Zheng, Y. Wang, *Semicond. Photon. Technol.* 11 (2005) 94.
- [210] G. Muthuraman, Y.-B. Shim, J.-H. Yoon, M.-S. Won, *Synth. Met.* 150 (2005) 165.
- [211] H. Varela, R.L. Bruno, R.M. Torresi, *Polymer* 44 (2003) 5369.
- [212] A. Guadarrama, C. De la Fuente, J.A. Acuna, M.D. Vazquez, M.L. Tascon, P. Batanero, *Quim. Anal.* 18 (1999) 209.
- [213] S. Yagi, M. Kimura, T. Koyama, K. Hanabusa, H. Shirai, *Polym. J.* 27 (1995) 1139.
- [214] C. Coutanceau, A. El Hourch, P. Crouigneau, J.M. Leger, C. Lamy, *Electrochim. Acta* 40 (1995) 2739.
- [215] N. Inagaki, S. Tasaka, Y. Ikeda, *J. Appl. Poly. Sci.* 55 (1995) 1451.
- [216] H. Eichhorn, M. Sturm, D. Woehle, *Macromol. Chem. Phys.* 196 (1995) 115.
- [217] J.R. Reynolds, M. Pyo, Y.J. Qiu, *J. Electrochem. Soc.* 141 (1994) 35.
- [218] A. El Hourch, A. Rakotondrainibe, B. Beden, P. Crouigneau, J.-M. Léger, C. Lamy, A.A. Tanaka, E.R. Gonzalez, *Electrochim. Acta* 39 (1994) 889.
- [219] A. El Hourch, S. Belcadi, P. Moisy, P. Crouigneau, J.-M. Léger, C. Lamy, *J. Electroanal. Chem.* 33 (1992) 1.
- [220] M. Kawashima, Y. Sato, M. Sato, M. Sakaguchi, *Polym. J.* 23 (1991) 37.
- [221] R.A. Bull, F.-R. Fan, A.J. Bard, *J. Electrochem. Soc.* 131 (1984) 687.
- [222] M. Kimura, T. Horai, K. Hanabusa, H. Shirai, *Chem. Lett.* 7 (1997) 653.
- [223] Y.J. Qui, J.R. Reynolds, *J. Polym. Sci., Part A: Polym. Chem.* 30 (1992) 1315.
- [224] S. Kurosawa, E. Tawara-Kondo, N. Minoura, N. Kamo, *Sens. Actuators B: Chem.* 43 (1997) 175.
- [225] S. Kurosawa, E. Tawara-Kondo, N. Kamo, *Anal. Chim. Acta* 337 (1997) 1.
- [226] A. Yu, W. Xu, W. Yang, Q. Jin, *Chin. Chem. Lett.* 2 (1991) 879.
- [227] Y. Osada, A. Mizumoto, *J. Appl. Phys.* 59 (1986) 1776.
- [228] A. Ferencz, N.R. Armstrong, G. Wegner, *Macromolecules* 27 (1994) 1517.
- [229] M.E. Boyle, J.D. Adkins, A.W. Snow, R.F. Cozzens, R.F. Brady Jr., *J. Appl. Poly. Sci.* 57 (1995) 77.
- [230] A. Pailletet, F. Bedioui, in: J.H. Zagal, F. Bedioui, J.P. Dodelet (Eds.), *N₄-Macrocyclic metal Complexes*, Springer, New York, 2006, p. 363.
- [231] R.G. Linford (Ed.), *Electrochemical Science and Technology of polymers*, Elsevier, London and New York, 1987.
- [232] J. Heinze, *Topics Curr. Chem.* 152 (1990) 1.
- [233] A. Merz, *Topics Curr. Chem.* 152 (1990) 49.
- [234] T.A. Skotheim (Ed.), *Handbook of Conducting Polymers*, vols. 1 and 2, Marcel Dekker, New York, 1986.
- [235] A. Deronzier, J.C. Moutet, *Acc. Chem. Res.* 22 (1989) 249.
- [236] D. Curran, J. Grimshaw, S.D. Perera, *Chem. Soc. Rev.* 20 (1991) 391.
- [237] J. Roncali, *Chem. Rev.* 92 (1992) 711.
- [238] T. Skotheim, M. Velasquez Rosenthal, C.A. Linkous, *J. Chem. Soc., Chem. Commun.* (1985) 612.
- [239] F. Mizutani, S.I. Lijima, Y. Tanabe, K. Tsuda, *J. Chem. Soc., Chem. Commun.* (1985) 1728.
- [240] M. Velasquez Rosenthal, T.A. Skotheim, C.A. Linkous, *Synth. Met.* 15 (1986) 219.
- [241] A. Elzing, A. Van Der Putten, W. Visscher, E. Barendrecht, *J. Electroanal. Chem.* 233 (1987) 113.
- [242] R. Jiang, S. Dong, *J. Electroanal. Chem.* 246 (1988) 101.
- [243] C.S. Choi, H. Tachikawa, *J. Am. Chem. Soc.* 112 (1990) 1757.
- [244] D.J. Walton, D.M. Hadingham, C.E. Hall, I.V.F. Viney, A. Chyla, *Synth. Met.* 41 (1991) 295.
- [245] B.R. Saunders, K.S. Murray, R.J. Fleming, *Synth. Met.* 47 (1992) 167.
- [246] N. Trombach, O. Hild, D. Schlottwein, D. Wöhrle, *J. Mater. Chem.* 12 (2002) 879.
- [247] D. Wöhrle, O. Hild, N. Trombach, R. Benders, G. Schnurpfel, O. Suvorova, *Macromol. Symp.* 186 (2002) 99.
- [248] J. Obirai, N. Pereira Rodrigues, F. Bedioui, T. Nyokong, *J. Porph. Phthal.* 7 (2003) 508.
- [249] I. Chambrier, M.J. Cook, D.A. Russell, *Synthesis* (1995) 1283.
- [250] K.L. Brown, J. Shaw, M. Ambrose, H.A. Mottola, *Microchem. J.* 72 (2002) 285.
- [251] S. Zhang, W.-L. Sun, Y.-Z. Xian, W. Zhang, L.-T. Jin, K. Yamamoto, S. Tao, J. Jin, *Anal. Chim. Acta* 399 (1999) 213.
- [252] M.E. Boyle, J.D. Adkins, A.W. Snow, R.F. Cozzens, R.F. Brady Jr., *J. Appl. Poly. Sci.* 57 (1995) 77.
- [253] J. Wang, *Anal. Lett.* 29 (1996) 1575.
- [254] G. Ramirez, E. Trollund, J.C. Canales, M.J. Canales, F. Armijo, M.J. Aguirre, *Bol. Soc. Chil. Quim.* 46 (2001) 247.
- [255] N.M. Alpatova, E.V. Ovsyannikova, L.G. Tomilova, O.V. Korenchenko, Y. Kon-drashov, *Russ. J. Electrochem.* 37 (2001) 1012.
- [256] K. Ozoemena, P. Westbroek, T. Nyokong, *J. Porph. Phthal.* 6 (2002) 98.
- [257] K. Ozoemena, T. Nyokong, *Microchem. J.* 75 (2003) 241.
- [258] K.L. Brown, H.A. Mottola, *Langmuir* 14 (1998) 3411.
- [259] Y.-H. Tse, P. Janda, H. Lam, A.B.P. Lever, *Anal. Chem.* 67 (1995) 981.
- [260] J. Obirai, T. Nyokong, *Electrochim. Acta* 49 (2004) 1417.
- [261] G. Ramirez, E. Trollund, M. Isaacs, F. Armijo, J. Zagal, J. Costamagna, M.J. Aguirre, *Electroanalysis* 14 (2002) 540.
- [262] N. Pereira Rodrigues, J. Obirai, T. Nyokong, F. Bedioui, *Electroanalysis* 17 (2005) 186.
- [263] N. Hu, J.F. Rusling, *Anal. Chem.* 63 (1991) 2163.
- [264] N.G. Kama, J.F. Rusling, *Langmuir* 12 (1996) 2645.
- [265] M. Ozsoz, A. Erdem, E. Kilinc, L. Gokgunec, *Electroanalysis* 8 (1996) 147.
- [266] T. Mafatle, T. Nyokong, *Anal. Chim. Acta* 354 (1997) 307.
- [267] S.J. Hart, A.A. Dowman, D.C. Cowell, *Biosens. Bioelectron.* 16 (2001) 887.
- [268] J. Oni, T. Nyokong, *Anal. Chim. Acta* 434 (2001) 9.
- [269] J. Oni, P. Westbroek, T. Nyokong, *Electroanalysis* 15 (2003) 847.
- [270] T.-F. Kang, G.-L. Shen, R.-Q. Yu, *Anal. Chim. Acta* 356 (1997) 245.
- [271] G.-J. Yang, J.-J. Xu, K. Wang, H.-Y. Chen, *Electroanalysis* 18 (2006) 282.
- [272] F.M. Zampa, A.C. de Brito, I.L. Kitagawa, J.L.C. Constantino, O.N. Oliveira Jr., N.H. Da Cunha, V. Zucolotto, R.D.S. Jose Jr., C. Eirás, *Biomacromolecules* 8 (2007) 3408.
- [273] V. Zucolotto, M. Ferreira, M.R. Cordeiro, J.L.C. Constantino, D.T. Balogh, A.R. Zanatta, W.C. Moreira, O.N. Oliveira Jr., *J. Phys. Chem. B* 107 (2003) 3733.
- [274] S. Griveau, J. Pavez, J.H. Zagal, F. Bedioui, *J. Electroanal. Chem.* 497 (2001) 75.
- [275] I. Zilbermann, J. Hayon, T. Katchalski, R. Ydgar, J. Rishpon, A.I. Shames, E. Korin, A. Bettelheim, *Inorg. Chim. Acta* 305 (2000) 53.
- [276] M. Thamae, T. Nyokong, *J. Electroanal. Chem.* 470 (1999) 126.
- [277] C.A. Caro, F. Bedioui, J.H. Zagal, *Electrochim. Acta* 47 (2002) 1489.
- [278] B. Agboola, K. Ozoemena, T. Nyokong, *Electrochim. Acta* 51 (2006) 6470.
- [279] B. Agboola, T. Nyokong, *Anal. Chim. Acta* 587 (2007) 116.
- [280] F. Matemadombo, T. Nyokong, *Electrochim. Acta* 52 (2007) 6856.
- [281] P. Tau, T. Nyokong, *J. Electroanal. Chem.* 611 (2007) 10.
- [282] Z.-H. Wen, T.-F. Kang, *Talanta* 62 (2004) 351.
- [283] B. Retamal, M.E. Vaschetto, J.H. Zagal, *J. Electroanal. Chem.* 431 (1997) 1.
- [284] S. Maree, T. Nyokong, *J. Electroanal. Chem.* 492 (2000) 120.
- [285] K. Ozoemena, P. Westbroek, *Electrochem. Commun.* 3 (2001) 529.
- [286] M. Sekota, T. Nyokong, *Electroanalysis* 9 (1999) 1257.
- [287] T.J. Mafatle, T. Nyokong, *J. Electroanal. Chem.* 408 (1996) 213.
- [288] B. Ballarin, M. Gazzano, J.L. Hidalgo-Hidalgo de Cisneros, D. Tonelli, R. Seeber, *Anal. Bioanal. Chem.* 374 (2002) 891.
- [289] B. Filanovsky, *Anal. Chim. Acta* 394 (1999) 91.

- [290] M.J. Aguirre, M. Isaacs, F. Armijo, L. Basáez, J.H. Zagal, *Electroanalysis* 14 (2002) 356.
- [291] A. Napier, J.P. Hart, *Electroanalysis* 8 (1996) 1006.
- [292] S. Griveau, V. Albin, T. Pauporté, J.H. Zagal, F. Bedioui, *J. Mater. Chem.* 12 (2002) 225.
- [293] J.H. Zagal, M.E. Vaschetto, B.A. Retamal, *J. Poly. Mater.* 44 (1999) 225.
- [294] M.J. Aguirre, M. Isaacs, F. Armijo, N. Bocchi, J.H. Zagal, *Electroanalysis* 10 (1998) 571.
- [295] S. Griveau, M. Gulppi, F. Bedioui, J.H. Zagal, *Solid State Ionics* 169 (2004) 59.
- [296] J.H. Zagal, M.A. Gulppi, G. Cárdenas-Jirón, *Polyhedron* 19 (2000) 255.
- [297] J.F. Silva, S. Griveau, C. Richard, J.H. Zagal, F. Bedioui, *Electrochem. Commun.* 9 (2007) 1629.
- [298] M. Gulppi, S. Griveau, F. Bedioui, J.H. Zagal, *Electrochim. Acta* 46 (2001) 3397.
- [299] E.F. Perez, L.T. Lauro, A.A. Tanaka, G. De Oliveira Neto, *Electrochim. Acta* 43 (1998) 1665.
- [300] X. Qi, R.O. Baldwin, *J. Electrochem. Soc.* 143 (1996) 1283.
- [301] A.K. Abass, J.P. Hart, *Sens. Actuators B* B41 (1997) 169.
- [302] N. Pereira-Rodrigues, R. Cofré, J.H. Zagal, F. Bedioui, *Bioelectrochemistry* 70 (1997) 147.
- [303] J. Obirai, T. Nyokong, *Electrochim. Acta* 50 (2005) 3296.
- [304] N. Sehlotho, T. Nyokong, *J. Electroanal. Chem.* 595 (2006) 161.
- [305] S. Komorshy-Lovrić, *J. Electroanal. Chem.* 397 (1995) 211.
- [306] A.M. Castellani, J.E. Gocalves, Y. Gushikem, *J. New Mater. Electrochem. Syst.* 5 (2002) 169.
- [307] R.C.S. Luz, F.S. Damos, A.A. Tanaka, L.T. Kubota, *Sens. Actuators B: Chem.* B114 (2006) 1019.
- [308] S. Maldonado, K.J. Stevenson, *J. Phys. Chem. B* 108 (2004) 11375.
- [309] D. Dong, B. Liu, J. Liu, N. Kobayashi, *J. Porph. Phthal.* 1 (1997).
- [310] G. Ramirez, E. Trollund, M. Isaacs, F. Armijo, J. Zagal, J. Costamagna, J.M. Aguirre, *Electroanalysis* 14 (2002) 540.
- [311] X. Huang, W.T. Kok, *Anal. Chim. Acta* 273 (1993) 245.
- [312] S. de Irazu, N. Unceta, M.B. Samedro, M.A. Goicolea, B.R. Barrio, *Analyst* 126 (2001) 495.
- [313] M. Siswana, K.I. Ozoemena, T. Nyokong, *Talanta* 69 (2006) 1136.
- [314] T. Nyokong, in: J.H. Zagal, F. Bedioui, J.P. Dodet (Eds.), *N4-Macrocyclic Metal Complexes*, Springer, New York, 2006 (Chapter 7).
- [315] J. Oni, T. Nyokong, *Electroanalysis* 14 (2002) 1165.
- [316] K.I. Ozoemena, T. Nyokong, D. Nkosi, I. Chambrier, M.J. Cook, *Electrochim. Acta* 52 (2007) 4132.
- [317] K. Ozoemena, T. Nyokong, *Electrochim. Acta* 51 (2006) 2669.
- [318] M.P. Siswana, K. Ozoemena, T. Nyokong, *Electrochim. Acta* 52 (2006) 114.
- [319] K. Ozoemena, J. Pillay, T. Nyokong, *Electrochem. Commun.* 8 (2006) 1391.
- [320] P.N. Mashazi, P. Westbroek, K.I. Ozoemena, T. Nyokong, *Electrochim. Acta* 53 (2007) 1858.
- [321] J.H. Zagal, F. Bedioui, J.P. Dodelet (Eds.), *N-4 Macrocyclic Complexes*, Springer, New York, 2006.
- [322] S.A. Wring, J.P. Hart, B.J. Birch, *Electroanalysis* 4 (1992) 299.
- [323] S.A. Wring, J.P. Hart, *Analyst* 117 (1992) 1281.
- [324] T.R. Ralph, M.L. Hitchman, J.P. Millington, F.C. Walsh, *J. Electroanal. Chem.* 375 (1994) 1.
- [325] Y.-H. Tse, P. Janda, A.B.P. Lever, *Anal. Chem.* 66 (1994) 384.
- [326] X. Qi, R.P. Baldwin, *Electroanalysis* 6 (1994) 353.
- [327] J.P. Hart, L.C. Hartley, *Analyst* 119 (1994) 259.
- [328] J.H. Zagal, M. Gulppi, C. Depretz, D. Lelièvre, *J. Porph. Phthal.* 3 (1999) 355.
- [329] P. Ardiles, E. Trollund, M. Isaacs, F. Armijo, M.J. Aguirre, *J. Coord. Chem.* 54 (2001) 183.
- [330] R.O. Lezna, S. Juanto, J.H. Zagal, *J. Electroanal. Chem.* 452 (1998) 221.
- [331] J.H. Zagal, M. Gulppi, M. Isaacs, G. Cárdenas-Jirón, M.J. Aguirre, *Electrochim. Acta* 44 (1998) 1349.
- [332] D. Schlettwein, T. Yoshida, *J. Electroanal. Chem.* 441 (1998) 139.
- [333] J.H. Zagal, M. Gulppi, C.A. Caro, G.I. Cárdenas-Jirón, *Electrochem. Commun.* 1 (1999) 389.
- [334] G.I. Cárdenas-Jirón, M.A. Gulppi, C.A. Caro, R. Del Rio, M. Páez, J.H. Zagal, *Electrochim. Acta* 46 (2001) 3227.
- [335] M. Gulppi, S. Griveau, J. Pavez, J.H. Zagal, F. Bedioui, *Electroanalysis* 15 (2003) 779.
- [336] S. Shahrokhian, J. Yazdani, *Electrochim. Acta* 48 (2003) 4143.
- [337] S. Shahrokhian, A. Hamzehloei, A. Thaghani, S.R. Mousavi, *Electroanalysis* 16 (2004) 915.
- [338] M.A. Gulppi, M.A. Paez, J.A. Costamagna, G. Cárdenas-Jirón, F. Bedioui, J.H. Zagal, *J. Electroanal. Chem.* 580 (2005) 50.
- [339] M.A. Gulppi, Ph.D. Thesis, University of Santiago de Chile, 2003.
- [340] J.A. Claussen, G. Ochoa, M. Paez, J. Costamagna, T. Nyokong, F. Bedioui, J.H. Zagal, *J. Solid State Electrochem.* 12 (2008) 473.
- [341] J. Telesford, P.D. Voegel, Abstracts: 230th ACS National Meeting, Washington DC, August 28–September 1, 2005, CHED-139.
- [342] P.D. Voegel, J. Telesford, 60th Southwest regional meeting of ACS, Fort Worth, Texas, September 29–October 4, 2004, SEPT04-315.
- [343] S.A. Wring, J.P. Hart, B.J. Birch, *Talanta* 38 (1991) 1257.
- [344] G. Ochoa, C. Gutierrez, I. Ponce, J.F. Silva, M. Páez, J. Pavez, J.H. Zagal, *J. Electroanal. Chem.* 639 (2010) 88.
- [345] A.J. Appleby, in: B. Conway, J.O'M. Bockris (Eds.), *Modern Aspects of Electrochemistry*, vol. 9, Plenum Press, 1974, p. 369.
- [346] T. Bligaard, J.K. Nørskov, S. Dahl, J. Matthiesen, C.H. Christensen, J. Sehested, *J. Catal.* 224 (2004) 206.
- [347] B.E. Conway, J. Jerkiewicz, *Electrochim. Acta* 45 (2000) 4075.
- [348] R. Parsons, *Trans. Faraday Soc.* 54 (1958) 1053.
- [349] R. Parsons, *Surf. Sci.* 2 (1964) 418.
- [350] R. Parsons, *Surf. Sci.* 18 (1969) 28.
- [351] S. Trasatti, *J. Electroanal. Chem.* 33 (1971) 351.
- [352] S. Trasatti, *J. Electroanal. Chem.* 39 (1972) 163.
- [353] S. Trasatti, in: C.W. Tobias, H. Gerischer (Eds.), *Advances in Electrochemistry and Electrochemical Engineering*, vol. 10, Interscience, New York, 1977, p. 213.
- [354] S. Trasatti, in: W.E. O'Grady, P.N. Ross, F.G. Will (Eds.), *Proceedings of the Symposium on Electrocatalysis*, The Electrochemical Society Proceeding Series, Pennington, NJ, 1982, p. 73.
- [355] H. Gerischer, *Z. Physik, Chem. N. F.* 8 (1956) 137.
- [356] J. O'M Bockris, A.K.M. Reddy, *Modern Electrochemistry*, vol. 2, First ed., Plenum Press, New York, 1997, p. 960.
- [357] J.M. Jaksic, N.M. Ristic, N.V. Krstajic, M.M. Jaksic, *Int. J. Hydrogen Energy* 23 (1998) 1121.
- [358] M.M. Jaksic, *Electrochim. Acta* 45 (2000) 4085.
- [359] M.M. Jaksic, *Int. J. Hydrogen Energy* 26 (2001) 559.
- [360] M.M. Jaksic, *Solid State Ionics* 136–137 (2000) 733.
- [361] R. Adzic, in: J. Lipkowski, P.N. Ross (Eds.), *Frontiers in Science*, Wiley-VCH, 1998, p. 197.
- [362] D. Wöhrle, D. Schlettwein, G. Schnurpfeil, G. Schneider, E. Karmann, T. Yoshida, M. Kaneko, *Polym. Adv. Technol.* 6 (1995) 18.
- [363] E. Karmann, D. Schlettwein, N.I. Jaeger, *J. Electroanal. Chem.* 405 (1996) 149.
- [364] H. Kalvelage, A. Mecklenburg, U. Kunz, U. Hoffmann, *Chem. Eng. Technol.* 23 (2000) 803.
- [365] J.P. Collman, R. Boulatov, C.J. Sunderland, in: K.M. Kadish, K.M. Smith, R. Guilard (Eds.), *The Porphyrin Handbook*, Academic Press, Boston, 2003, p. 1 (Chapter 23).
- [366] J.H. Zagal, M. Páez, A.A. Tanaka, J.R. dos Santos, C. Linkous, *J. Electroanal. Chem.* 339 (1992) 13.
- [367] Y.H. Tse, P. Janda, H. Lam, J. Zhang, W.P. Pietro, A.B.P. Lever, *J. Porph. Phthal.* 1 (1997) 3.
- [368] J. Pavez, M. Páez, A. Ringuedé, F. Bedioui, J.H. Zagal, *Solid State Electrochem.* 9 (2005) 21.
- [369] G. Lalonde, R. Cote, D. Guay, J.P. Dodelet, L.T. Weng, P. Bertrand, *Electrochim. Acta* 42 (1997) 1378.
- [370] A.L. Boukamp-Wijnol, W. Visscher, J.A.R. van Veen, *Electrochim. Acta* 43 (1998) 3152.
- [371] M. Lefevre, J.P. Dodelet, P. Bertrand, *J. Phys. Chem. B* 106 (2002) 8705.
- [372] A.L. Boukamp-Wijnol, W. Visscher, J.A.R. Van Veen, J.A.R. Boellaard, A.M. Van der Kraan, S.C. Tang, *J. Phys. Chem. B* 106 (2002) 12993.
- [373] M. Lefevre, J.P. Dodelet, *Electrochim. Acta* 48 (2003) 2749.
- [374] N. Kobayashi, W.A. Nevin, *Appl. Organomet. Chem.* 10 (1996) 579.
- [375] J.H. Zagal, M.J. Aguirre, L. Basaez, J. Pavez, L. Padilla, A. Toro-Labbé, in: F.C. Anson, R.R. Adzic, K. Kinoshita (Eds.), *Oxygen Electrochemistry*, The Electrochemical Society Symposium Series 95–26, 1995, p. 89.
- [376] I. Bytheway, M.B. Hall, *Chem. Rev.* 94 (1994) 639.
- [377] G. Wang, N. Ramesha, A. Hsua, D. Chub, R. Chenc, *Mol. Simul.* 34 (2008) 1051.
- [378] R. Chen, H. Li, D. Chu, G. Wang, *J. Phys. Chem. C* 113 (2009) 20689.
- [379] Z. Shi, J. Zhang, *J. Phys. Chem. C* 111 (2007) 7084.
- [380] A. van der Putten, A. Elzing, W. Visscher, E. Barendrecht, *J. Electroanal. Chem.* 221 (1987) 95.
- [381] S. Zecevic, B. Simic-Glavaski, E. Yeager, A.B.P. Lever, P.C. Minor, *J. Electroanal. Chem.* 196 (1985) 339.
- [382] S.H. Kim, D.A. Scherson, *J. Electroanal. Chem.* 64 (2002) 3091.
- [383] I.C. Stefan, Y.B. Mo, S.Y. Ha, S. Kim, D.A. Scherson, *Inorg. Chem.* 42 (2003) 4316.
- [384] J.A.R. van Veen, C. Visser, *Electrochim. Acta* 24 (1979) 921.
- [385] J.A.R. van Veen, J.F. van Baar, C.J. Croese, J.G.F. Coolegem, N. de Wit, H.A. Colijn, *Ber. Bunsenges. Phys. Chem.* 85 (1981) 693.
- [386] J.H. Zagal, G. Cárdenas-Jirón, *J. Electroanal. Chem.* 489 (2000) 96.
- [387] G.I. Cárdenas-Jirón, J.H. Zagal, *J. Electroanal. Chem.* 497 (2001) 55.
- [388] M.D. Newton, *Chem. Rev.* 91 (1991) 767.
- [389] R.G. Pearson, *Proc. Natl. Acad. Sci. USA* 83 (1986) 8440.
- [390] R.G. Parr, R.G. Pearson, *J. Am. Chem. Soc.* 105 (1983) 7512.
- [391] J. Ulstrup, *J. Electroanal. Chem.* 79 (1977) 191.
- [392] A. Rosa, E.J. Baerends, *Inorg. Chem.* 33 (1994) 584.
- [393] K.W. Hipps, X. Lung, X.D. Wang, U. Manzur, *J. Phys. Chem. B* 100 (1996) 11207.
- [394] C. Hinnen, F. Coowar, M. Savy, *J. Electroanal. Chem.* 264 (1989) 167.
- [395] D. van den Ham, C. Hinnen, G. Magner, M. Savy, *J. Phys. Chem.* 91 (1987) 4743.
- [396] F. Coowar, O. Contamin, M. Savy, G. Scarbeck, *J. Electroanal. Chem.* 246 (1998) 119.
- [397] J.H. Zagal, P. Bindra, E. Yeager, *J. Electrochem. Soc.* 127 (1980) 1506.
- [398] A. Elzing, A. van der Putten, W. Visscher, E. Barendrecht, *J. Electroanal. Chem.* 233 (1987) 99.
- [399] A. Elzing, A. van der Putten, W. Visscher, E. Barendrecht, *J. Electroanal. Chem.* 200 (1986) 313.
- [400] C.A. Fierro, M. Mohan, D.A. Scherson, *Langmuir* 6 (1990) 1338.
- [401] J. Ouyang, K. Shigehara, A. Yamada, F.C. Anson, *J. Electroanal. Chem.* 297 (1991) 489.
- [402] A. van der Putten, A. Elzing, W. Visscher, E. Barendrecht, *J. Electroanal. Chem.* 214 (1986) 523.
- [403] C. Song, L. Zhang, J. Zhang, *J. Electroanal. Chem.* 587 (2006) 293.
- [404] J.A.R. van Veen, J.F. van Baar, K.J. Krose, *J. Chem. Soc. Faraday Trans. 77* (1981) 2827.
- [405] J.A.R. van Veen, H.A. Colijn, *Ber. Bunsenges. Phys. Chem.* 85 (1981) 700.

- [406] C. Coutanceau, A. Rakotondrainibe, P. Crouigneau, J.M. Léger, C. Lamy, J. Electroanal. Chem. 386 (1995) 173.
- [407] A. Elzing, A. van der Putten, W. Visscher, E. Barendrecht, C. Hinnen, J. Electroanal. Chem. 279 (1990) 137.
- [408] N. Phougat, P. Vasudevan, J. Power Sources 69 (1997) 161.
- [409] A. Elzing, A. van der Putten, W. Visscher, E. Barendrecht, Recl. Trav. Chim. Pays-Bas 109 (1990) 31.
- [410] J.H. Zagal, M. Pérez, J. Sturm, S. Ureta-Zañartu, J. Electroanal. Chem. 181 (1984) 295.
- [411] R.A. Sheldon, J.K. Kochi, Metal-Catalysed Oxidations of Organic Compounds, Academic Press, New York, 1981.
- [412] J.A.R. van Veen, J.F. van Baar, Rev. Inorg. Chem. 4 (1982) 293.
- [413] F. van den Brink, W. Visscher, E. Barendrecht, J. Electroanal. Chem. 172 (1984) 301.
- [414] S. Baranton, C. Coutanceau, E. Garnier, J.M. Léger, J. Electroanal. Chem. 590 (2006) 100.
- [415] L. Bouwkamp-Wijnol, W. Visscher, J.A.R. van Veen, Electrochim. Acta 39 (1994) 1641.
- [416] J.P. Collman, K. Kim, J. Am. Chem. Soc. 108 (1986) 7847.
- [417] L. Bouwkamp-Wijnol, B.J. Palys, W. Visscher, J.A.R. van Veen, J. Electroanal. Chem. 406 (1996) 195.
- [418] O. Ikeda, H. Fukuda, H. Tamura, J. Chem. Soc. Faraday Trans. 82 (1986) 1561.
- [419] A.B. Anderson, R.A. Sidik, J. Phys. Chem. B 108 (2004) 5031.
- [420] G. Magner, M. Savy, G. Scarbeck, J. Riga, J.J. Verbist, J. Electrochem. Soc. 128 (1981) 1674.
- [421] R. Baker, D.P. Wilkinson, J. Zhang, Electrochim. Acta 53 (2008) 6906.
- [422] L. Zhang, C. Song, J. Zhang, H. Wang, D.P. Wilkinson, J. Electrochem. Soc. 152 (2005) A2421.
- [423] S. Baranton, C. Coutanceau, C. Roux, F. Hahn, J.-M. Léger, J. Electroanal. Chem. 577 (2005) 223.
- [424] Y. Lu, R.G. Reddy, Electrochim. Acta 52 (2007) 2562.
- [425] N. Villeneuve, F. Bedioui, Electroanalysis 15 (2003) 59.
- [426] T. Malinski, Z. Taha, Nature 358 (1992) 676.
- [427] F. Lantoiné, S. Trévin, F. Bedioui, J. Devynck, J. Electroanal. Chem. 392 (1995) 85.
- [428] S. Trévin, F. Bedioui, J. Devynck, J. Electroanal. Chem. 408 (1996) 261.
- [429] A. Ciszewski, G. Milczarek, Electroanalysis 10 (1998) 791.
- [430] N. Diab, W. Schumann, Electrochim. Acta 47 (2001) 265, and references cited therein.
- [431] A.V. Kashevskii, A.Y. Safronov, O. Ikeda, J. Electroanal. Chem. 510 (2001) 86, and references cited therein.
- [432] F. Bedioui, S. Trévin, J. Devynck, F. Lantoiné, A. Brunet, M.A. Devynck, Biosens. Bioelectron. 12 (1997) 205.
- [433] M. Pontié, H. Lecture, F. Bedioui, Sens. Actuators: B 56 (1999) 1.
- [434] I. Zibermann, J. Hayon, T. Katchalski, R. Ydgar, J. Rishpon, A.I. Shames, E. Korin, A. Bettelheim, Inorg. Chim. Acta 305 (2000) 53.
- [435] J. Jin, T. Miwa, L. Mao, H. Tu, L. Jin, Talanta 48 (1999) 1005.
- [436] C. Caro, J. Zagal, F. Bedioui, J. Electrochem. Soc. 150 (2003) E95.
- [437] S.L. Vilakazi, T. Nyokong, Electrochim. Acta 46 (2000) 453.
- [438] L. Mao, K. Yamamoto, W. Zhou, L. Jin, Electroanalysis 12 (2000) 72.
- [439] I. Zibermann, J. Hayon, T. Katchalski, O. Raveh, J. Rishpon, A.I. Shames, A. Bettelheim, J. Electrochem. Soc. 144 (1997) L228.
- [440] G.R. Richter-Addo, J. Porph. Phthal. 4 (2000) 354.
- [441] J.Z. Li, X.Y. Pang, R.Q. Yu, Anal. Chim. Acta 297 (1994) 437.
- [442] J.N. Younathan, K.S. Wood, T.J. Meyer, Inorg. Chem. 31 (1992) 3280.
- [443] F. Bedioui, S. Trévin, V. Albin, M.G. Gomez-Villegas, J. Devynck, Anal. Chim. Acta 341 (1997) 177.
- [444] R. Lin, M. Bayachou, J. Greaves, P.J. Farmer, J. Am. Chem. Soc. 119 (1997) 12689.
- [445] N. Chebotareva, T. Nyokong, J. Coord. Chem. 46 (1999) 433.
- [446] D. Mimica, J.H. Zagal, F. Bedioui, J. Electroanal. Chem. 497 (2001) 106.
- [447] J.R. Rocha, L. Kosminsky, T.R.L.C. Paixao, M. Bertotti, Electroanalysis 13 (2001) 155.
- [448] C. Caro, F. Bedioui, G. Gardenas Jiron, J. Zagal, J. Electrochem. Soc. 151 (2004) E32.
- [449] R.G. Parr, W. Yang, J. Am. Chem. Soc. 106 (1984) 4049.
- [450] G.I. Cárdenas-Jirón, J. Phys. Chem. A 106 (2002) 3202.
- [451] G.I. Cárdenas-Jirón, C.A. Caro, D. Venegas-Yazigi, J.H. Zagal, J. Mol. Struct. (Theochem.) 580 (2002) 193.
- [452] G.I. Cárdenas-Jirón, D.A. Venegas-Yazigi, J. Phys. Chem. A 106 (2002) 11938.
- [453] G.I. Cárdenas-Jirón, Int. J. Quantum Chem. 91 (2003) 389.
- [454] C. Hansch, A. Leo, R.W. Taft, Chem. Rev. 91 (1991) 165.
- [455] X. Li, S. Zhang, C. Sun, J. Electroanal. Chem. 553 (2003) 139.
- [456] S.V. Guerra, L.T. Kubota, C.R. Xavier, S. Nakagaki, Anal. Sci. 15 (1999) 1231.
- [457] S. Antoniadou, A.D. Jannakoudakis, E. Theodoridou, Synth. Met. 30 (1989) 295.
- [458] J. Jiang, Y. Bian, F. Furuya, W. Liu, M. Choi, M. Kobayashi, H.W. Li, Q. Yang, T. Ng, D.K.P. Mak, Chem. Eur. J. 7 (2001) 5059.
- [459] A.M. Moliner, J.J.J. Street, Environ. Qual. 18 (1989) 487.
- [460] S.M. Golabi, H.R. Zare, J. Electroanal. Chem. 465 (1999) 168.
- [461] H. Razmi-Nerbin, M.H. Pournaghi, J. Solid State Electrochem. 6 (2002) 126.
- [462] E.F. Pérez, G. Neto, A.A. Tanaka, L.T. Kubota, Electroanalysis 10 (1998) 111.
- [463] S. Golabi, F.J. Noor-Mohammadi, Solid State Electrochem. 2 (1998) 30.
- [464] K. Tamura, T. Kahara, J. Electrochem. Soc. 123 (1976) 776.
- [465] F. Steinbach, M. Zobel, Z. Phys. Chem. N. F. 111 (1978) 113.
- [466] F. Steinbach, M. Zobel, J. Chem. Soc. Faraday Trans. 82 (1979) 113.
- [467] F.J. Cookson, T.D. Smith, J.F. Boas, P.R. Hicks, J.R. Pilbrow, J. Chem. Soc. Dalton 18 (1976) 1791.
- [468] D.M. Wagnerova, E. Schwertnerova, J. Veprek-Siska, Collect. Czech. Chem. Commun. 38 (1973) 756.
- [469] E. Schwertnerova, D.M. Wagnerova, J. Veprek-Siska, Z. Chem. 14 (1974) 311.
- [470] L.J. Boucher, in: G.A. Melson (Ed.), Coordination Chemistry of Macrocyclic Compounds, Plenum Press, New York, 1979.
- [471] K. Brinck, Ms.Sci.Thesis, University of Santiago de Chile, 1985.
- [472] T.A. Albright, J.K. Burdett, M.H. Whango, Orbital Interaction in Chemistry, Wiley-Interscience, New York, 1985.
- [473] V. Paredes-García, G.I. Cárdenas-Jirón, D. Venegas-Yazigi, J.H. Zagal, M. Pérez, J. Costamagna J. Phys. Chem. A 109 (2005) 1196.
- [474] D.A. Venegas-Yazigi, G.I. Cárdenas-Jirón, J.H. Zagal, J. Coord. Chem. 56 (2003) 1269.
- [475] G. Ochoa, D. Geraldo, C. Linares, T. Nyokong, F. Bedioui, J.H. Zagal, ECS Trans. 19 (2009) 97.
- [476] J.H. Zagal, S. Griveau, K. Ozoemena, T. Nyokong, F. Bedioui, J. Nanosci. Nanotechnol. 9 (2009) 2201.
- [477] E.F. Perez, G. de Oliveira Neto, A.A. Tanaka, L.T. Kubota, Electroanalysis 10 (1998) 111.
- [478] K.I. Ozoemena, Sensors 6 (2006) 874.
- [479] I. Ponce, J.H. Zagal, 10th International Conference on Frontier Polymeric and Advanced Materials, Santiago, Chile, 2009.
- [480] K. Becker, C. Schulz, S. Kaus, M. Seiwert, B. Seifert, Int. J. Hyg. Environ. Health 206 (2003) 15.
- [481] A. Cienaitė, J.N. Huckins, D.A. Alvarez, W.L. Cranor, R.W. Gale, V. Kauneliene, P.-A. Bergqvist, Atmos. Environ. 41 (2007) 2844.
- [482] L.R. Sharma, G. Singh, A. Sharma, B. Electrochem. 4 (1988) 679.
- [483] A. García de la Rosa, E. Castro-Quezada, S. Gutiérrez-Granados, F. Bedioui, A. Alatorre-Ordaz, Electrochem. Commun. 7 (2005) 853.
- [484] A.A. Ordaz, J.M. Rocha, F.J.A. Aguilar, S. Gutiérrez-Granados, F. Bedioui, Anal. Chem. 72 (2000) 238.
- [485] F. Vijchez-Aguado, S. Gutiérrez-Granados, S. Sucar-Succar, C. Bied-Charreton, F. Bedioui, New J. Chem. 21 (1997) 1009.
- [486] X.-E. Jiang, L.-P. Guo, X.-G. Du, Talanta 61 (2003) 247.
- [487] M. Chicharro, A. Zapardiel, E. Bermejo, M. Moren, E. Madrid, Anal. Bioanal. Chem. 373 (2002) 277.
- [488] W.G. Kiflom, O.S. Wandiga, N.G. Kamau, Pure Appl. Chem. 73 (2001) 1907.
- [489] C. Berrios, J.F. Marco, C. Gutiérrez, M.S. Ureta-Zañartu, Electrochim. Acta 54 (2009) 6417.
- [490] C. Berrios, M.S. Ureta-Zañartu, C. Gutiérrez, Electrochim. Acta 53 (2007) 792.
- [491] C. Berrios, J.F. Marco, C. Gutiérrez, S.-M. Ureta-Zañartu, J. Phys. Chem. B 112 (2008) 12644.
- [492] E.B. Bustos, G.M. Jimenez, B.R. Diaz-Sanchez, E. Juaristi, T.W. Thomas, A.L. Godínez, Talanta 72 (2007) 1586.
- [493] H. Yao, Y. Sun, X. Lin, Y. Tang, L. Huang, Electrochim. Acta 52 (2007) 6165.
- [494] K. Miyazaki, G. Matsumoto, M. Yamada, S. Yasui, H. Kanedo, Electrochim. Acta 44 (1999) 3809.
- [495] J. Li, X. Li, Sens. Actuators B 124 (2007) 469.
- [496] S. Alwarappan, K.S. A/Butcher, D.K.Y. Wong, Sens. Actuators B 128 (2007) 299.
- [497] B.E.K. Swamy, B.J. Venton, Analyst 132 (2007) 876.
- [498] P. Wang, Y. Li, X. Huang, L. Wang, Talanta 73 (2007) 431.
- [499] K.I. Ozoemena, T. Nyokong, D. Nkosi, I. Chambrier, M.J. Cook, Electrochim. Acta 52 (2007) 4132.
- [500] L.M. Santos, R.P. Baldwin, Anal. Chem. 59 (1987) 1766.
- [501] C. Sun, X. Zhang, D. Jiang, Q. Gao, H. Xu, Y. Sun, X. Zhang, J. Chen, J. Electroanal. Chem. 411 (1996) 73.
- [502] Z. Sun, H. Tachikawa, Anal. Chem. 64 (1992) 1112.
- [503] F. Muzutani, S. Yabuki, S. Iijima, Anal. Chim. Acta 300 (1995) 59.
- [504] T.-F. Kang, G.-L. Shen, R.-Q. Yu, Anal. Lett. 30 (1997) 647.
- [505] E. Crouch, D.C. Cowell, S. Hoskins, R.W. Pittson, J.P. Hart, Biosens. Bioelectron. 21 (2005) 712.